ATOMIC FORCE MICROSCOPY FOR SORPTION STUDIES

A Thesis
Presented to
The Academic Faculty

By

Viriya Vithayaveroj

In Partial Fulfillment
of the Requirements for the Degree
Doctor of Philosophy in Environmental Engineering
School of Civil and Environmental Engineering

Georgia Institute of Technology
September 2004

ATOMIC FORCE MICROSCOPY FOR SORPTION STUDIES

Approved by:

Dr. Sotira Yiacoumi, advisor

Dr. Costas Tsouris, co-advisor

Dr. Ching-Hua Huang

Dr. Michael Sacks

Dr. Rina Tannenbaum

Date Approved

September 21, 2004

Dedicated to

My Beloved Family, Vichit, Vipa, Pasinee, Parkpoom, and Sasis Vithayaveroj,

and My Fiancé, Polapat Udomphol.

ACKNOWLEDGEMENTS

I would like to express my sincere gratitude to my Ph.D. advisors Dr. Sotira Yiacoumi and Dr. Costas Tsouris for their guidance and encouragement. I have benefited greatly from their direction and review of this study. My appreciation is also given to Dr. Ching-Hua Huang, Dr. Michael Sacks, and Dr. Rina Tannenbaum for being my committee members and for providing me with valuable insight, comments, and suggestions, which improved the presentation of this thesis.

I thank Dr. Guangxuan Zhu for his assistance and discussion on experimental methods and equipment. I am also thankful to Andrea Bé and Therese Rehkopf for their assistance and their friendship during the past few years. I would like to thank Goragot Lertpatanakul and Victor Romero for editing this thesis.

I would like to express my gratitude to several friends, especially Kasemsan and Supinda, who made my life at Georgia Tech all the more memorable. My thanks also go to my fellow graduate students, Monica, Tony, Kun-Lin, Thorben, Jeremy, and Chia-Hung, for the exchange of ideas and their friendship. I am especially thankful to Patricia for numerous discussions and her friendship throughout my study at Georgia Tech.

I am grateful to my parents, sister, brothers, and fiancé for their unconditional love, support, and encouragement that have enabled me to successfully complete my graduate studies.

Financial support for this work was provided by the National Science Foundation through a Career Award to Dr. Sotira Yiacoumi (BES-9702356), Georgia Institute of Technology, and the U. S. Department of Energy, Office of Basic Energy Sciences, Division of Chemical Sciences through Oak Ridge National Laboratory.

TABLE OF CONTENTS

LIST OF FIGURES

LIST OF SYMBOLS

a	Point where the potential presents a minimum
A	Hamaker constant (J)
A_{eff}	Effective area (m^2)
C_D	Debye coefficient
C_K	Keesom coefficient
C_L	London coefficient
D	Separation distance (m)
$\bar{e}$	Electron charge = 1.6×10^{-19} C
F	Force (N)
$F_{electrostatic}$	Electrostatic forces (N)
F_{vdw}	Van der Waals forces (N)
h	Planck's constant = 6.626×10^{-34} J s
$h\upsilon_1$, $h\upsilon_2$	first ionization potentials of the molecules
I	Ionic strength of the solution (M)
k	Spring constant (N m^{-1})
k_B	Boltzmann constant = 1.38×10^{-23} J K^{-1}
M	Mass of the added particle
N_o	Avogadro's constant = 6.022×10^{-23} mol^{-1}
r	Distance between the atoms or molecules (m)

R	Radius of the particle tip (m)
T	Absolute temperature (K)
u_1, u_2	Dipole moments of the molecules
V_D	Debye potential (J)
V_K	Keesom potential (J)
V_L	London potential (J)
V_{vdw}	Van der Waals potential (J)
x	deflection of cantilever (m)
y	Radius of an effective area (m)
z	Valence of the symmetric electrolyte in the solution
α, α'	Angles of two perpendicular/parallel sides
α_{01}, α_{02}	Electronic polarizabilities of the molecules
ε	Permittivity of the medium = 8.85×10^{-12} C^2 N^{-1} m^{-2}
ε_o	Vacuum dielectric constant
$\varepsilon_1, \varepsilon_2, \varepsilon_3$	Dielectric constants of the three media
$\varepsilon(i\upsilon)$	Dielectric constant at the imaginary frequency axis $i\upsilon$.
κ	Inverse of the double-layer thickness (m^{-1})
ρ	Number density of ions of valence z at any point between two surfaces
σ	surface charge density (C m^{-2})
$\sigma_{silica}, \sigma_{glass}$	charge densities of a silica particle and a glass plate (C m^{-2})
υ_0, υ	resonance frequencies before and after tip loading (Hz)
ψ	electrostatic potential (mV)
ψ_m	electric potential at the midplane (mV)

ψ_0	surface potential of particles (mV)
CE	Counter electrode
CTAB	Cetyltrimethylammonium bromide
DLVO	Derjaguin-Landau-Verwey-Overbeek
EDL	Electrical double layer
E_{pzc}	Potential of zero charge
IEP	Isoelectric point
OCP	Open circuit potential
pH_{pzc}	Point of zero charge
RE	Reference electrode
SDS	Sodium dodecyl sulfate
WE	Working electrode

SUMMARY

Sorption plays an important role in natural waters as well as in water treatment processes. Sorption of ions, such as metal and surfactant ions, may lead to variations in interparticle forces and, thus, changes in the stability of colloidal particles. Interactions between ions and colloidal particles modify the molecular structure of the surface, the surface charge, and the electrical potential between colloidal particles. These modifications to the surface and to the electrical double layer due to ion sorption are reflected in the interaction force between a particle and another surface, which was measured in this study by atomic force microscopy (AFM). The objective of this research was to improve the understanding of sorption dynamics and equilibrium by using AFM as a tool. The Derjaguin–Landau–Verwey–Overbeek (DLVO) theory, which includes electrostatic and van der Waals forces, was used to explain the interactions between surfaces. Experimental data and theoretical results were compared to probe DLVO and other interparticle forces. This research was divided into four parts and details for each part are given below.

In the first part, AFM was used to investigate the sorption of copper ions from aqueous solutions by silica particles. Changes in interaction forces indicated the occurrence of copper sorption. The influence of metal ion concentration and solution ionic strength on surface forces was studied under transient conditions. Results showed that as the metal ion concentration was decreased, charge reversal occurred and a longer

period of time was required for the system to reach equilibrium. The ionic strength had no significant effect on sorption kinetics. Furthermore, neither metal concentration nor ionic strength exhibited any effect on sorption equilibria, indicating that for the experimental conditions used in this study, the surface sites of the silica particle were fully occupied by copper ions. The concentration limit that could have a measurable effect by AFM was also determined. Theoretical calculations based on the DLVO theory were compared with direct force measurements. A good agreement was found at all conditions except at very small separations.

In the second part, the phase of silicon nitride used in AFM cantilevers was first determined. Results from both the zeta potential and AFM measurements indicated that silicon nitride employed in this study was either alpha phase or electronic grade, which consists of 94% alpha phase and 6% beta phase. Force-volume AFM was used to detect heterogeneously charged regions on surfaces. Interaction forces between a silica substrate and a silicon nitride AFM tip were measured before and after copper sorption. An attractive force was found throughout the surface before copper ion sorption. The magnitude of attractive force increased at a higher pH. After sorption, the force was less attractive. The higher the concentration of copper ions, the less attractive the force became. Copper sorption was low as expected at pH 4.5. The formation of islands was observed at a higher pH, and the interaction force in those regions was repulsive. The higher the concentration of copper ions in the system, the larger the number of islands was detected. The regions without islands still presented attractive interaction. The island regions on the surface are a result of the sorption of copper ions.

In the third part, AFM was used to measure interaction forces between a gold sample and a silicon nitride tip of the AFM in aqueous electrolyte solutions. Various values of electrostatic potential were externally applied between the sample, which served as the working electrode, and a reference electrode immersed into the solution. The interaction was a strong function of the solution pH and the applied potential. An attractive force was initially found at open circuit when the solution pH was below 7. A series of force measurements showed that the force became more attractive as the applied potential was more negative. On the other hand, the force was more repulsive when a more positive potential was applied. At pH values higher than 7, the interaction force was repulsive without any applied potential. As the gold sample was held at negative potentials, the forces showed a repulsive interaction. The interaction force transformed to an attractive force at positive potentials. The potential of zero charge of the gold sample was identified from force measurements in this study. The experimental results were compared to the DLVO predictions.

In the fourth part, the total interaction force between a standard silicon nitride AFM tip and a gold-coated plate in the presence of cationic surfactant, cetyltrimethylammonium bromide (CTAB), was measured under various values of applied potential. An attractive force was found in the system without surfactant molecules present, which corresponded to their zeta potentials. A repulsive force was observed in surfactant solutions. As the surfactant concentration increased, the repulsion became stronger and the decay length was also longer. The features of force curves were similar under a range of applied potential values from –1000 to 250 mV (vs. Ag/AgCl). At a higher positive potential, the repulsive force was weaker, the decay length was

shorter, and the instability distance decreased indicating the formation of a monolayer. Results from the AFM electrochemical study were compared to measurements obtained by cyclic voltammetry.

In summary, AFM was employed in this work to investigate the effects of sorption of metal and surfactant ions on surface charge and the interaction force between surfaces. The results are of importance in natural and engineered systems for the aggregation of colloidal particles with implications in separations as well as naturally occurring facilitated transport. It was also demonstrated that an external electrostatic potential may be applied to modify the surface charge and to control the interaction force between two surfaces, and therefore, the stability of particles in aqueous systems.

CHAPTER 1

INTRODUCTION

1.1. Surface Force Interactions

Interparticle interactions play a fundamental role in colloidal and interface science. These forces principally consist of electrical double layer, van der Waals, Born, hydration, and steric interactions. These interactions are dominant in short distances and depend significantly on the surface properties (Elimelech et al., 1995).

In the case where the interactions are due to electrical charge, interparticle forces are controlled by the presence of charging groups on the surface and their chemical nature. Electrical interactions between colloidal particles in aqueous systems influence particle stability, aggregation, and deposition. Particles in aqueous media are usually charged. In an electrolyte solution, the distribution of ions around a charged particle is not uniform and gives rise to an electrical double layer. The charge on the surface of a particle is balanced by oppositely charged counterions in the solution. These counterions are subject to two opposing influences: electrostatic attraction that tends to localize the counterions close to the particles, and the natural tendency of the ions to diffuse throughout the solution due to thermal fluctuations.

Surface properties are affected by surface group dissociations, sorption of chemical species, or application of an external potential. Specific sorption of ions on the surface may occur and modify the surface charge. In the case of ionic surfactants,

hydrophobic interaction leads to strong sorption, and the surface acquires a charge characteristic of the surfactant ion.

Atomic force microscopy (AFM) has recently been employed to acquire images of surfaces with nanoscale resolution, as well as direct measurements of interaction forces between approaching surfaces, such as particle–particle (Ducker and Senden, 1992; Li et al., 1993), particle–plate (Larson et al., 1995; Li et al., 1993; Considine et al., 2000a), and particle–bubble (Butt, 1994; Fielden et al., 1996) surfaces. These interaction forces include DLVO forces, e.g., electrostatic and van der Waals forces, as well as non-DLVO forces like steric, hydration, and hydrophobic forces. In many cases, the measured forces were found to be in agreement with theoretical predictions.

The use of AFM to study changes in topography and surface forces as a result of sorption has also been reported. However, investigations of sorption of metal ions using AFM have been very limited. The first study was done by Larson and Pugh (1998), who studied sorption of copper ions onto a silicon nitride probe. A more recent study (Chin et al., 2002) was focused on the use of AFM to measure the surface force between a silica particle and a smooth glass plate in an aqueous solution, both with and without the presence of copper ions. The force between the particle and the surface was found to change from repulsive to attractive with time, due to sorption of copper ions. Experimental results agreed with the calculated data based on the DLVO theory for constant surface charge.

Besides being employed to measure topographic images in a variety of conditions, AFM has also been extended to create force images related to the physical or chemical nature of various surfaces (Weaver et al., 1991; Meyer et al., 1992; Kado et al.,

1992). Imaging the spatial distribution of surface charge due to molecular functional groups on surfaces in aqueous solution was studied by measuring electrostatic forces (Butt, 1992; Senden et al., 1994; Manne et al., 1994; Ishino et al, 1997). In addition, surface charge mapping has also been performed on surfaces with modified charge by polyelectrolytes and metal ion species (Kramer et al., 1998; Estel et al., 2000; Miyatani et al., 1997; Miyatani et al., 1998, Johnson et al., 2003).

Double-layer forces in an aqueous solution play a key role in numerous interfacial processes. Early studies employed AFM to investigate the influence of solution pH and ionic strength (Butt, 1991; Weisenhorn et al., 1992; Atkins and Pashley, 1993; Li et al., 1993; Senden et al., 1994; Raiteri et al., 1996b; Karaman et al., 1997). Recently, the dependence of double-layer forces on externally applied potential has gathered attention in many research areas (Raiteri et al., 1996a; Hiller et al., 1996; Fréchette and Vanderlick, 2001). Potential-dependent interactions have been studied for solid surface materials (Hu et al., 1997; Döppenschmidt and Butt, 1999; Arai and Fujihira, 1996), as well as for soft materials such as polymer films (Ishino et al., 1994; Wang et al., 2002). In most cases, the measured forces were found to be strongly influenced by the applied potential.

Sorption of surfactant molecules onto solid surfaces has been studied over the years due to the numerous practical applications of surfactants. The type and concentration of both background electrolytes and surfactant molecules were found to affect the structure of surfactant molecules adsorbed onto the surface and also the sorption behavior itself (Rabinovich et al., 1994; Xu et al., 1996; Bremmell et al., 1999; Nalaskowski et al., 1999; Liu et al., 2001; McNamee et al., 2001). The mixture between

two surfactants that have different surface-aggregate structures can lead to the transformation of the individual surfactant structures (Ducker and Wanless, 1996). The mole fraction of surfactant in bulk solutions plays an important role in the organization and shape of aggregates at interfaces. Studies on the changes in the electrokinetic properties of surfaces due to the sorption of surfactant were performed quantitatively (Whitby et al., 2001). Applying an electric field to the system (Yang et al., 2001) would affect the sorption dynamics and equilibrium of surfactants, and these effects can also be captured by force measurements using AFM. As electrosorption increases the local concentration of surface-active ions at the electrode interface, it could lead to the formation of various structures of surfactant such as spherical, semispherical, cylindrical, and semicylindrical micelles, as well as bilayers.

There are several implications of the AFM capabilities that need to be explored further for sorption studies. The research presented in this dissertation focuses on employing AFM to provide a quantitative understanding of sorption of different species from aqueous solutions and on the effect of sorption on interparticle forces.

1.2. Scope and Objectives

The hypothesis behind this research is that Atomic Force Microscopy (AFM) can be used to capture changes in the surface interaction force caused by sorption of ions, which add electrical charge to the surface, and thereby can be employed as a tool to study sorption at the nano-scale. Once this hypothesis is verified, four different systems are investigated including (1) copper ion sorption from aqueous solutions onto a single silica particle, (2) partial copper ion sorption from aqueous solutions onto a quartz silica

surface, (3) electrosorption of electrolytes onto a gold surface, and (4) electrosorption and phase transition of surfactant molecules onto a gold surface. The main objective of these studies is to improve the current understanding of sorption dynamics and equilibrium on various surfaces and under the influence of an externally applied electric field. The Derjaguin–Landau–Verwey–Overbeek (DLVO) theory, which includes electrostatic and van der Waals forces, is used to explain surface interactions and probe DLVO and other interparticle forces.

The specific objectives identified for this research are:

1. Measure colloidal surface forces between a particle and a plate using atomic force microscopy (AFM).
2. Compare measured and theoretical forces to probe the DLVO theory.
3. Investigate the effects of metal ion sorption on colloidal forces, including concentration and ionic strength.
4. Assess the applicability of AFM on detecting heterogeneously charged regions on the surface.
5. Examine the influences of pH, ionic strength, and electric-field strength on electrosorption.
6. Study the effects of surfactant concentration on the surface force and formation of micellar structures.

The methodology to achieve each of these goals and the organization of this thesis are described in the following section.

1.3. Organization of Thesis

Chapter 1 presents the background and motivation of this research. The scope and objectives of this work are also discussed in this chapter. A literature review pertinent to this research, including colloidal interactions and direct force measurements using AFM, is presented in Chapter 2.

Chapter 3 describes the investigation of metal ions sorption by a single particle using AFM at different values of solution ionic strength and metal ion concentration. Results of direct force measurements and potential energy calculations based on the DLVO theory are compared. The concentration limit that can have a measurable effect by AFM is also determined.

Chapter 4 shows an assessment of the applicability of AFM on surface charge mapping, which means detection of heterogeneously charged regions on the surface. Surface charge of the sample substrate is controlled by regulating the pH. The heterogeneity of surface charge is enhanced by partial sorption of copper ions on the substrate, thus, modifying the surface charge at the sorption sites. The interaction force between the silica surface and a chemically inert tip are obtained along with images of the surface. Comparisons between the charge distributions before and after sorption are presented and discussed. In addition, the phase of a silicon nitride AFM tip is determined.

Influences of applied potential on the interaction forces between a gold sample and a silicon nitride tip in aqueous electrolyte solutions are presented in Chapter 5. Various potentials are applied between the sample, which served as the working electrode, and a reference electrode. The interaction force is a strong function of the solution pH and the applied potential. However, the ionic strength shows no effect on the

interaction force. The potential of zero charge for the gold sample is identified. The experimental results are compared with the DLVO predictions.

A study of cationic surfactant sorption on a gold surface is presented in Chapter 6. The influence of the adsorbed surfactant molecules on surface forces is examined. The effect of cationic surfactant on the formation of various micellar structures is also investigated both with and without an electric field applied.

A summary, conclusions, and recommendations for future studies are presented in Chapter 7.

1.4. Significance of Study

The research work described in this thesis is expected to provide a better understanding of sorption mechanisms at the molecular scale under various chemical environments. The study of sorption kinetics using only a single particle eliminates heterogeneity in the system and provides more accurate results using smaller quantities of reactants. In addition, the study of colloidal interactions under conditions of heterogeneous charge development is an important contribution to the current understanding of particle–particle interaction forces, as well as the analysis of solid–liquid separation processes that mainly consider a uniform constant surface charge.

The findings from this research have many potential applications. First, they can be used to evaluate sorption and particle aggregation models. Second, they will be valuable in the design and optimization of sorption and particle aggregation processes for the remediation of contaminated sites with toxic metals, as well as for the prediction of metal ion transport in natural surface and subsurface systems. The results can also be

utilized in mineral processes and in the removal of metal ions from industrial wastes. Furthermore, variations in the interaction force between surfaces, due to sorption of charged species, can be used to develop sensors. More specifically, this concept can be employed in sensors based on microcantilevers, which detect changes in bending and oscillation frequency caused by sorption. The electrical double layer force provides an additional parameter that can be sensed by microcantilevers.

The knowledge obtained from the electrosorption study allows a better understanding of the role of electrostatic forces in sorption processes and the manipulation of the sorption capacity by charged surfaces by applying an external potential to the interface.

AFM is also being used as a technique to study the changes in interaction forces due to sorption and electrosorption of surfactant molecules. Application of an electric field has been reported to enhance aqueous cleaning, a phenomenon attributed to electrosorption (Rowe, 2000). The findings of the study on sorption and electrosorption mechanisms of surfactant molecules have direct application in particle stabilization, as well as aqueous cleaning processes of metal surfaces, where formation of different structures determine the efficiency of the process. An understanding of surfactant-cleaning processes is needed to improve cleaning systems. Improvements in these aqueous surfactant solution systems can enhance their efficiency and reduce the impact of industrial cleaning systems on the environment.

CHAPTER 2

BACKGROUND

2.1. Surface Interactions

Information on intermolecular and surface interactions has been provided in the literature by a variety of measurements. These measurements can be divided into two methods, direct and indirect. The indirect method assumes a relationship between the forces and the property measured. For example, information on the short-range attractive potential between molecules can be obtained by performing experiments on the boiling points (Choi et al., 1994), latent heats of vaporization (Bhat and Agarwal, 1996), or lattice energies (Rae and Mason, 1968). Measurements from molecular beam scattering experiments (Balooch and Hamza, 1996), nuclear magnetic resonance (NMR) (Victor et al., 1999; Zhang et al., 2003), X-ray and neutron scattering of liquids and solids (Imae et al., 1999; Harada et al., 2001; Philip et al., 2003) can be employed to obtain short-range repulsion information. Short-range information on solute–solvent and solute–solute interactions can be acquired by measuring solubility (Batchelor et al., 2004), miscibility (Bouslah and Amrani, 2001), or osmotic pressure (Zimmerman et al., 1995). Adsorption isotherms provide information on the interactions of molecules with surfaces. Measurements that provide information on the forces between particles and surfaces include adhesion measurements, surface tension studies, contact angle measurements, total internal reflection microscopy (TIRM), and coagulation studies. However, the

measurements mentioned above are often inadequate when providing the detailed information needed to evaluate models predicting the interaction force as a function of separation distance between surfaces. In order to obtain this information, more direct force measurements are required. The challenge in such direct measurements is located in measuring forces on the order of 1 nN with a length-scale resolution of 1 nm. The first direct measurements of intermolecular forces were performed by using an electrobalance along with an optical technique (Derjaguin et al., 1954; Derjaguin and Abrikossova, 1956). Later, the surface forces apparatus (SFA) was invented and used to measure the interaction force between two macroscopic surfaces (Israelachvili and Adams, 1978; Israelachvili, 1987).

Recently, there have been numerous attempts to measure interparticle forces at the molecular scale. Atomic force microscopy (AFM) was developed from the original SFA to allow measurements of forces at an atomic scale. AFM has been employed to both image surfaces as well as measure surface forces in various environments. Results of several AFM studies have led to information on surface properties such as surface charge density (Butt, 1991; Butt, 1992), the Hamaker constant (Larson et al., 1993; Biggs and Mulavaney, 1994; Hartley et al., 1998), hydrophobicity/hydrophilicity (Ducker et al., 1994), and contact angle (Preuss and Butt, 1998b).

2.2. Colloidal Interaction Forces

2.2.1. Van der Waals Forces

The van der Waals Force between atoms and molecules is the sum of three different forces: (a) the Keesom force, (b) the Debye force, and (c) the London force

(Israelachvili, 1992). All of these forces are proportional to $1/r^6$ (r is the distance between the atoms or molecules).

(a) The Keesom force, an orientation force, is the dipole–dipole interaction between two atoms or molecules. The corresponding potential is (Israelachvili, 1992)

$$V_K(r) = -\frac{u_1^2 u_2^2}{3(4\pi\varepsilon_o\varepsilon)^2 k_B T r^6} = -\frac{C_K}{r^6} \tag{2.1}$$

where V_K is the Keesom potential, u_1 and u_2 are the dipole moments of the molecules, ε_o is the vacuum dielectric constant, ε is the dielectric constant of the medium, k_B is the Boltzmann constant, T is the temperature, and C_K is the Keesom coefficient. This equation is valid when $k_B T > u_1 u_2/4\pi\varepsilon_0\varepsilon r^3$.

(b) The Debye force, an induction force, is the dipole–induced dipole interaction between two atoms or molecules, and its associated potential is (Israelachvili, 1992):

$$V_D(r) = -\frac{u_1^2\alpha_{02} + u_2^2\alpha_{01}}{(4\pi\varepsilon_o\varepsilon)^2 r^6} = -\frac{C_D}{r^6} \tag{2.2}$$

where V_D is the Debye potential, α_{01} and α_{02} are the electronic polarizabilities of the molecules, and C_D is the Debye coefficient.

(c) The London force is also known as the dispersion force. It is the instantaneous dipole–induced dipole interaction and is of quantum-mechanical nature. It is the most dominant force in terms of contribution to van der Waals forces. The London interaction energy is given by (London, 1937):

$$V_L = -\frac{3}{2}\frac{\alpha_{01}\alpha_{02}}{(4\pi\varepsilon_o)^2 r^6}\frac{(h\upsilon_1)(h\upsilon_2)}{h\upsilon_1 + h\upsilon_2} = -\frac{C_L}{r^6} \tag{2.3}$$

where V_L is the London potential, $h\upsilon_1$ and $h\upsilon_2$ are the first ionization potentials of the molecules, h is the Planck constant, and C_L is the London coefficient.

Therefore, the total van der Waals potential (V_{vdW}) is

$$V_{vdW} = -\frac{C_K + C_D + C_L}{r^6}. \tag{2.4}$$

Since the van der Waals force is a result of electric and magnetic polarization and propagation of the electric field, the Hamaker constant, A, depends on the material and the medium. The Hamaker constant, A_{132}, based on the Liftshitz theory for media 1 and 2 interacting across the medium 3 may be expressed in terms of McLachlan equation (1963) as

$$A \cong \frac{3}{4}k_B T\frac{\varepsilon_1 - \varepsilon_3}{\varepsilon_1 + \varepsilon_3}\frac{\varepsilon_2 - \varepsilon_3}{\varepsilon_2 + \varepsilon_3} + \frac{3h}{4\pi}\int_{\upsilon_1}^{\infty}\frac{\varepsilon_1(i\upsilon_n) - \varepsilon_3(i\upsilon_n)}{\varepsilon_1(i\upsilon_n) + \varepsilon_3(i\upsilon_n)}\frac{\varepsilon_2(i\upsilon_n) - \varepsilon_3(i\upsilon_n)}{\varepsilon_2(i\upsilon_n) + \varepsilon_3(i\upsilon_n)}d\upsilon. \tag{2.5}$$

Here, ε_1, ε_2, and ε_3 are the dielectric constants of the three media, and $\varepsilon(i\upsilon)$ is the dielectric constant at the imaginary frequency axis $i\upsilon$. The first term is the zero-frequency energy of the van der Waals interaction and includes the Debye and Keesom forces. The latter is the London dispersion contribution.

The Hamaker constant can be simplified and expressed as

$$A_{132} \approx \pm\sqrt{A_{131}A_{232}}\,, \tag{2.6}$$

or

$$A_{132} \approx \left(\sqrt{A_{11}} - \sqrt{A_{33}}\right)\left(\sqrt{A_{22}} - \sqrt{A_{33}}\right), \tag{2.7}$$

where A_{11} is for media 1 and 1 interacting across vacuum.

2.2.2. Double-Layer Forces

Surfaces with high dielectric constant are usually charged when they are immersed in water. The charging mechanisms may occur via ionization or dissociation of surface groups, or via adsorption of ions from the solution. The final surface charge is balanced by an oppositely charged stagnant region of counterions, which is adjacent to the surface within the Stern layer (Figure 2.1), and by a cloud of ions in rapid thermal motion after the first layer. The combination of these two layers is known as the diffuse electrical double layer. The simplest way to express the double-layer force is through the Poisson–Boltzmann equation, the combination of the Poisson equation and the Boltzmann distribution of counterions.

$$\frac{d^2\psi}{dx^2} = \frac{2\bar{e}zN_o}{\varepsilon}\sinh\left(\frac{z\bar{e}\psi}{k_BT}\right) \tag{2.8}$$

When charged particles move closer to each other, the diffuse layers are overlapping. These diffuse layers regulate the interaction between particles. As a result, the potential at the Stern layer plays a more important role in colloidal interaction than the potential at the particle surface. However, there are some difficulties in determining the Stern layer potential. Therefore, a better way to express the electrostatic double-layer interaction is through the zeta potential, which is established through the motion of particles in an electric field (e.g., Hiemenz and Rajagopalan, 1997).

Derjagiun and Landau (1941) and Verwey and Overbeek (1948) established the DLVO theory to describe both the magnitude and range of the double-layer force, which are determined by the surface potential and the double layer thickness. Surface potentials can be affected by the ionic strength and the adsorbing counterions in the system. On the other hand, the double layer thickness depends on the concentration and valence of the counterions in the solution. The theory demonstrates that higher ionic strength can lead to higher counterion concentration in the diffuse layer, which subsequently decreases the thickness of the diffuse layer.

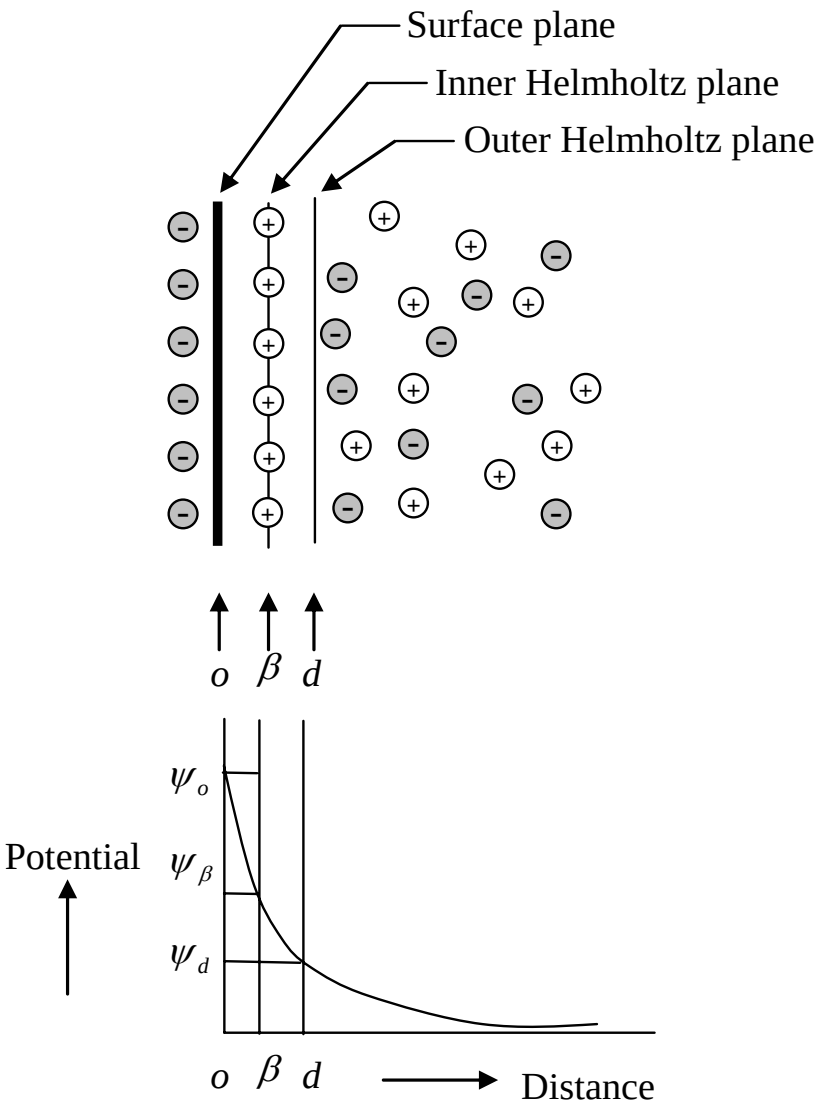

Figure 2.1. Schematic of the electrical double layer.

2.2.3. Solvation Forces

The DLVO theory cannot describe the reciprocal interaction of two surfaces approaching at distances of less than a few nanometers due to the limitations in its application at small separations, as well as the presence of other short-range forces. These surface forces, which include solvation forces, hydration forces, hydrophobic forces, and steric forces, are known as non-DLVO forces.

Solvation forces occur when the solvent density is changed as the liquid molecules are coerced to order in almost distinct layers between the two interacting surfaces. Usually, these forces exhibit an oscillatory behavior.

2.2.4. Hydration Forces

Hydration forces arise when water molecules strongly bind to hydrophilic surfaces. The strength of the forces depends on the energy needed for disrupting the hydrogen-bonding network and/or dehydrating two surfaces as they approach each other. These forces are always repulsive and present an exponential decrease with separation distance. However, the origin of the exponential decay is still unknown.

There are two types of hydration forces. The first one is a steric hydration force between fluid-like amphiphilic surfaces. This is a very strong short-range force that arises from the overlap of the excited chain and headgroup, which extended from the amphiphilic surfaces as they move closer to each other. The second force is a long-range repulsive hydration force between solid crystalline hydrophilic surfaces such as silica, mica, and certain clays. This force occurs when strong hydrogen-bonding surface groups

modify the hydrogen-bonding network of liquid water molecules adjacent to them. The strength and range of the forces increase with the hydration number of the cations.

2.2.5. Hydrophobic Forces

A hydrophobic interaction is a long-range attractive force, and its origin is still unknown. However, it is found to arise when the surfaces, which cannot bind to water molecules via ionic or hydrogen bonds, approach each other (Israelachvili, 1992). The hydrophobic force can be much stronger than the van der Waals attraction when the Hamaker constant of the system is quite small. The magnitude of the hydrophobic force decreases with the decrease in hydrophobicity of the interacting surfaces.

2.2.6. Steric Forces

When two surfaces covered with chain molecules approach each other, the chains extend out into the solution and overlap each other. At this point, the surface will experience a repulsive force due to the unfavorable entropy associated with the compression of the chains between the surfaces. In the case of polymers, this force is known as steric force.

2.3. Atomic Force Microscopy (AFM)

The atomic force microscope (AFM) (Figure 2.2) was invented in 1986 by Binnig, Quate, and Gerber. It uses a sharp tip to scan the surface of a sample. The tip is mounted at the end of a cantilever, which bends in respond to the force exerted on the tip by the sample.

AFM consists of two main modules (Figure 2.3). The first module consists of the piezoelectric scanner that moves the sample in the X, Y, and Z directions. The second module is called the AFM detection system. This system includes a laser source, a cantilever, a mirror, a photodiode, a photodetector, and computer control. The laser is focused onto the back of the reflective cantilever. As the tip scans the surface of the sample, the laser beam is bounced off the cantilever into the photodiode. The difference in light intensities between the upper and lower photodiodes is sent to the photodetector, and the signal is then sent off to the computer control feedback loop. The feedback loop attempts to keep the cantilever deflection constant by maintaining a constant distance between the cantilever and the sample. This can be done by moving the scanner at each (X, Y) position in the Z direction, hence, adjusting the voltage applied to the scanner. The voltage, then, is converted to a cantilever deflection. The standard cantilever tips are typically Si_3N_4 or silicon.

Figure 2.2. Digital Instrument MultiMode™ AFM.

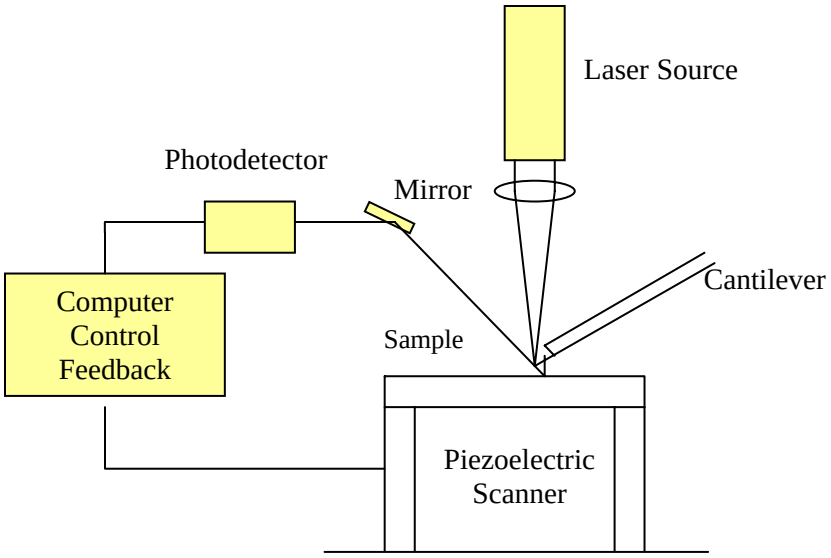

Figure 2.3. Schematic of an atomic force microscopy setup.

2.3.1. Anatomy of a Force Curve

At the beginning (Figure 2.4), the probe tip is far away from the sample surface (A). However, if the tip experiences a long range attractive or repulsive force, it will deflect downwards or upwards before making contact with the surface. As the cantilever tip approaches the surface, the cantilever enters the range of surface forces and may jump into contact if it experiences a sufficient attractive force from the sample (B). Once the tip touches the surface (C), the fixed end of the cantilever still moves closer to the surface producing an increase in the cantilever deflection until retraction starts. The process is reversed when the cantilever reaches a desired force value (D). As the cantilever is withdrawn, adhesion or bonds formed during contact with the surface may cause the cantilever to adhere to the sample some distance past the initial contact point on the approach curve. At this point (E), the adhesion is broken, the cantilever is set free from the surface and the cycle may start again.

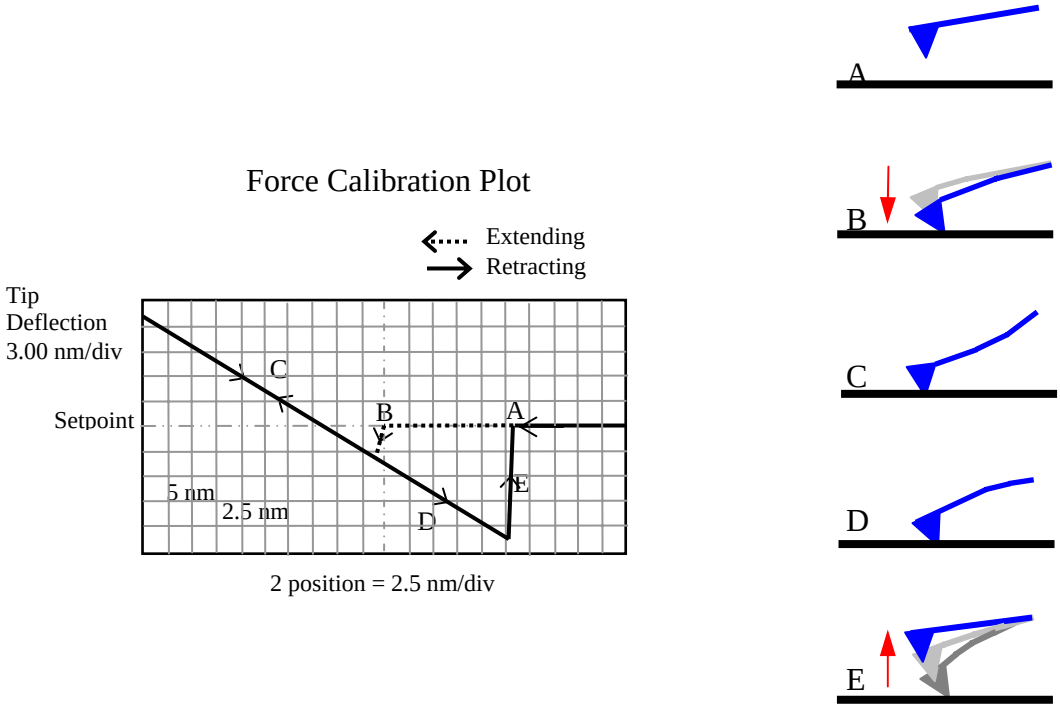

Figure 2.4. Anatomy of force curve.

2.3.2. Principles of AFM and Data Analysis

AFM controls the movement of the sample by applying a voltage to the piezoelectric tube, while the deflection of the cantilever is monitored using a laser beam. The beam is focused at the end of the cantilever and reflected to a photodiode. Deflection-versus-displacement data are converted to ASCII format by the NanoScope software (Digital Instruments, Santa Barbara, CA) and imported into a spreadsheet program. In order to obtain a force-versus-separation curve, the zero values for force and distance are defined. The zero value for force is set at the point for which the deflection is constant. Zero distance was determined to be the position at which the deflection of the tip was the same as the displacement of the sample. The force is then calculated by means of Hooke's law,

$$F = kx \tag{2.9}$$

where F is force, k is the spring constant, and x is tip deflection. The separation distance is the sum of the tip deflection and the sample displacement.

2.3.3. Force Volume AFM

Force volume imaging mode is the technique in which force plots are measured across the surface of a sample at regular intervals. In each X–Y position, there is a cumulative force curve in the Z direction for a selected interacting area. In this imaging mode, an electronic feedback loop maintains the forces between the tip and the sample at a specified setpoint instead of maintaining a constant separation distance.

2.3.4. Studies on Surface Interactions by AFM

AFM has been a useful tool in several fields of research, such as surface science, materials engineering, biochemistry, and biology. AFM force–distance curves are very important in the study of surface interactions with both theoretical and practical implications. Besides rendering images of surface with nanoscale resolution, AFM has been used extensively in direct measurement of interaction forces between approaching surfaces such as particle–particle (Larson et al., 1993; Veeramasuneni et al., 1996), particle–plate (Larson et al., 1995; Li et al., 1993; Considine et al., 2000a), and particle–bubble (Snyder et al., 1997; Wangsa-Wirawan et al., 2001). These forces were measured between similar as well as dissimilar surfaces.

Influences of solution conditions such as pH and ionic strength were investigated (Chin et al., 2002; Ducker and Senden, 1992; Li et al., 1993). The measured force was discovered to decay exponentially with distance when the ionic strength increases and the pH decreases. The comparison between experimental data and the prediction of the Poisson–Boltzman equation (Ducker and Senden, 1992; Toikka and Hayes, 1997), as well as DLVO theory was performed in some cases (e.g. Chin et al., 2002; Larson et al., 1995). A good agreement was clearly shown in those studies. The type of solution also plays a role in the interfacial forces. For example, alcohol was found to suppress the long-range electrostatic repulsive force and enhance the attractive force with increasing weight fraction of alcohol (Kanda et al., 1998).

AFM has been used to examine both DLVO forces and non-DLVO forces (Rabinovich and Yoon, 1994; Nalaskowski et al., 1999; Adler et al, 2001). For instance,

the interaction between bacteria and the silicon nitride surface of the AFM tip was dominated by steric force (Camesano and Logan, 2000). The steric force and the thickness of polymer layers on the surface of the bacteria were affected by the solution pH. A repulsive hydration force was found to exist between similarly charged hydrophilic particles, while attractive forces exist between oppositely charged hydrophilic particles in solutions of high ionic strength (Veeramasuneni et al., 1998). Both short- and long-range hydrophobic attractive forces were analyzed by Rabinovich and Yoon (1994) and Nalaskowski et al. (1999), but with different systems.

AFM can also be used to evaluate surface charge density. Based on the force measurements between silica and α-alumina surfaces for different solution pH, the zeta potential was found to be in agreement with the values obtained from direct electrokinetic measurements (Veeramasuneni et al., 1996). A similar work was conducted by Butt (1992), who used AFM to determine the local surface charge densities of plasma membranes of *Halobacterium halobium* in electrolyte solutions. His previous work (Butt, 1991) revealed that the electrostatic force increases with increasing surface charge density and decreases roughly exponentially with distance. It can be reduced by imaging in high salt concentrations. The electrical double layer was also examined (Hüttl et al., 1997; Ishino et al., 1994). A repulsive force due to overlapping of the electrical double layers of similar approaching surfaces in intermediate-pH aqueous electrolyte solutions was observed (Toikka and Hayes, 1997).

Information obtained from AFM measurements including the surface charge densities (Butt, 1992; Hartley et al., 1998), steric interaction (Considine et al., 2000a; Camesano and Logan, 2000), and the functional groups on surfaces (Ishino et al., 1994;

Frisbie et al., 1994) is helpful for determining the structure of biological macromolecules and understanding their functions through interparticle forces. In addition, AFM has been successfully employed to determine the Hamaker constant in various systems (Larson et al., 1993; Biggs and Mulvaney, 1994; Hartley et al., 1998) and to evaluate the roughness of interfaces (Crossley et al., 1995; Nalaskowski et al., 1999).

Studies of the surface force between colloidal probes and air–bubble interfaces have attracted attention in the past decade. A repulsive force was observed between a hydrophilic particle and a bubble, while the force between a hydrophobic particle and a bubble was strongly attractive (Butt, 1994; Fielden et al., 1996; Considine and Drummond, 2000b). The dependence of particle–bubble interactions on surfactant molecules was also studied (Ducker et al, 1994; Preuss and Butt, 1998a). The force between a hydrophobic particle and an air–bubble interface was found to become repulsive when surfactant was added to the aqueous solution. The contact angle and adhesion force also decreased simultaneously. For hydrophilic particles, different behaviors were observed depending on the adsorption of the surfactant on the particle surface.

Besides particle–bubble interactions, surface interaction forces for oil–particle (Snyder et al., 1997), oil–water (Hartley et al, 1999), and protein inclusion bodies with bubbles (Wangsa-Wirawan et al., 2001) were also determined. AFM was also applied to measure the contact angle (Ducker et al, 1994; Preuss and Butt, 1998b).

AFM can be applied in order to obtain “force images” from the surface, which means that data of force profiles at different points on the surface can be directly associated with topographic characteristics. The charged state and spatial distributions of

functional groups on the substrates can thus be evaluated in various solution conditions (Ishino et al., 1997; Hartley et al., 1998). Besides mapping biological materials such as bilayer membranes and DNA molecules (Hartley et al., 1998; Johnson et al., 2003), this approach can be used to study surfaces that are modified with polyelectrolyte and metal species (Kramer et al., 1998; Estel et al., 2000; Miyatani et al., 1997; Miyatani et al., 1998).

Using AFM to study changes in topography and surface forces as a result of sorption was recently reported. The type and concentration of both electrolyte solutions and surfactant were shown to have an effect on the structure of surfactant molecules adsorbed onto the surface and also on the sorption behavior (Rabinovich et al., 1994; Xu et al., 1996; Bremmell et al., 1999; Nalaskowski et al., 1999; Liu et al., 2001; McNamee et al., 2001). The structure transformation of a mixture of two surfactants having different surface-aggregate structures was investigated by Ducker and Wanless (1996). The shape of aggregates at interfaces can be controlled by the mole fraction of surfactant in the bulk solution. Changes in the electrokinetic properties of surfaces due to the adsorption of surfactant were quantitatively performed (Whitby et al, 2001).

Temperature is an important parameter when determining the structure of adsorbed surfactant molecules (Liu and Ducker, 1999; Gadegaard et al, 1999). Binding-site competition between cations in the electrolyte solution and cationic surfactant was observed (Ducker and Wanless, 1999). Protons were found to produce more defects in the aggregate of surfactant than potassium ion. The presence of surfactant slowed adsorption of hydrogen ions, but had no effect on potassium ions. AFM provides not only information on force changes due to sorption of surfactant, but also images of the

structure of macromolecules, such as copolymer (Gadegaard et al, 1999) and blend components (Karim et al., 1999).

In this study, AFM is used as a tool to investigate sorption kinetics of metal ions by a single silica particle, electrosorption of surfactant molecules by an externally charged surface, as well as charge distribution on a silica surface. These studies are necessary to better understand natural systems and to devise technologies that can reduce concentrations of metal ions and particulates in waters.

CHAPTER 3

MODIFICATION OF SURFACE FORCES BY METAL ION SORPTION

3.1. Objectives

The study of metal ion sorption using only a single particle is performed by means of atomic force microscopy (AFM). The interaction force between a silica probe and a glass plate with the presence of metal ions in solution is monitored as a function of time. The effects of solution ionic strength and concentration of metal ions are determined. Further investigation to find the maximum concentration that has no effect on the original force is conducted. AFM force measurements are compared with the calculations using the Derjaguin–Landau–Verwey–Overbeek (DLVO) theory.

3.2. Introduction

Sorption plays an important role in both natural waters as well as in water treatment processes and is one of the techniques used to remove metal ions from aqueous solutions. Uptake of metal ions from aqueous solution, however, is limited by interactions between ions and surfaces in contact with the solution. Moreover, fate and transport of metal ions are controlled by their reactions with surfaces at the solid/liquid interface. For example, inorganic colloids such as clays, metal oxides, and carbonates have been reported as effective sorbents of metal ions through ion exchange and surface

complexation reactions (Dzombak and Morel, 1987; Shuman, 1988; Zachara et al., 1989). It is also noted that surface properties of the sorbent, such as surface charge and electrical double layer, change continuously during sorption of metal ions (Subramaniam et al., 2001; Chin et al., 2002). As a result, physical transport, chemical reactivity, and/or bio-availability of the pollutants are altered during the sorption process.

Earlier studies have shown that sorption of ions from aqueous solutions by colloidal particles affects colloidal stability, mobility, and reactivity (James and Healy, 1972a; James and Healy, 1972b; Dzombak and Morel, 1990; Liang and Morgan, 1990; Crawford et al., 1996; Stumm and Morgan, 1996; Colic et al., 1998). This sorption process also has significant influences on interparticle forces and the zeta potential of the colloidal sorbent. In most cases, reactions of metal ions with functional groups on the surface of the particles are time dependent (Yiacoumi and Tien, 1995). A quantitative understanding of the changes in surface properties caused by chemical interactions between the particles and the ions present in the surrounding environment is critical for the prediction and control of the behavior of colloidal systems. This knowledge can be obtained by using AFM that provides direct and real-time measurements of colloidal forces during sorption of ions.

Previous studies (Subramaniam, 2000; Chin, 2002) showed a qualitative agreement in transient behavior of charge reversal of copper uptake by silica between a macroscopic batch experiment and AFM measurements. However, a much stronger charge reversal monitored by AFM measurements was observed due to a high ratio of copper concentration to silica particle concentration. An agreement between the measured forces by AFM and the DLVO theory suggested that the transient zeta potential

of silica particle during sorption of copper ions can be reliably determined by representing the direct force measurements with the DLVO theory. This method provided a way to measure the zeta potential of particles that cannot be directly measured under low colloidal concentration.

The extent of metal ion sorption by colloidal particles is strongly influenced by several factors such as solution pH, ionic strength, size and type of the substrate, concentration of metal ions and particles, reaction time, and temperature (Subramaniam et al., 2001). In this study, an AFM is employed to elucidate the influences of ionic strength and concentration of metal ions on sorption and colloidal behavior.

3.3. Materials and Methods

3.3.1 Colloidal Probe Preparation

In this part of the work, 3-μm silica particles with a density of 1.96 g cm^{-3} from Bangs Laboratories, Inc. (Fishers, IN), were used as colloidal probes. The particles were nonporous and had hydroxyl (–OH) surface groups. A silica particle was glued to the end of a tipless contact-mode cantilever (Digital Instruments, Santa Barbara, CA) with epoxy (ITWDevcon, Danver, MA) by means of a micromanipulator and a camera/monitor system. Two sharp-tip needles were attached to the micromanipulator. The first one was used to transfer epoxy glue to the end of the cantilever, and the second was used to pick up a silica particle and place it on the top of the epoxy. Consequently, the free surface of the colloidal probe is glue free.

The spring constant is a critical factor in the conversion of deflection data to force and can be estimated from the geometry, mass, and Young's modulus of a cantilever

(Rabinovich and Yoon, 1994; Veeramasuneni et al., 1996; Veeramasuneni et al., 1998). In order to have more accurate force data, the spring constants of cantilevers were verified by using the "cantilever tune" function in AFM. The resonant frequencies were measured before and after a particle was glued on the cantilever. The resonant frequency of a cantilever changes after an additional mass is loaded. The mass of the added particle, *M*, was calculated from its density reported by manufacturer. Particle size was determined by scanning electron microscopy (SEM). The spring constant of the cantilever, *k*, was then calculated by the method of Cleveland et al. (1993):

$$k = (2\pi)^2 \frac{M}{\left(1/\nu^2\right) - \left(1/\nu_0^2\right)} \tag{3.1}$$

where ν_0 and ν are the resonant frequencies of a cantilever before and after the loading of particle, respectively. The cantilever with 3-μm silica particle tip is shown in Figure 3.1.

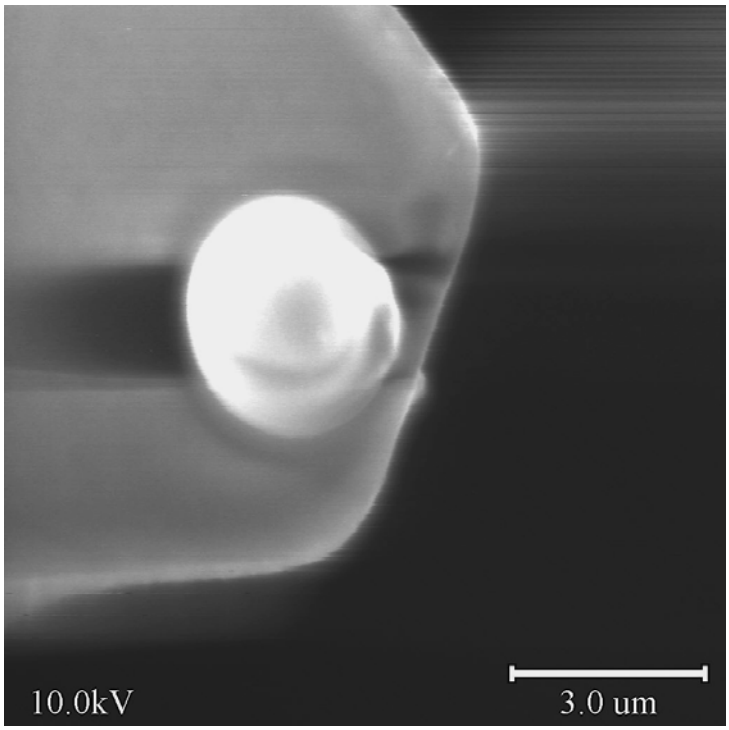

Figure 3.1. A 3-μm silica particle tip is shown in the SEM photomicrograph.

3.3.2. Sample Preparation

The substrate was a nonsorptive borosilicate glass coverslip. The glass coverslips (Ted Pella, Inc., Redding, CA) were cleaned by soaking them overnight in a 1-N HCl solution (Fisher Scientific, Fair Lawn, NJ). They were then immersed in acetone (Aldrich, Milwaukee, WI) for 30 min, boiled in a mixture of $5H_2O$:$1H_2O_2$:$1NH_4OH$ at 85°C for 25 min, washed with chromic acid (LabChem Inc., Pittsburgh, PA) for 25 min, and then reimmersed in water. This cleaning procedure was reported by Nalaskowski et al. (1999) who tested its efficiency by contact angle measurements and found that the surfaces were fully wettable by water. Glass substrates also underwent plasma cleaning (model PDC-32G, Harrick Scientific Corp., Ossining, NY) before being used to remove any residual organic contaminants. No residues were detected on the surfaces by AFM. The smoothness of the surface was determined by AFM images obtained using a silicon nitride tip (Digital Instruments, Santa Barbara, CA). Water of 18-MΩ/cm resistivity at 25°C was prepared by an E-pure system (model D4631, Barnstead Thermolyne Co., Dubuque, IA).

The zeta potential measurements of the silica particles and the glass coverslips were carried out using a ZetaPlus zeta potential analyzer (Brookhaven Instrument Corp., Holtsville, NY). The coverslips were crushed into a powder and then washed using the same procedure for the glass coverslips. The zeta potential of the crushed glass coverslips was found to be similar to that of silica particles. Similar results were found by Chin (2002), who measured the zeta potentials of the silica particles, the glass beads, and the glass coverslips.

3.3.3. Force Measurements and Data Analysis

Interaction forces between the small probe and the substrate were measured using AFM (model MMAFM-2, Digital Instruments, Santa Barbara, CA). Fresh solutions at different values of ionic strength (as NaCl) and copper concentration [as $Cu(NO_3)_2$] were prepared by using triply distilled 18-MΩ deionized water. Because sorption of copper ions onto silica particles occurs at intermediate pH values (Subramaniam et al., 2001; Chin et al., 2002), all solutions were prepared at pH 5.5. An O-ring was used to seal the fluid cell of the AFM to prevent flooding and to isolate the cell from possible contamination from the ambient environment. Initially, the colloidal probe was immersed in NaCl solution. Then, at the beginning of the sorption experiment, the metal ion solution was manually injected into the cell.

As the substrate moved toward and away from the particle via a piezoelectric tube, the deflection of the cantilever was monitored. Deflection-versus-displacement data were converted to ASCII format by the NanoScope software (Digital Instruments, Santa Barbara, CA) and imported into a spreadsheet program. To achieve a force-versus-separation curve, the zero values for force and distance were defined. The zero value for force was set at the point at which the deflection was constant. Zero distance was determined to be the position at which the deflection of the tip was the same as the displacement of the sample. The force was then calculated by means of Hooke's law, $F = kx$, where F is force, k is the spring constant, and x is tip deflection. The separation distance was the sum of the tip deflection and the sample displacement. Five measurements were averaged in each experiment.

3.4. Theoretical Calculations

3.4.1. Derjaguin–Landau–Verwey–Overbeek (DLVO) Theory

According to the DLVO theory of colloidal stability, the interaction force can be separated into two contributions: a repulsive electrostatic interaction and an attractive van der Waals force (Israelachvili, 1992). The total interaction force, F_{DLVO}, is taken as a sum of these two terms.

$$F_{DLVO} = F_{electrostatic} + F_{vdW} \tag{3.2}$$

where $F_{electrostatic}$ and F_{vdW} refer to the electrostatic and van der Waals components, respectively.

To describe electrostatic interaction force between sphere–flat plate interactions, a linearized form of the Poisson–Boltzmann equation and the Derjaguin approximation was used. The electrostatic interaction force is calculated from

$$F_{electrostatic} = \frac{4\pi\sigma_{silica}\sigma_{glass}R}{\varepsilon\kappa} e^{-\kappa D} \tag{3.3}$$

where σ_{silica} and σ_{glass} are the charge densities of a silica particle and a glass plate, respectively; R is the radius of the particle tip; ε is the permittivity of water; κ is the inverse of the double-layer thickness; and D is the separation distance. The inverse of the double-layer thickness is described as

$$\kappa \equiv 5.552 \times 10^{-6} \sqrt{I / \varepsilon k_B T} \tag{3.4}$$

where k_B is the Boltzmann constant; T is the absolute temperature; and I is the ionic strength.

Within the Derjaguin approximation, a simple expression for the nonretarded van der Waals forces, is given by

$$F_{vdW} = -\frac{AR}{6D^2} \tag{3.5}$$

where A is the Hamaker constant.

The total force is

$$F_{DLVO} = \frac{4\pi\sigma_{silica}\sigma_{glass}R}{\varepsilon\kappa} e^{-\kappa D} - \frac{AR}{6D^2} \tag{3.6}$$

The measured zeta potentials of sphere and substrate were converted to surface charge densities by using the Grahame equation (Hiemenz and Rajagopalan, 1997) and assuming that the zeta potential is the same as the surface potential:

$$\sigma = 0.117[I]^{1/2} \sinh(\psi_0 / 51.4) \tag{3.7}$$

where ψ_0 is the surface potential in mV and the surface charge density, σ, is expressed in C m^{-2}. This model is based on the assumption that the surface charge remains constant as

the two surfaces approach each other. Previous studies (Larson et al., 1993; Li et al., 1993; Veeramasuneni et al., 1996) showed that the constant-surface-charge assumption is better than the constant-surface-potential assumption because of the large changes of surface potential as the two double layers interpenetrate. In addition, Chin (2002) also proved that the constant-surface-charge model can correctly describe the AFM force measurements using the same system employed in this study.

3.4.2. Hamaker Constant

Based on Lifshitz theory (Hiemenz and Rajagopalan, 1997), the Hamaker constant (A) can be determined using the following expressions:

$$A_{12} \approx \sqrt{A_{11}A_{22}} \tag{3.8}$$

$$A_{131} \approx A_{313} \approx A_{11} + A_{33} - 2A_{13} \tag{3.9}$$

$$A_{131} \approx \sqrt{A_{11}} - \sqrt{A_{33}} \tag{3.10}$$

$$A_{132} \approx \pm\sqrt{A_{131}A_{232}} \tag{2.6}$$

$$A_{132} \approx \left(\sqrt{A_{11}} - \sqrt{A_{33}}\right)\left(\sqrt{A_{22}} - \sqrt{A_{33}}\right) \tag{2.7}$$

where A_{12} is for media 1 and 2 interacting across vacuum, and A_{132} is for media 1 and 2 interacting across the medium 3. The Hamaker constant for silica in water was measured by means of physical property measurements such as Tabor-Winterton approximation, single oscillator, and simple spectral method (Ackler et al., 1996). It was reported to vary from 1.6×10^{-21} J to 3.2×10^{-21} J, therefore, the average value 2.2×10^{-21} J is used here. The Hamaker constant of glass in water, experimentally measured by Rabinovich and Derjaguin (1987), was found to be 1.3×10^{-20} J. Thus, the calculated Hamaker constant for silica and glass in water, $A_{silica\text{-}water\text{-}glass}$ is 5.4×10^{-21} J.

3.5. Results and Discussion

Studies of both equilibrium and dynamics of copper ion uptake by silica particles under various solution conditions are presented here. In all sorption studies, a repulsive force was initially observed, which is attributed to an electrostatic repulsion between the negatively charged silica particle tip and the negatively charged glass surface. As copper ions were introduced into the system, they began to be sorbed onto the surface of the silica particle. Consequently, the surface charge of silica was reversed from negative to positive and the repulsive force was gradually replaced by an attractive force.

In all measurements, the experimental data were compared with theoretical calculations. In non-sorption experiments, the experimentally determined zeta potentials of the silica particles and the glass were used for the theoretical calculations of interparticle forces. On the other hand, the zeta potential of the glass plate was set as a constant value in the calculations since copper ions do not sorb on the glass plate (Chin, 2002), while the one corresponding to the silica particle was determined from the

comparison between experimental data and the calculation results based on the DLVO theory in sorption experiments. In Figures 3.2–3.10, symbols are used to represent force measurements at different times during sorption and the calculated results are represented by lines.

3.5.1. Effect of Metal Ion Concentration

The effect of copper concentration on the interaction force between a colloidal silica probe and a glass substrate was investigated. The forces were measured for solutions of varying copper ion concentration at a background electrolyte concentration of 0.005 M and pH 5.5. In a previous study, Chin et al. (2002) observed an immediate change in the measured force due to sorption of copper ions, with the surface charge of the silica particle being reversed from negative (–48 mV) to positive (2 mV) in 10 min.

Figure 3.2 presents the total measured force for 7.6×10^{-6} M copper concentration, which is 10 times lower than the concentration used by Chin et al. (2002). As shown in this figure, sorption ensued more slowly than in the previous study, with the charge reversal occurring in 60 min. Because the concentration gradient was lower, a longer period of time was required for the surface of the silica particle to be totally sorbed by copper ions. The interaction force reached equilibrium approximately after 160 min. Similar experiments were repeated at the same pH and ionic strength with 1.5×10^{-6} M and 7.6×10^{-7} M copper concentrations, as shown in Figures 3.3 and 3.4, respectively. Sorption of copper ions onto a silica tip took place slowly because of the lower concentration gradient. A time of about 180 min was required for the interaction force to reach equilibrium in the case of 1.5×10^{-6} M copper concentration, while the time required

for the case of 7.6×10^{-7} M copper concentration was 240 min. From these results, it is concluded that as the metal ion concentration is decreased, more time is required for the interaction force to reach equilibrium.

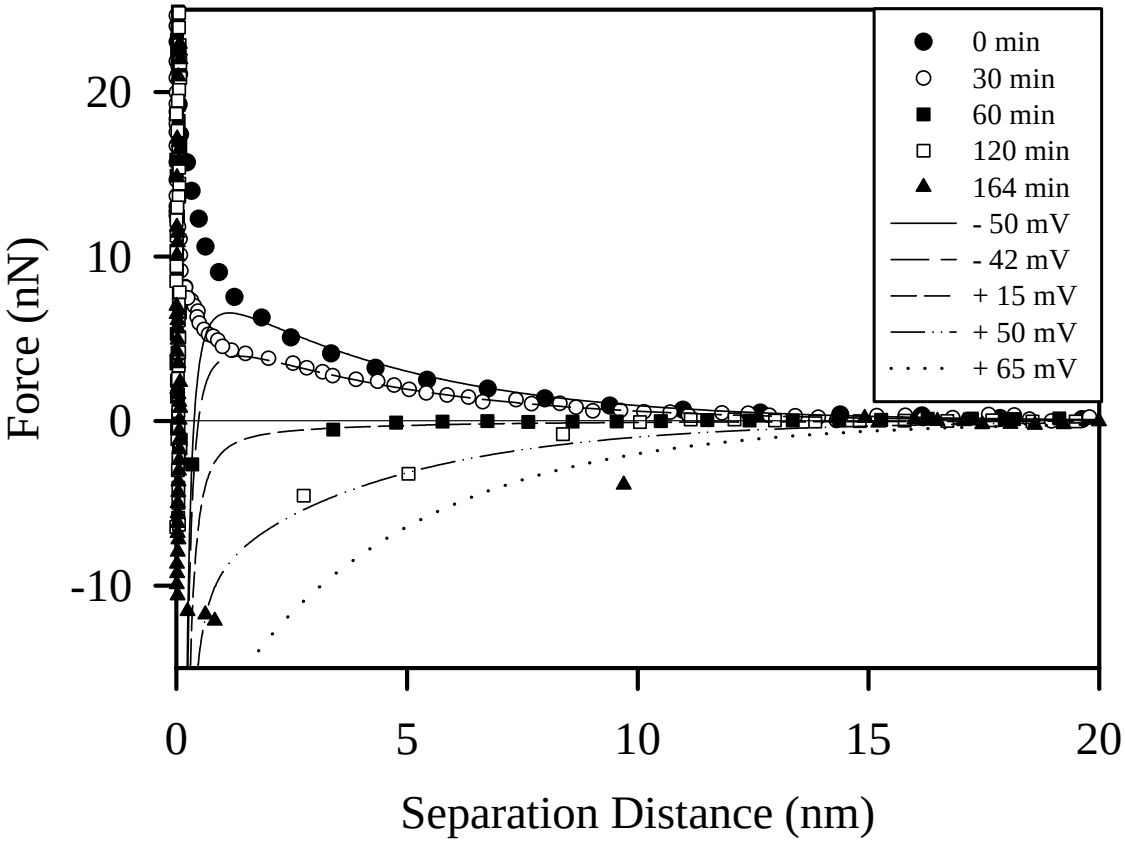

Figure 3.2. Dynamic force-profile measurements during sorption of copper ions by a silica tip. Ionic strength = 0.005 M NaCl, pH = 5.5, copper concentration = 7.6×10^{-6} M, $A = 5.43\times10^{-21}$ J.

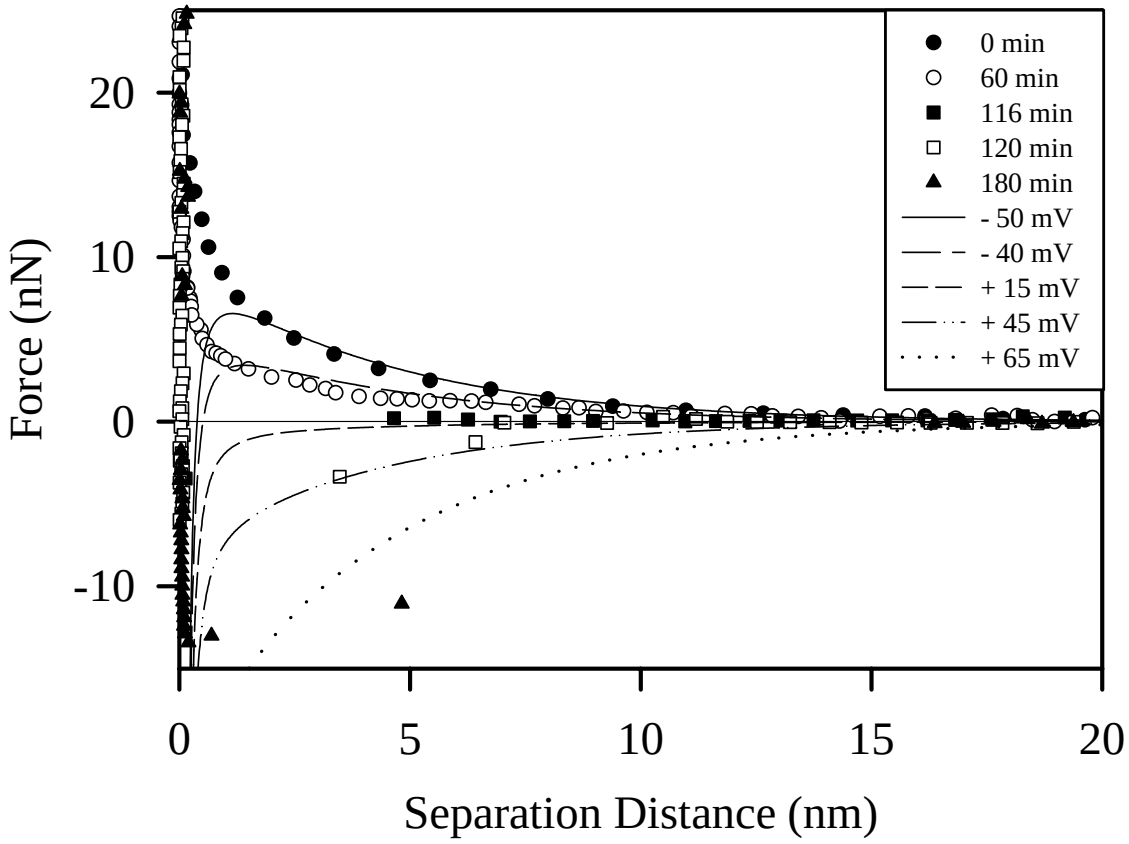

Figure 3.3. Dynamic force-profile measurements during sorption of copper ions by a silica tip. Ionic strength = 0.005 M NaCl, pH = 5.5, copper concentration = 1.5×10^{-6} M, $A = 5.43\times10^{-21}$ J.

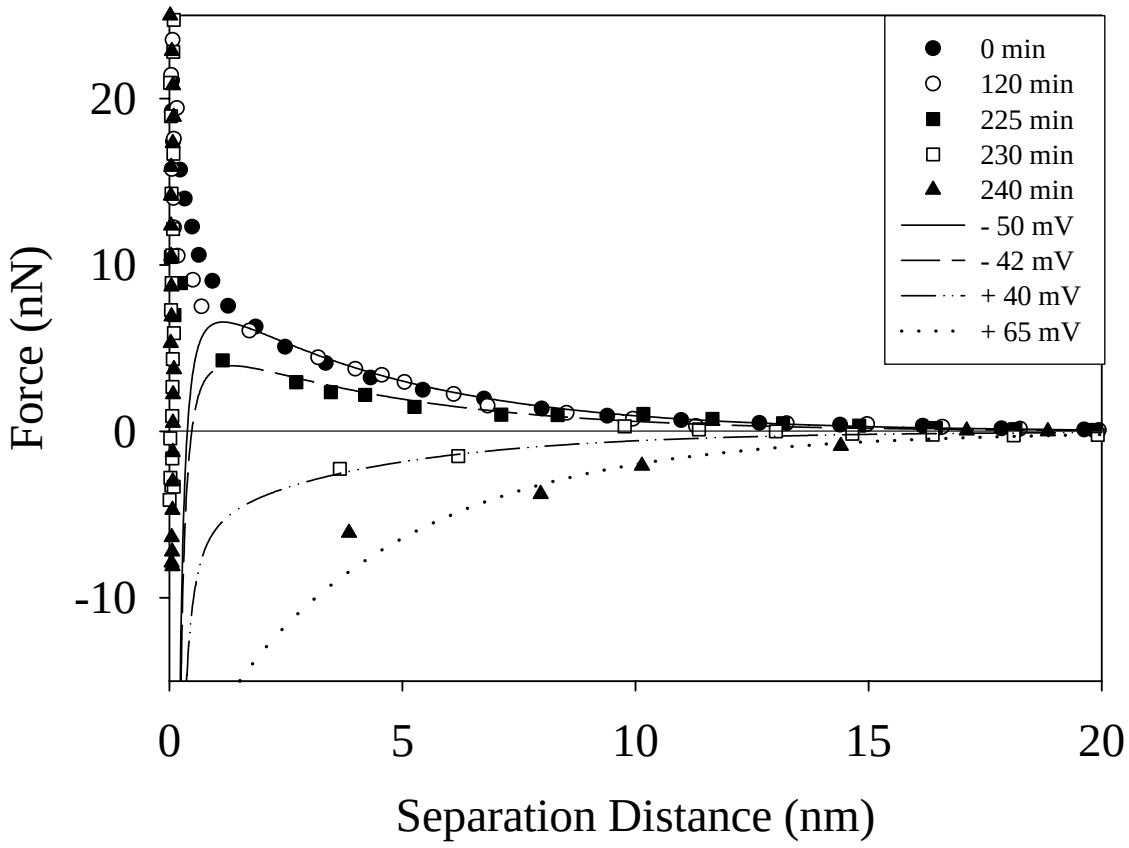

Figure 3.4. Dynamic force-profile measurements during sorption of copper ions by a silica tip. Ionic strength = 0.005 M NaCl, pH = 5.5, copper concentration = 7.6×10^{-7} M, $A = 5.43\times10^{-21}$ J.

A study of metal ion sorption equilibrium using various metal ion concentrations is shown in Figure 3.5. At equilibrium, a strong attractive force was found in all solution conditions, revealing that the surface of the silica particle was fully covered by copper ions. The surface charge was positive in all cases. Therefore, at equilibrium, the surface charges of a silica sphere and a glass plate have opposite signs, which lead to an attractive force. The measured forces for all solution conditions demonstrated the same behavior. The zeta potential of the silica particle at equilibrium was estimated to be +65 mV, which matched the calculated result according to DLVO theory based on Eq. (3.6). This behavior shows that for the concentration range used in these experiments, the metal ion concentration had no effect on sorption at equilibrium, which can be explained by the full monolayer coverage of the sorption sites.

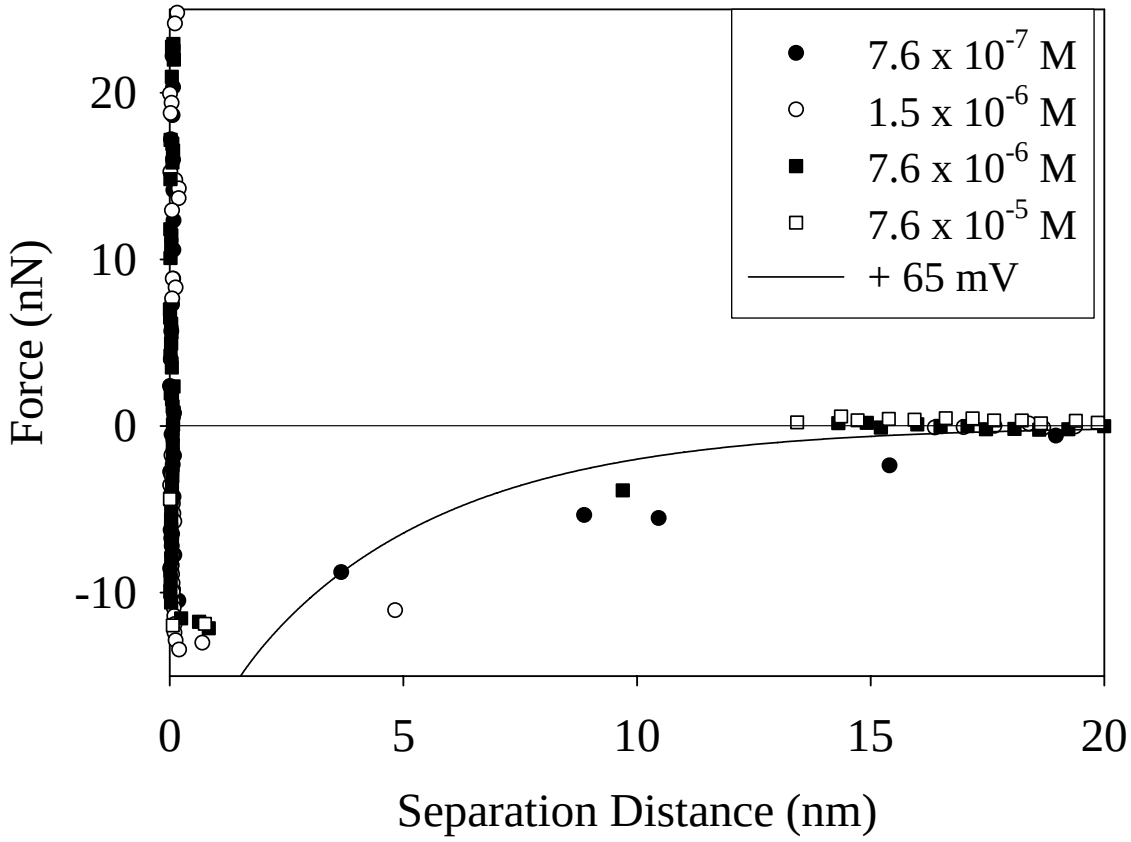

Figure 3.5. Equilibrium state of sorption of copper ions by a silica tip.
Ionic strength = 0.005 M NaCl, pH = 5.5, $A = 5.43\times10^{-21}$ J.

Concentration Limit

An additional experiment was performed, using the same system, in order to find the maximum concentration that would not change the interaction force from originally repulsive to attractive, i.e. the detection capacity of the experimental setup. Figure 3.6 shows that, when the concentration decreased to 1.5×10^{-11} M and 1.5×10^{-14} M, the measured interparticle force became weak attraction while the force became repulsive at a copper concentration of 1.5×10^{-16} M. Thus, the maximum concentration that has no effect on the original force is 1.5×10^{-16} M.

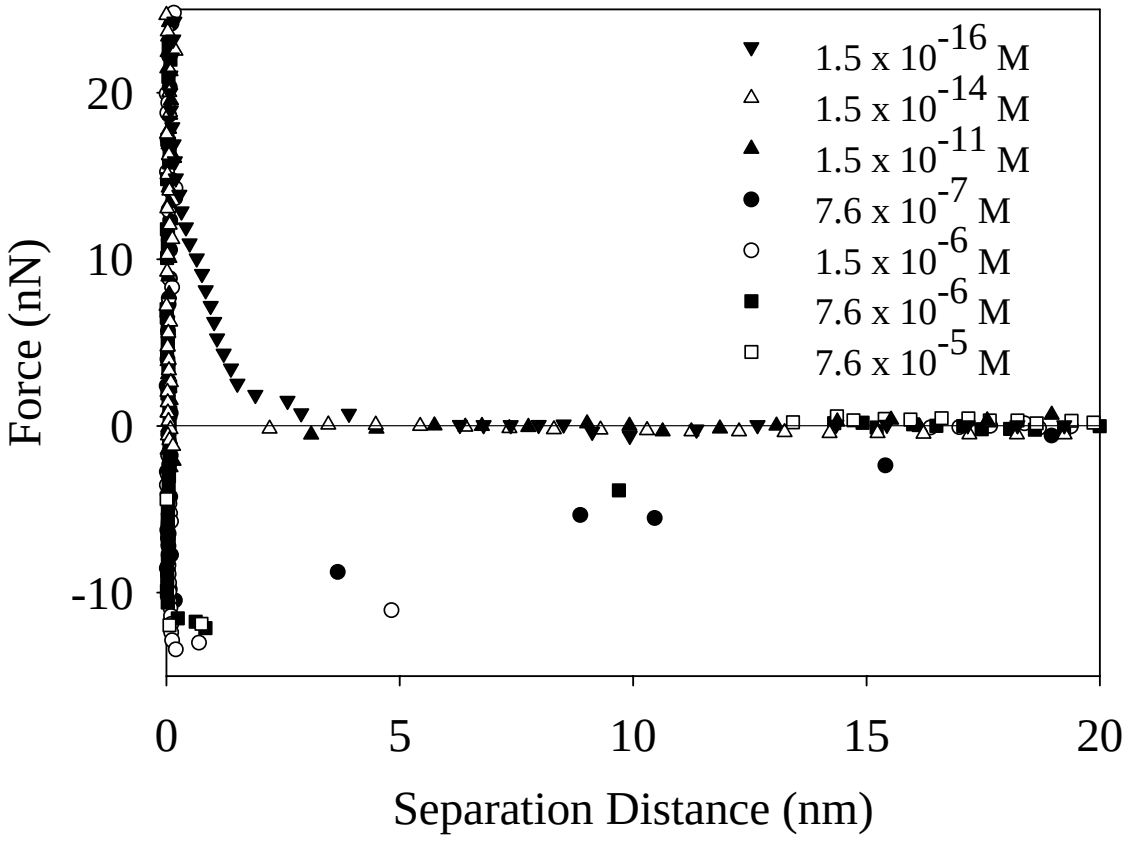

Figure 3.6. Equilibrium state of sorption of copper ions by a silica tip.
Ionic strength = 0.0005 M NaCl, pH = 5.5, $A = 5.43\times10^{-21}$ J.

3.5.2. Effect of Ionic Strength

All sorption experiments were conducted at 7.6×10^{-5} M copper ion concentration and pH 5.5, using different ionic strengths. The force–distance profiles between a silica sphere and a glass plate in a variety of NaCl solutions without copper ions (shown in Figure 3.7) indicate that the magnitude of the electrostatic repulsion decreases with increasing ionic strength. This behavior can be explained by Eq. (3.3), in which the decay length is reduced as the ionic strength is increased due to the compression of the electrical double layer. As the ionic strength is increased, as shown in Eq. (3.4), this value overcomes the repulsion caused by an increase in the surface charge density.

The theoretical calculations of interparticle forces as shown in this Figure were performed using the experimentally determined zeta potentials of the silica particles and the glass. Good agreement between AFM force measurements and the DLVO theory was observed in all solution conditions examined. It is indicated that the constant-surface-charge model can correctly predict the interaction force between two charged surfaces. A discrepancy between experimental data and the DLVO theory at very small separation distances is probably due to non-DLVO repulsion. Similar results were observed by Chin (2002), who employed the constant-surface-charge model to describe the measured interaction force between a silica particle and a glass plate obtaining from AFM.

Figure 3.8 presents the curves for the force-versus-separation distance for the silica/glass system at a copper concentration of 7.6×10^{-5} M in a 0.05 M NaCl solution. This figure clearly shows that sorption is a relatively fast process. Surface charge reversal occurred 2 min after the copper ion solution was introduced into the system, and the system reached equilibrium in approximately 60 min.

Figure 3.9 shows the results of the same experiment performed with the use of 0.0005 M NaCl solution. Although, sorption dynamics are similar to those noted for 0.05 M NaCl solution, a longer period of time elapsed before reversal of the surface charge occurred. A repulsive force was still observed at 2 min after the copper solution was introduced into the system, and the system reached equilibrium in about 60 min.

Equilibrium measurements of the same copper concentration but performed with solutions of different ionic strength are illustrated in Figure 3.10. All force curves exhibited a strong attractive force at equilibrium, confirming the findings of Subramaniam et al. (2001) that ionic strength has no significant effect on sorption equilibria.

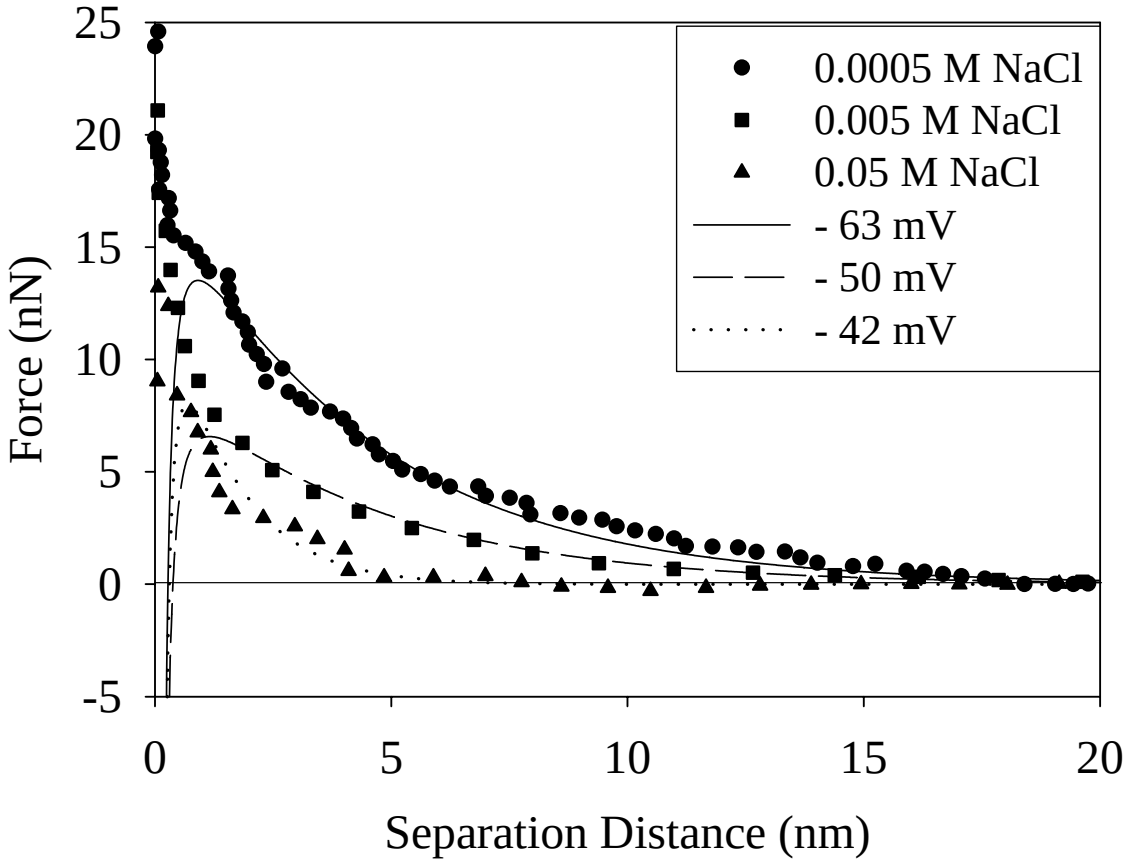

Figure 3.7. Effect of ionic strength on the force-profile measurements at equilibrium. pH = 5.5.

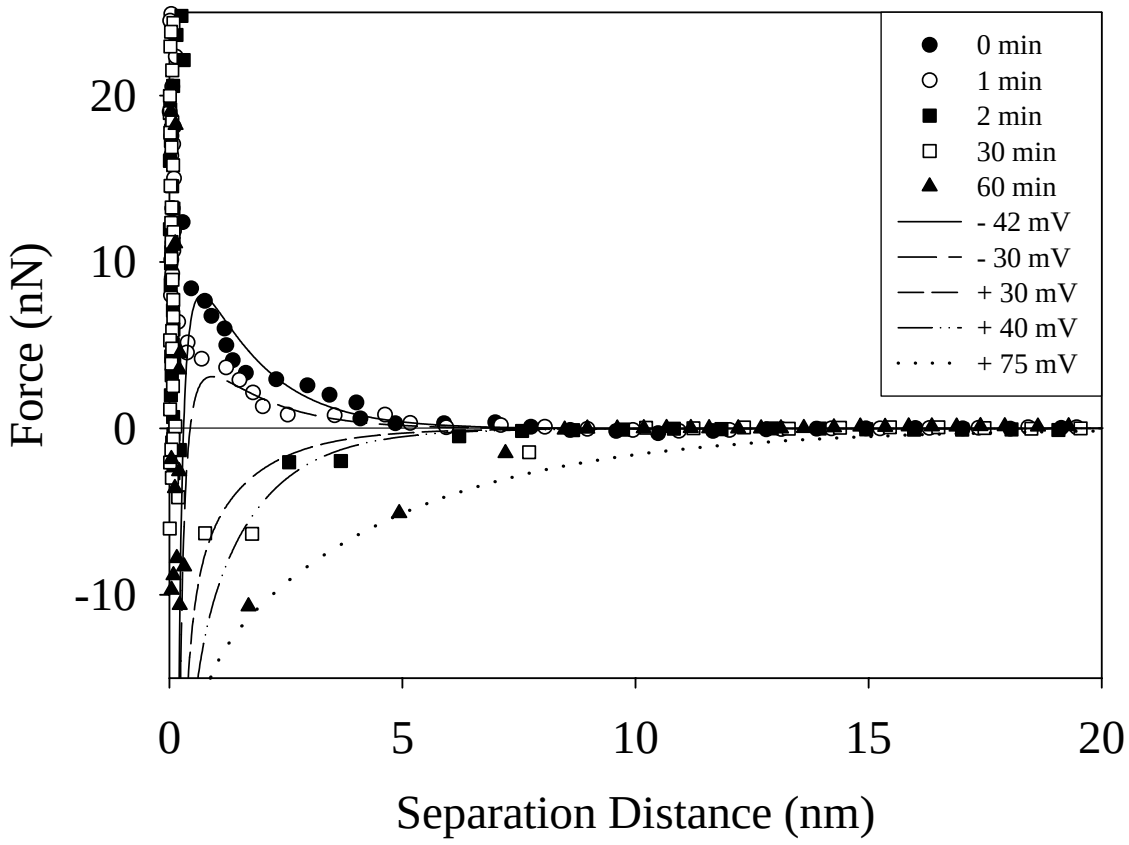

Figure 3.8. Dynamic force-profile measurements during sorption of copper ions by a silica tip. Ionic strength = 0.05 M NaCl, pH = 5.5, copper concentration = 7.6×10^{-5} M, $A = 5.43\times10^{-21}$ J.

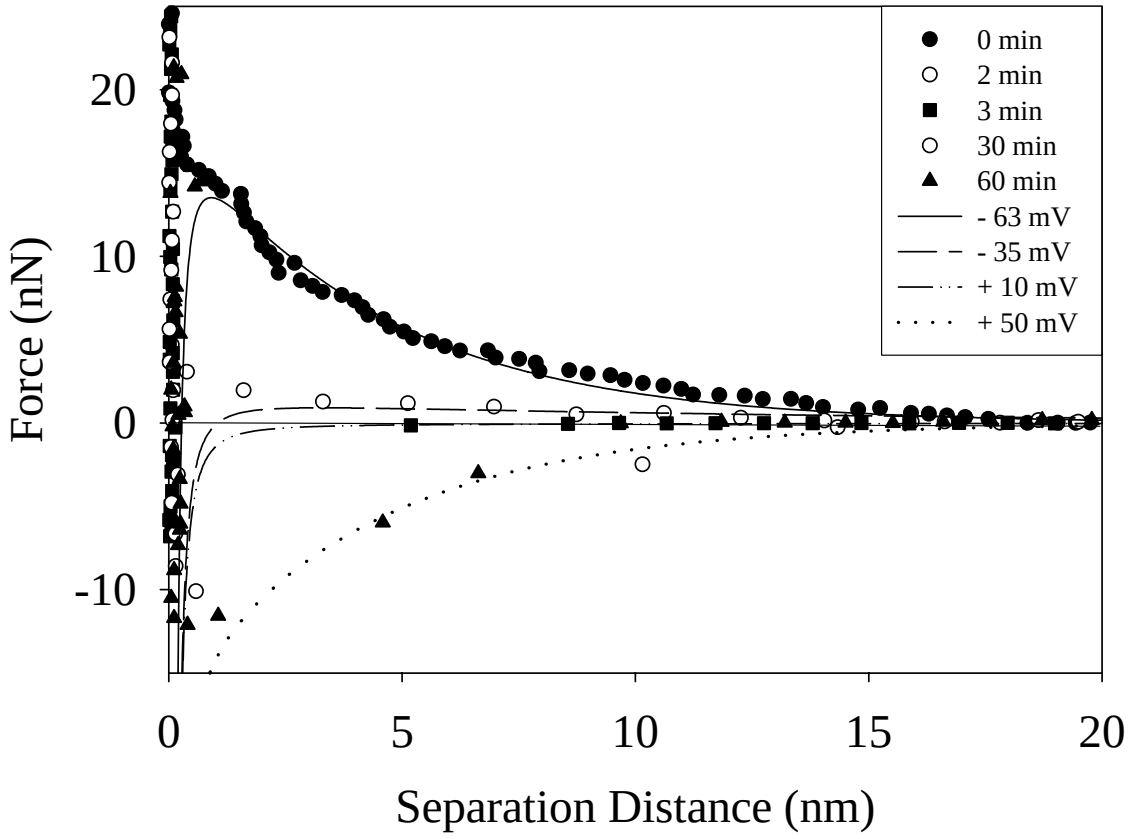

Figure 3.9. Dynamic force-profile measurements during sorption of copper ions by a silica tip. Ionic strength = 0.0005 M NaCl, pH = 5.5, copper concentration = 7.6×10^{-5} M, $A = 5.43\times10^{-21}$ J.

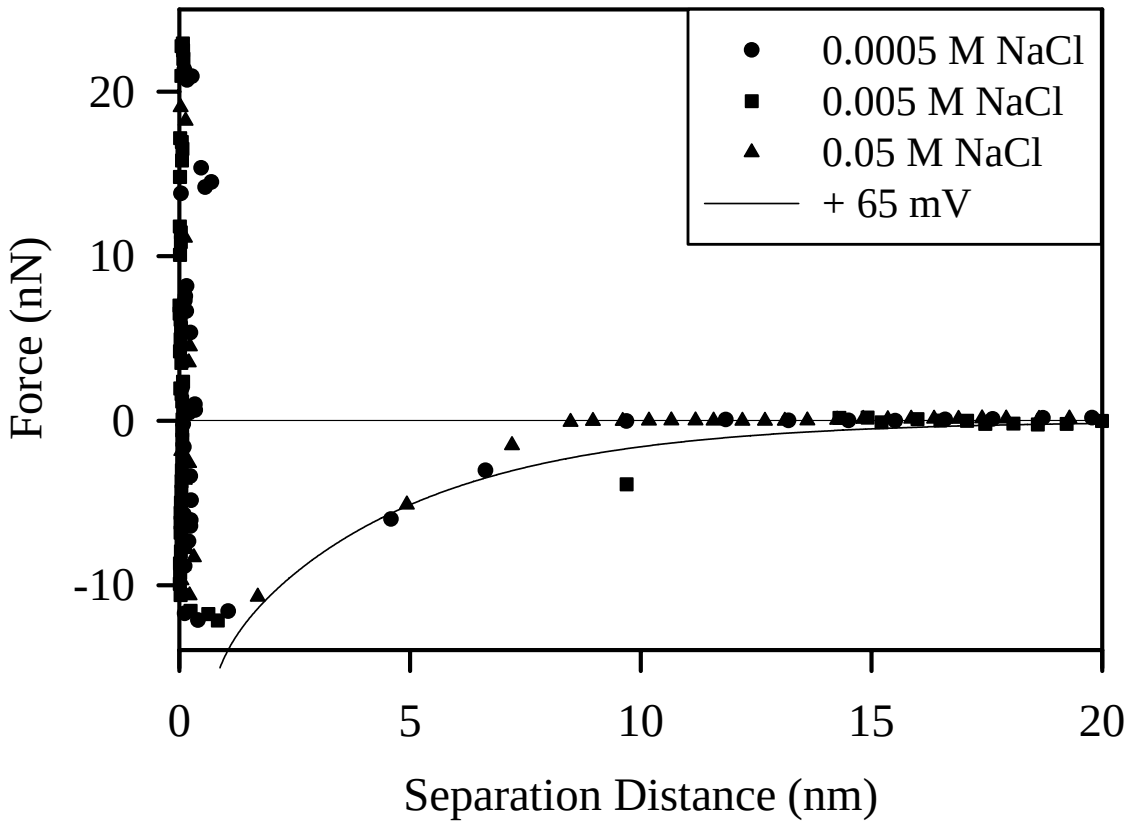

Figure 3.10. Equilibrium state of sorption of copper ions by a silica tip. pH = 5.5, copper concentration = 7.6×10^{-5} M, $A = 5.43\times10^{-21}$ J.

3.6. Summary

AFM is used to investigate the influence of metal concentration and ionic strength on metal ion sorption. Changes in interaction forces as a function of time demonstrate surface charge reversal; hence, sorption did occur. This study shows that metal concentration has an effect on sorption dynamics, with decreases in metal ion concentration causing charge reversal to occur more slowly and the system to require a longer period of time to reach equilibrium. The maximum concentration that has no effect on the original force is found. The ionic strength has no significant effect on sorption kinetics. In addition, neither metal concentration nor ionic strength exhibits any effect on sorption equilibria, indicating that for the experimental conditions used in this study, the surface sites of the silica particle are fully covered by copper ions.

CHAPTER 4

SURFACE CHARGE MAPPING BY ATOMIC FORCE MICROSCOPY

4.1. Objectives

The objective of the present work is to assess the applicability of atomic force microscopy (AFM) to surface charge mapping, i.e., the detection of heterogeneously charged regions on a surface. Silica substrate is used as the model system, as its surface charge can be controlled by regulating pH. Partial sorption of copper ions on the silica substrate is used to enhance surface charge heterogeneities by modifying the surface charge at the sorption sites. The interaction force between the silica surface and a chemically inert tip is monitored, and images of the surface are simultaneously obtained. Comparisons between the charge distributions before and after sorption are presented and discussed. In addition, the phase of a silicon nitride AFM tip is determined.

4.2. Introduction

Colloidal particles and surfaces acquire surface charge in aqueous electrolyte solutions by chemical processes like protonation and deprotonation of surface groups, as well as sorption of metal ions or other molecules. The surface charge may be heterogeneously distributed on the surface depending on surface characteristics and the presence of active sites for the charging process (Van Megan and Snook, 1980). Electrostatic forces, resulting from the presence of charge on the surface of particles, play

a key role on the behavior of particles in natural aquatic environments as well as in separations processes. The study of colloidal interactions under conditions of heterogeneous-charge development is an important contribution to the current understanding of particle–particle interaction forces and the analysis of solid–liquid separations processes that mostly contemplates uniform constant surface charge.

AFM has been used to provide images of surfaces at the nanoscale, as well as direct measurements of the interaction force between two approaching surfaces (Butt, 1992; Li et al., 1993; Veeramesuneni et al., 1996; Toikka and Hayes, 1997). Changes in topography and interaction forces as a result of sorption have also been investigated using AFM (Kramer et al., 1998; Larson and Pugh; 1998; Subramanian and Ducker, 2000; Liu et al., 2001; Chin et al., 2002; Vithayaveroj et al., 2003). In recent years, AFM has been applied to obtain "force images" of surfaces which means that data of force profiles at different points of the surface can be directly associated with topographic characteristics (Terán Arce et al., 2003).

Ishino et al. (1997) modified SiO_2 substrates with polar functional groups by the Langmuir–Blodgett method and measured the interactions between the standard silicon nitride tip and sample surfaces covered with charged functional groups in aqueous solutions. The results showed that AFM can detect the spatial distribution of the charged functional groups on the substrate by associating them with specific images of adhesion force.

Kramer et al. (1998) employed AFM force imaging to monitor two-dimensionally a partial sorption of cationic polyelectrolytes on an oxidized silicon wafer. Sorption of polycations on the silica wafer drastically affected the interaction force between a

standard AFM tip and the silica surface. Before sorption, an electrostatic repulsion during approach and a relatively small adhesion during retraction were detected. After sorption, the repulsion was replaced by a long range electrostatic attraction during approach, and the adhesive force increased strongly during retraction due to polyelectrolyte bridging between the substrate and the tip. The location of sites covered by electrolyte could be directly related to regions on the surface where strong adhesive forces were detected. Different coverages of the polycation were found to qualitatively correspond to the results of x-ray photoelectron spectroscopy (XPS) and electrokinetic measurements. The same research group (Estel et al., 2000) employed a similar technique to study the sorption of polyelectrolyte complexes, which consisted of a mixture of polycations and polyanions, using an identical model system. They found that the sorbed polyelectrolyte complex could lead to a heterogeneous surface with a wide variety of interaction features due to the balance of cationic and anionic charges. The interaction forces were strongly influenced by solution pH.

Indentation curves of commercially available elastomers were obtained by the application of force imaging AFM (Terán Arce et al., 2003). The location of calcium carbonate inclusions was detected through a change in the adhesion force. Applications of scanning electron microscopy with energy-dispersive x-ray alaysis (SEM/EDX) showed that the “pits” and the “holes” observed during force image could be directly linked to calcium inclusions.

Other forms of AFM have also been used in surface charge mapping. Pulsed-force mode atomic force microscopy was applied to map the charge distribution on a sample surface in water (Miyatani et al., 1997; Miyatani et al., 1998). The sample

consisted of a quartz (SiO_2) substrate plate partially covered by an Al_2O_3 film. Both, a topographic image and an electrical double-layer force image showed the surface with some circular regions. Force–distance curves were recorded both inside the circular region and on the surrounding area in aqueous solutions of various pH values. The results showed that the circular regions always bear negative charge in solutions with pH 3–11 indicating that those regions correspond to bare quartz substrate since the isoelectric point (IEP) of SiO_2 has been reported to be around pH 2. On the other hand, the IEP of the surrounding area was determined to be around pH 10 which suggested that this area is Al_2O_3.

Johnson et al. (2003) adapted an electric force microscope for mapping surface charge density in aqueous solutions. This technique provided high-resolution images at typical AFM scanning rates; therefore, it was suggested that it could be applied in the study of charge mapping of soft biological materials such as fluid-phase-supported bilayer membranes and DNA molecules.

Most of the studies using conventional AFM have focused on mapping the sorption sites of long organic molecules by monitoring adhesive forces. In the present work, the same principle is applied in order to detect the presence and location of chemical groups bearing different charge on the surface by monitoring electrostatic forces.

4.3. Materials and Methods

The system of study consisted of an amorphous silica plate and a standard silicon nitride tip embedded in a background electrolyte. Silica was selected for this study

because its charging process can be controlled by adjusting the pH of the solution. The requirement of a high lateral resolution was met by using standard silicon nitride tips. Partial sorption of copper ion was used to enhance surface charge heterogeneities. The conditions of pH and ionic strength were selected according to three criteria: 1) surface charge of the silica substrate and the silicon nitrite tip, 2) predominance of electrostatic forces over van der Waals forces, and 3) absence of precipitated copper species. The concentrations of copper ion solutions injected into the system were selected in order to ensure partial coverage of the surface.

4.3.1. Preparation of Silica Surfaces, Standard Silicon Nitride Tips, and Silicon Nitride Particles

The substrates were amorphous silica plates (fused quartz silica plates, Ted Pella, Inc., Redding, CA). The silica plates were cleaned by soaking them for more than 12 h in a concentrated H_2SO_4 solution (Fisher Scientific, Fair Lawn, NJ). They were rinsed with DI water before each experiment. They were accepted for sorption measurements if silica surfaces were completely wet after exposing to water. The smoothness of the surfaces was determined by AFM images obtained using a standard silicon nitride tip (Digital Instruments, Santa Barbara, CA). The silicon nitride tips were sequentially rinsed with DI water, hydrochloric acid (Fisher Scientific, Fair Lawn, NJ), DI water, methanol (Fisher Scientific, Fair Lawn, NJ), and DI water. They were blow-dried with nitrogen gas before use. The goal was to completely remove organic contaminants. Three different types of silicon nitride particles (alpha phase, beta phase, and electronic grade) were purchased

from Alfa Aesar (Ward Hill, MA). The particles were cleaned with DI water several times before use.

4.3.2. Chemicals

Water of 18-MΩ/cm resistivity at 25 ºC, prepared by an E-pure system (model D4631, Barnstead Thermolyne Co., Dubuque, IA), was used for the cleaning procedures and for the preparation of solutions.

Copper ion solutions were prepared from copper nitrate (Fisher Scientific, Fair Lawn, NJ). A solution of hydrochloric acid of concentration 1 N was used for adjusting the pH of the solutions. The pH of the solutions were measured and found to be consistent throughout the experiments.

Background electrolyte solutions for adjusting the ionic strength were prepared from sodium chloride (enzyme grade, Fisher Scientific, Fair Lawn, NJ). All concentrations of ions in solution were considered for the estimation of ionic strength.

4.3.3. Zeta Potential Measurements

Measurements of the zeta potential of both surfaces, silica and silicon nitride particles, were obtained by a Lazer Zee Meter (model 501, Pen Kem Inc., Bedford Hills, NY) using sodium chloride solutions as background electrolyte and dilute hydrochloric acid solutions for adjusting the pH.

4.3.4. AFM Measurements

The interaction force between a silicon nitride cantilever tip and a silica surface was measured by a Nanoscope IIIa atomic force microscope (Digital Instruments, Santa Barbara, CA) equipped with a fluid cell. In order to discard any contamination or introduction of particles to the system, the copper solutions were filtered right before injection to the system with a filtration medium of 0.2-μm pores.

The force volume mode was used in this work because it provides not only image and a single interaction force curve, but also complete force versus distance curves at different points on the surface. In this mode, force curves are obtained while the AFM tip scans the sample surface. Therefore, a two-dimensional array of force versus distance curves is acquired. Each curve can be analyzed and several quantities characterizing the interaction–force curves can be calculated. The force at a constant distance from the surface can be displayed and analyzed for the whole array and an image of the interaction forces can be created with lateral resolution. Due to the limitation of accumulated data, however, the force measurements can be carried out only at 64 × 64 spots on the surface; and furthermore, the number of data points per approach and separation curve is limited to 64. In this study, 32 × 32 surface points with 256 data points per approach and separation were recorded in order to acquire a higher resolution in the force curves. The force volume mode was appropriate for this study.

4.4. Results and Discussion

4.4.1. Silicon Nitride Phase Determination

A study of the surface charge development of the silicon nitride tip was necessary in order to understand its interaction with the silica surface. Electrokinetic experiments with three types of commercially available silicon nitride crystals and amorphous silica were performed using a Lazer Zee Meter to determine the behavior of the zeta potential of the surfaces of interest.

The surface of silicon nitride in aqueous solution is composed of amphoteric silanol and basic silylamine--secondary (silylamine, $–Si_2NH_2$) and possible primary (silylamine, $–SiNH_3$) amines, though the latter is rapidly hydrolyzed--surface groups (Teschke et al., 2001). The phase of silicon nitride depends on the dominant surface group. The presence of silanol groups on silicon nitride surface is the cause of its acidic behavior resulting in low isoelectric point, while the presence of amine groups results in high isoelectric point (Čerovic et al, 2002). Figure 4.1 shows the zeta potential curves of the three types of silicon nitride particles studied. The isoelectric points are found at pH 3.2 (beta phase), pH 7.2 (alpha phase) and pH 7.9 (electronic grade). The latter two curves are very close, since 94% of electronic grade silicon nitride particle is composed of alpha phase. These values fall in the range of the isoelectric point of silicon nitride, which is pH 6 – 8.5, reported in the literature (Davis et al., 1978; Harame et al., 1987; Nietzsche and Friedrich, 1989; Bousse and Mostarshed, 1991; Senden and Drummond, 1995; Raiteri et al., 1998a). These results indicate that alpha phase and electronic grade silicon nitride have more amine groups on the surfaces than silanol groups. Silica presents an isoelectric point around 2. These results were compared with measurements

of the interaction force between silica and silicon nitride tip at different pH conditions. Figure 4.2 presents the measurements of the interaction force.

At pH 2.15 and pH 3, the interaction forces between the tip and the plate is attractive instead of repulsive. This behavior corresponds to pH values that are very close to the isoelectric point, and therefore one expects the van der Waals attractive force to dominate over the weak electrostatic force. At the pH range of 3.90 to 6.90, the forces are all attractive due to the opposite charge of silicon nitride and silica. And repulsive forces are detected from pH 8.10 to pH 9.10 as expected. Based on these results, it can be concluded that the silicon nitride tip employed in this study behaves as silicon nitride of either alpha phase or electronic grade.

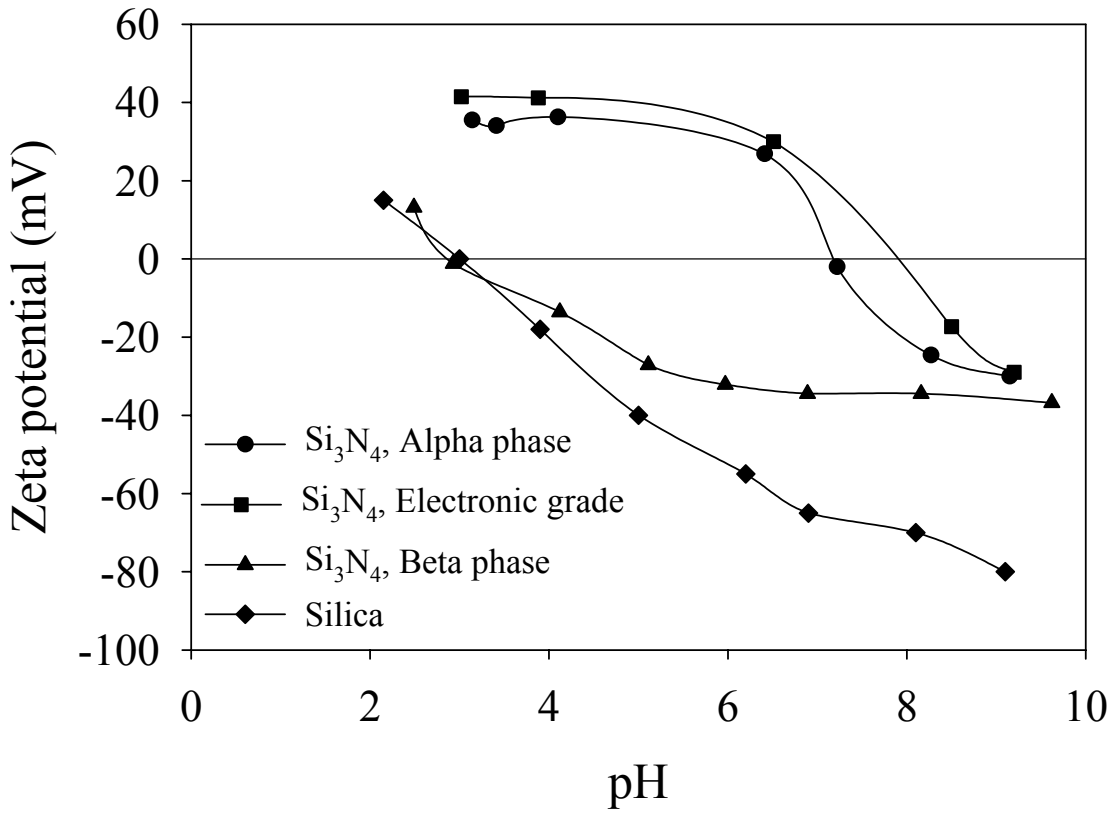

Figure 4.1. Zeta potential of silica particles and three types of silicon nitride particles as a function of pH.

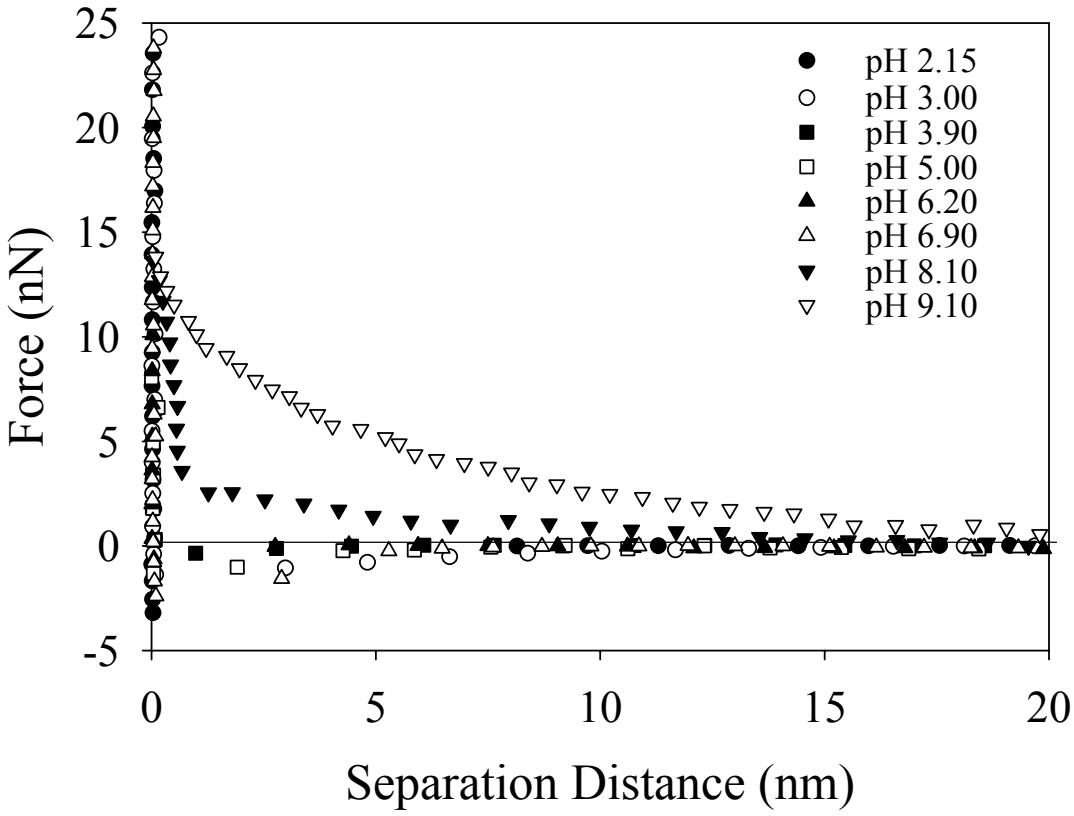

Figure 4.2. Interaction force profiles between a Si_3N_4 tip and a silica plate in a 0.0005 M NaCl solution.

4.4.2. Surface Charge Mapping

In order to select the experimental conditions, the equilibrium of copper uptake by silica as a function of pH (Figure 4.3) was examined from a previous study. Copper uptake starts taking place at pH 3, and at pH around 7 there is complete coverage of the surface (Subramaniam et al., 2003). Therefore, the pH values of 4.5 and 5.5 were chosen to ensure that partial copper sorption would take place and that no precipitation would occur in the system. It was also expected that sorption at pH 5.5 would occur in a larger extent than at pH 4.5, since the equilibrium curve is shifted to lower pH values as concentration increases. In this work, the copper ion solutions were prepared with higher concentrations than those in Chapter 3 to ensure that sorption sites would be detected by AFM. The surface area of the silica plate is considerably larger than the surface area of the single silica particle.

Figure 4.4a depicts an image of a silica plate in the electrolyte at pH 4.5 before the introduction of copper ions to the system. The sample surface is smooth, with a roughness of about 5 nm. Although the interaction force was measured throughout the surface, only three regions are presented here. In this case, the interaction force in all regions is attractive (Figure 4.4b), with a magnitude of –1 to –1.5 nN.

The same situation can be observed at pH 5.5 (Figure 4.5), with the difference that the attractive forces are stronger in concordance to the electrokinetic measurements. In each case, copper solutions were introduced into the system and allowed to sit for several hours, so that the system would reach equilibrium. Because the silicon nitride tip in this work exhibits more amine groups on the surface; therefore, copper sorption occurred on the tip is insignificant since amine groups do not complex with copper ions.

Figure 4.6 presents the interaction forces at pH 4.5 and a concentration of 1.5×10^{-3} M copper ions. When the positively charged copper ions sorb onto the silica, they modify the negative charge on the silica surface. As a result, silica has a less negative charge and lead to the diminution of the magnitude of force to an average of –0.5 nN.

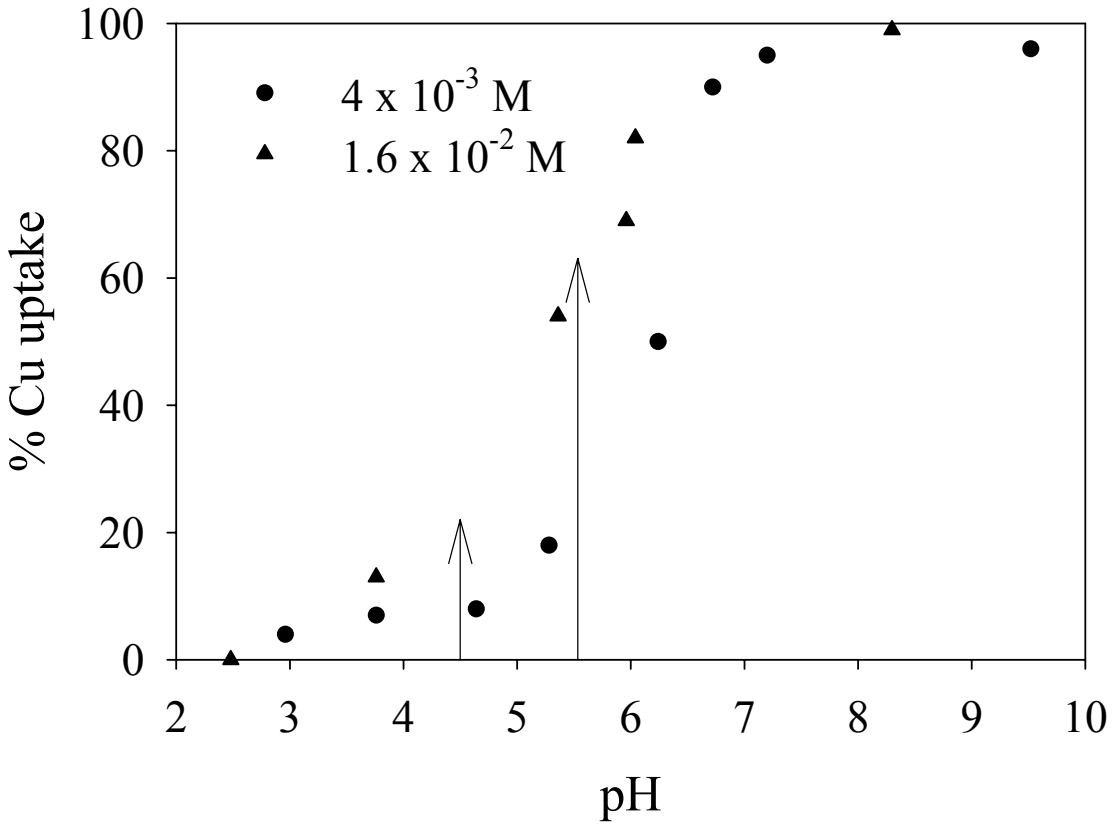

Figure 4.3. Equilibrium of copper uptake by silica as a function of pH (Subramaniam et al., 2003).

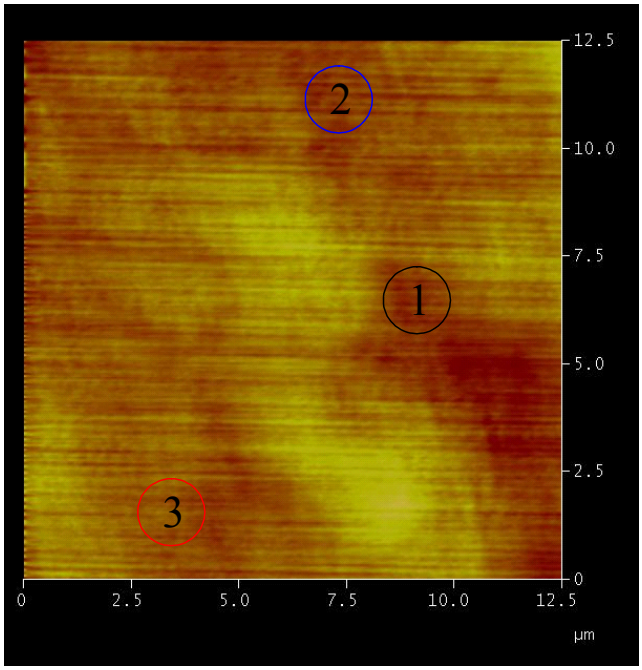

(a)

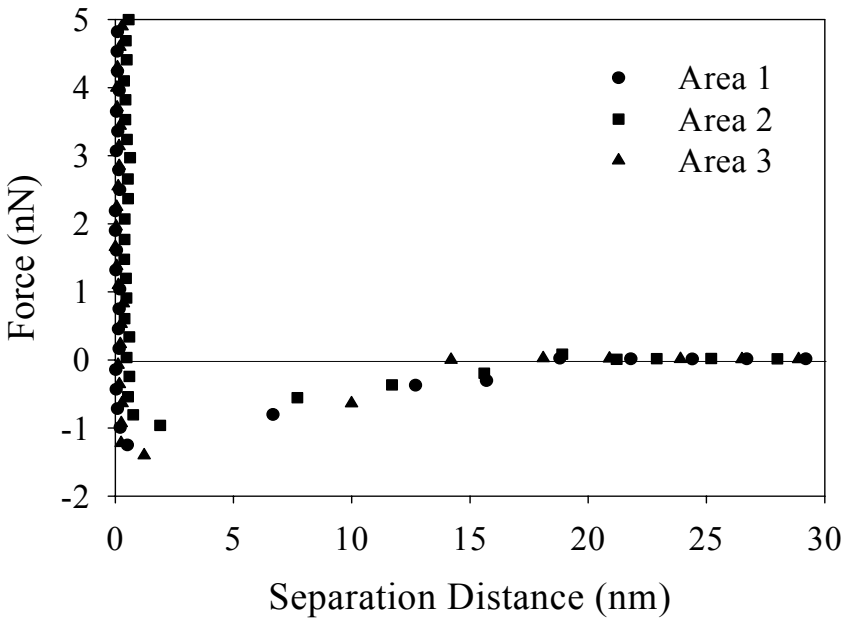

(b)

Figure 4.4. (a) An image of a silica plate and (b) force profiles between a Si_3N_4 tip and a silica plate before copper sorption at pH 4.5, ionic strength = 0.0005 M.

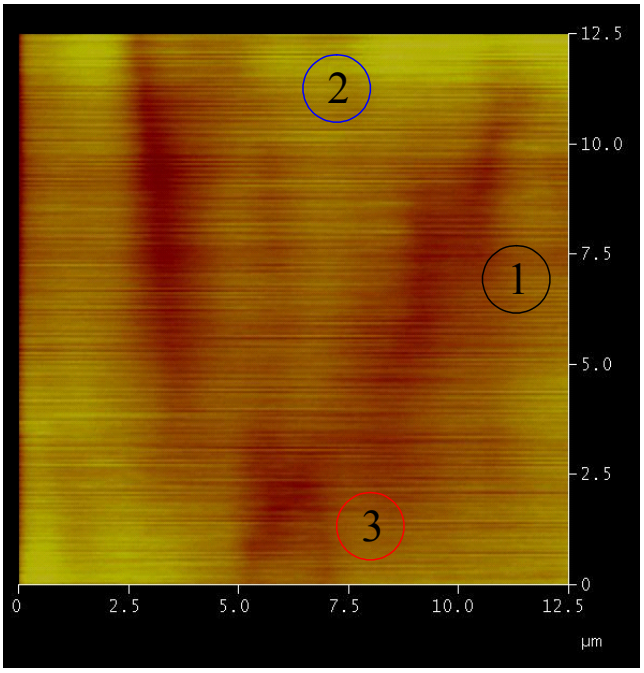

(a)

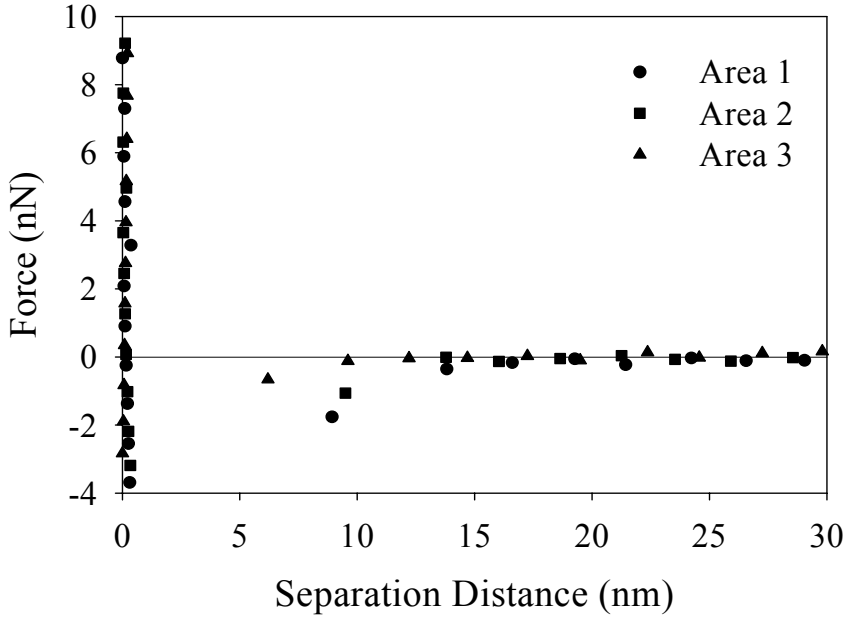

(b)

Figure 4.5. (a) An image of a silica plate and (b) force profiles between a Si_3N_4 tip and a silica plate before copper sorption at pH 5.5, ionic strength = 0.0005 M.

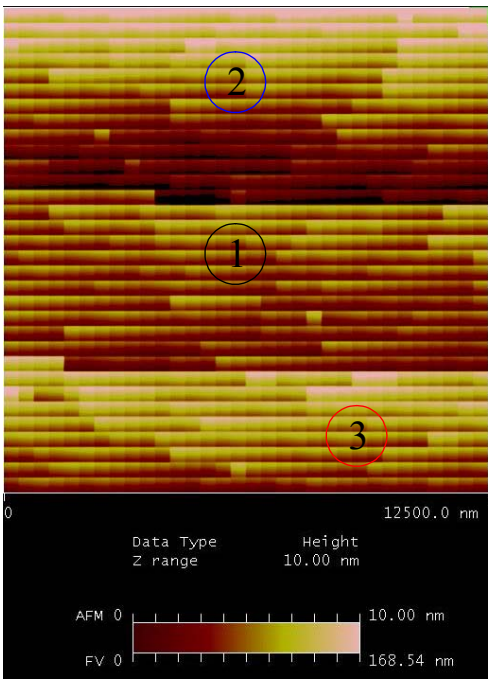

(a)

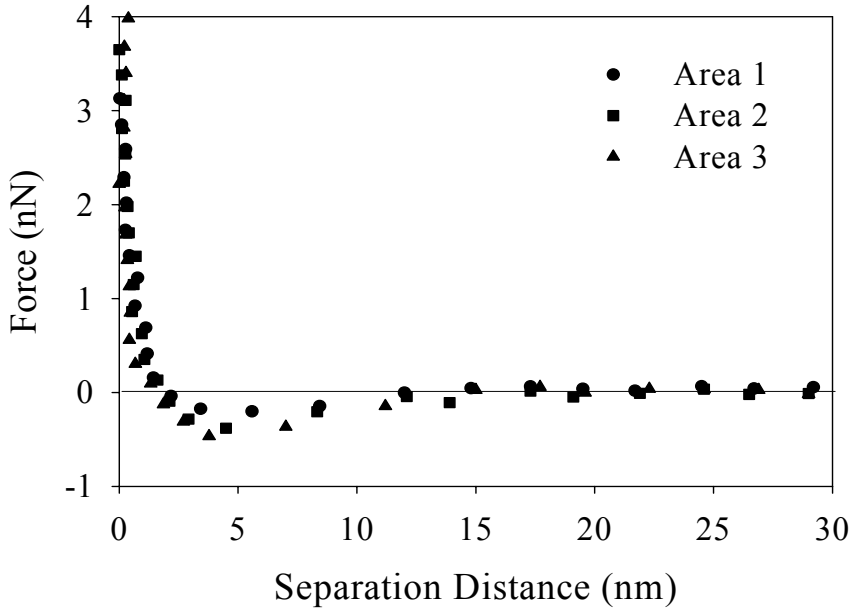

(b)

Figure 4.6. (a) An image of a silica plate and (b) force profiles between a Si_3N_4 tip and a silica plate after copper sorption at pH 4.5,
copper concentration = 1.5×10^{-3} M, ionic strength = 0.0005 M.

Figure 4.7 presents the results for pH 4.5 with a copper ion concentration of 7.6×10^{-3} M. In this case, the magnitude of the attractive force also decreased but at a higher degree. This observation agrees with the behavior of the equilibrium of copper previously mentioned (Figure 4.3) that the higher the metal concentration, the more copper ions uptake by silica. As a result, silica has a much less negative surface charge and the magnitude of force is greatly decreased.

Figure 4.8 presents the results for pH 4.5 and a copper ion concentration of 3.04×10^{-2} M. Although no features could be observed on the surface, force measurements showed that every measured force had become repulsive. This is the result of complete coverage of the surface by copper ions.

Figure 4.9 presents the results at pH 5.5 and a copper ion concentration of 1.5×10^{-3} M. "Islands", which had a repulsive force associated with them, were observed on the surface. The presence of these islands may be a result of selective copper sorption on the silica plate. On the other hand, the dark, shallow areas did still present attraction although of a lower magnitude than before copper ion sorption.

Figure 4.10 corresponds to pH 5.5 and a copper ion concentration of 7.6×10^{-3} M. More "islands" were observed. In this case, a strong repulsive force was associated with the "island" regions. Weak attractive forces were detected on the shallow areas.

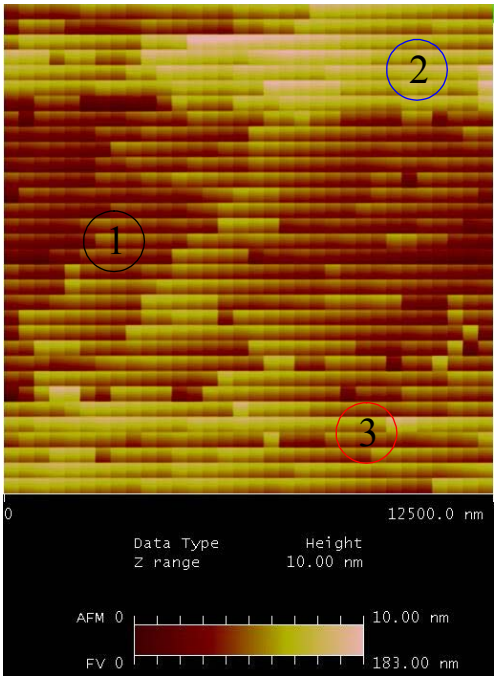

(a)

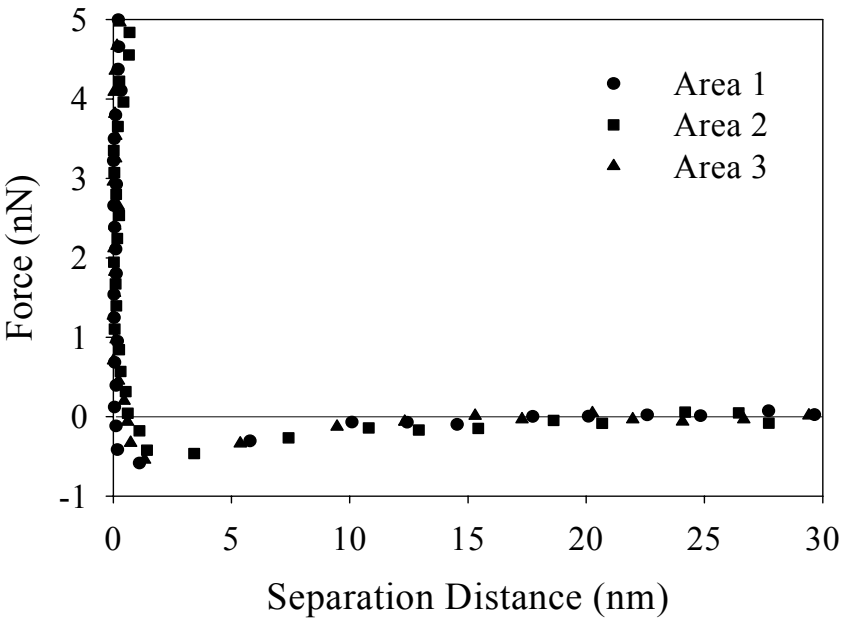

(b)

Figure 4.7. (a) An image of a silica plate and (b) force profiles between a Si_3N_4 tip and a silica plate after copper sorption at pH 4.5,
copper concentration = 7.6×10^{-3} M, ionic strength = 0.0005 M.

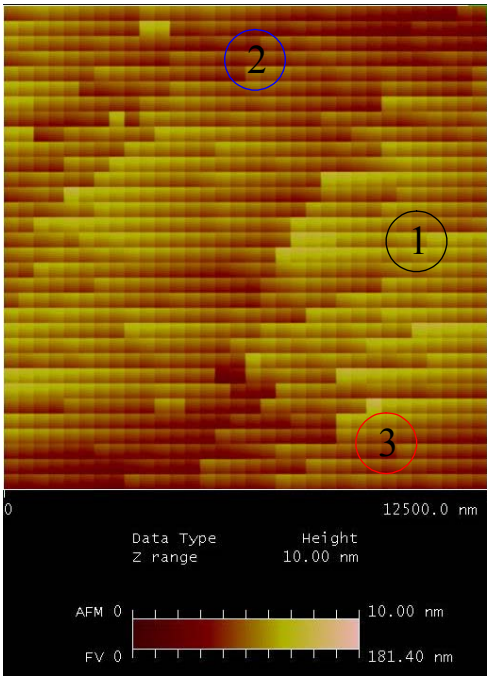

(a)

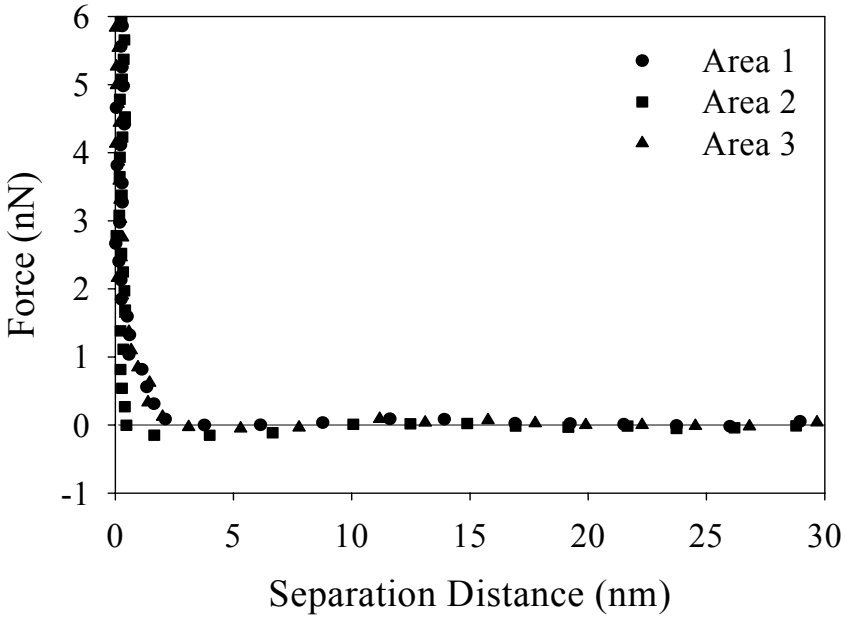

(b)

Figure 4.8. (a) An image of a silica plate and (b) force profiles between a Si_3N_4 tip and a silica plate after copper sorption at pH 4.5,
copper concentration = 3.04×10^{-2} M, ionic strength = 0.0005 M.

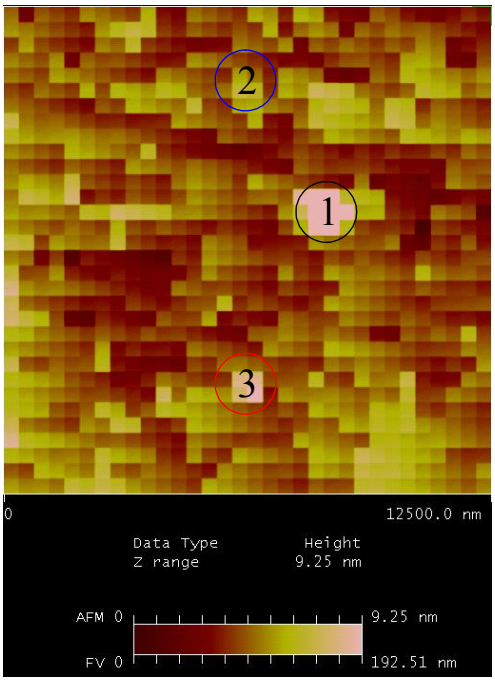

(a)

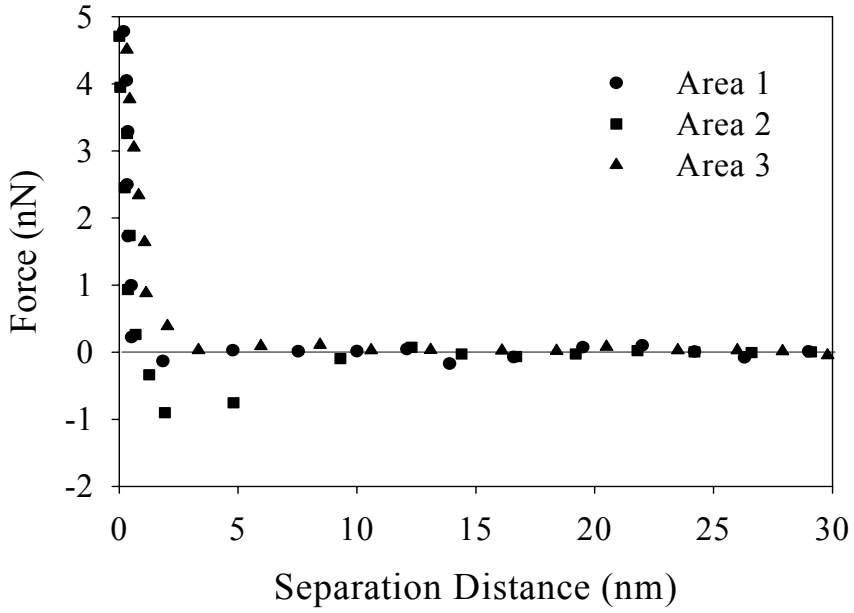

(b)

Figure 4.9. (a) An image of a silica plate and (b) force profiles between a Si_3N_4 tip and a silica plate after copper sorption at pH 5.5,
copper concentration = 1.5×10^{-3} M, ionic strength = 0.0005 M.

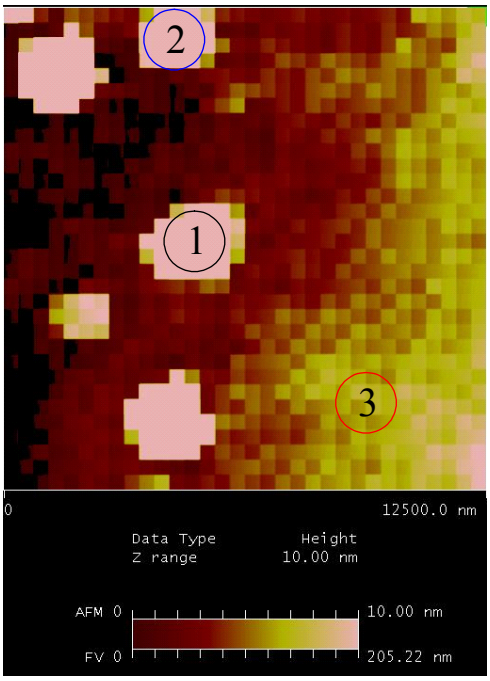

(a)

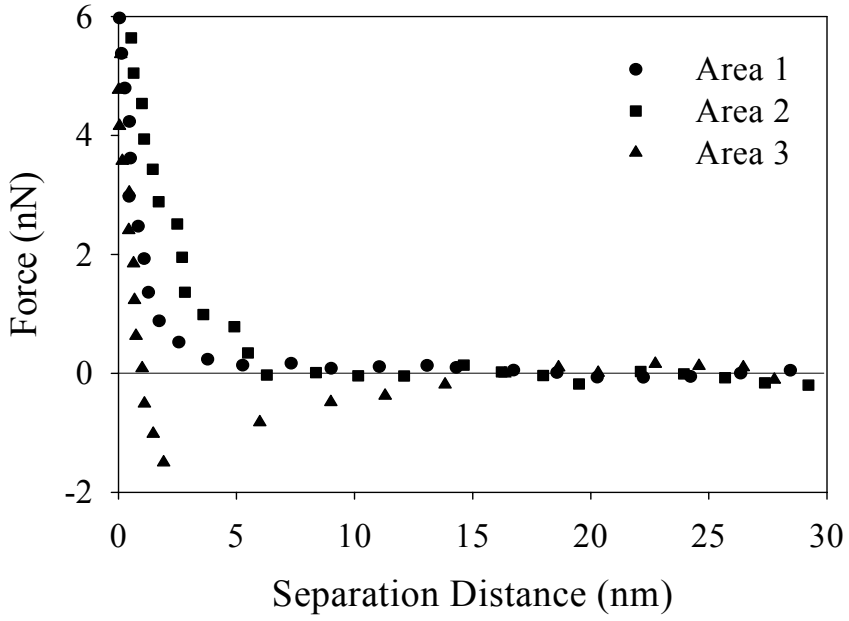

(b)

Figure 4.10. (a) An image of a silica plate and (b) force profiles between a Si_3N_4 tip and a silica plate after copper sorption at pH 5.5,
copper concentration = 7.6×10^{-3} M, ionic strength = 0.0005 M.

There are two possible explanations for the presence of the "islands": 1) they either correspond to a copper precipitate or 2) they correspond to regions of the surface bearing a different charge that results in abrupt changes in the magnitude of the interaction force. The latter situation would force the feedback control system of the AFM to move the surface away from the tip, creating the image of obstacles or islands. Similar observations were reported in studies cited in the introduction of this work.

These islands are believed not to be precipitates even though the copper concentrations used in this study are very close to the solubility of copper ions at the higher value of experimental pH. The assessment of copper ion solubility was performed based on calculations of speciation of copper in aqueous solution without taking into account the sorption of copper ions onto the surface. Sorption will decrease the amount of free copper in solution. Moreover, the zeta potential measurements of tenorite precipitates showed that these particles bear negative charge at all pH values (Figure 4.11). If the islands were tenorite particles, the interaction force measured between the silicon nitride tip and those spots would be attractive, since the silicon nitride tip is positively charged at the pH conditions used in this study.

In order to test that the presence of the islands is a result of electrostatic effects, the experiments were repeated at a higher ionic strength (0.05 M). At this higher ionic strength, compression of the electrical double layer should result in shorter ranges of the electrostatic forces. Figure 4.12 presents measurements of the interaction force at pH 5.5 and a copper ion concentration of 7.6×10^{-3} M. The "islands" could still be observed on the surface, but their size and average height were reduced, and so were the forces associated with them.

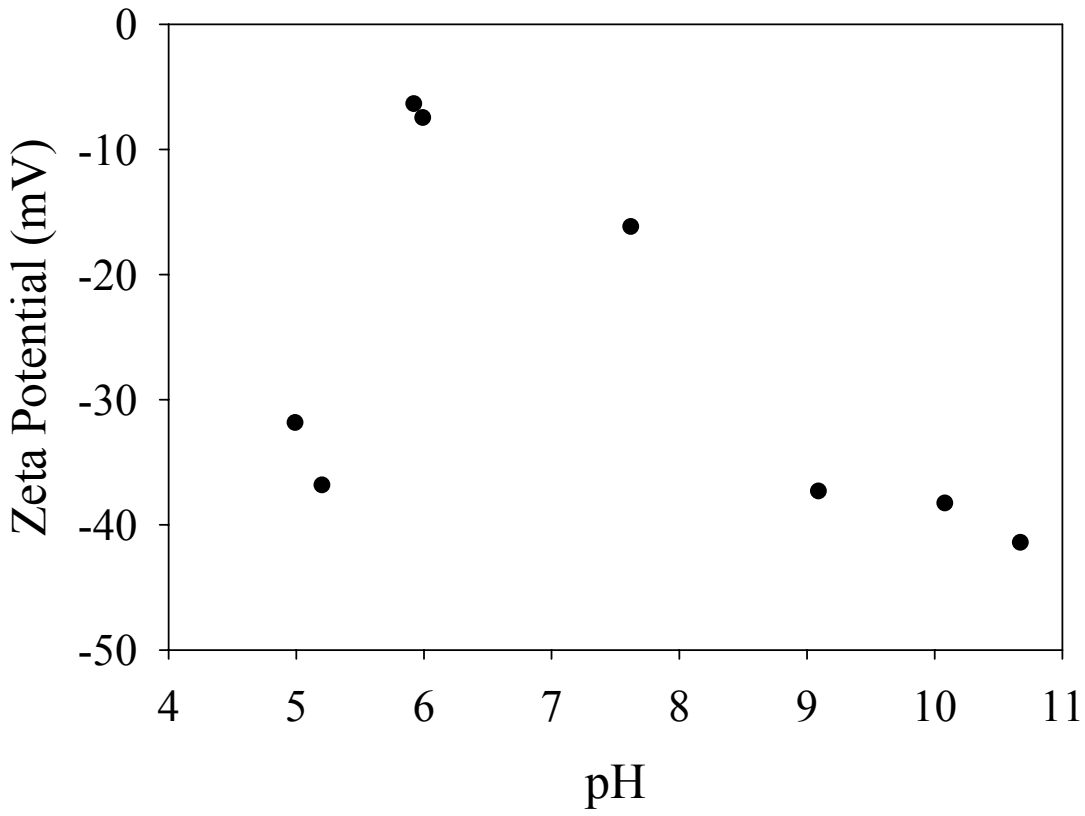

Figure 4.11. Zeta potential measurements of tenorite precipitates (Sung, 1999).

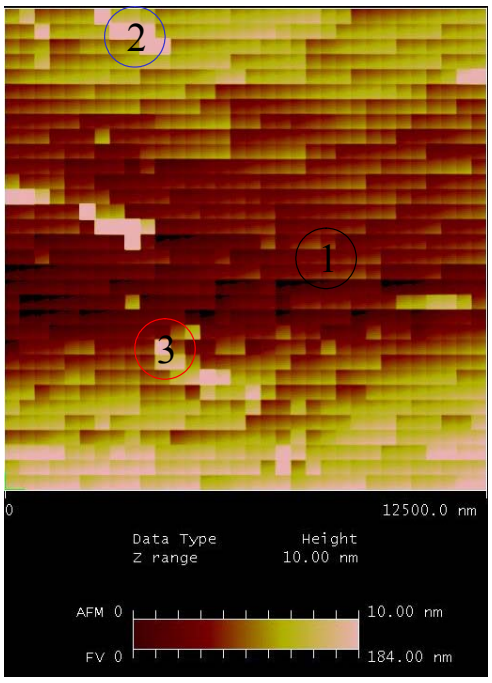

(a)

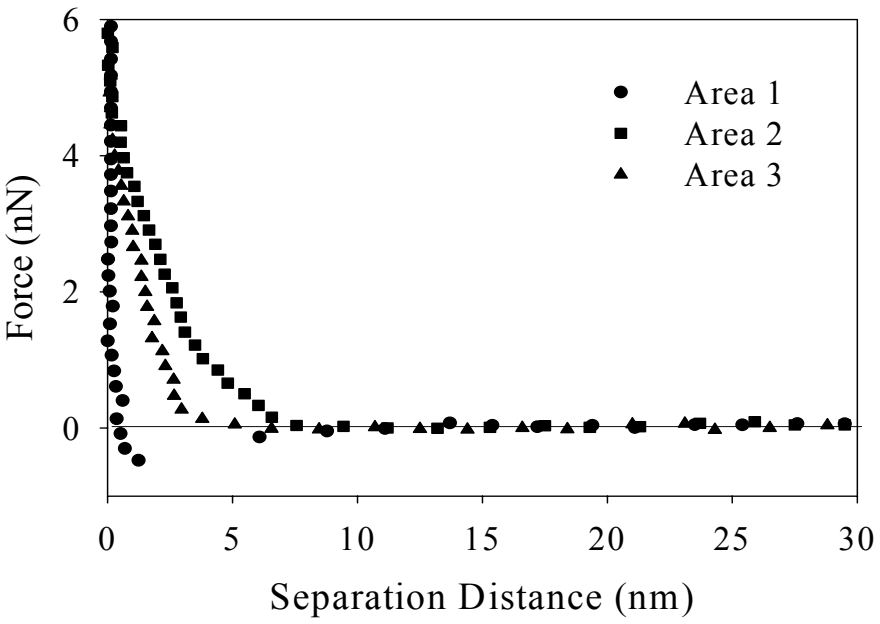

(b)

Figure 4.12. (a) An image of a silica plate and (b) force profiles between a Si_3N_4 tip and a silica plate after copper sorption at pH 5.5, copper concentration = 7.6×10^{-3} M, ionic strength = 0.05 M.

4.5. Summary

Results from both the zeta potential and AFM measurements indicate that the silicon nitride employed in this study is either alpha phase or electronic grade. The AFM experimental results demonstrate that force-volume AFM can be used to detect heterogeneously charged regions on a silica substrate surface. Measurements of the interaction force before copper ion sorption show an attractive force throughout the surface. The attractive force increases in magnitude with higher pH. After the injection of copper ion solution, the interaction force in general is less attractive. The higher the concentration of copper ions, the less attractive the force becomes. Copper sorption is low as expected at pH 4.5. No actual islands are observed at this pH.

At a higher pH, the formation of islands is observed, and the interaction force in those regions is repulsive. The higher the concentration of copper ions in the system, the larger the number of islands detected with a strong repulsive force associated with them. However, some regions without islands do still present attractive interaction. The islands represent the positively charged regions on the surface that might result from the sorption of copper ions.

CHAPTER 5

MODIFICATION OF THE ELECTROSTATIC FORCE BY AN EXTERNALLY APPLIED POTENTIAL

5.1. Objectives

The aim of this study is to measure the interaction forces between surfaces with various applied potentials in aqueous electrolyte solutions. Recently, atomic force microscopy (AFM) was shown to have the ability to provide direct measurements of surface forces with high precision. We use this procedure to probe the electrostatic double layer forces and their dependence on pH, applied potential, and ionic strength. Experimental results are compared to forces calculated with the Poisson–Boltzmann equation. The potential of zero charge of the gold sample is identified. The contribution of this study is a better understanding of charged interfaces, the role of electrostatic forces in sorption phenomena and the role of an externally applied potential to the interface to manipulate the sorption of charged species.

5.2. Introduction

Electrical double-layer forces in aqueous solutions play an important role in numerous interfacial processes including colloidal stability, polyelectrolyte sorption, ion partitioning in biological and polymer membranes, and electrochemical processes. The development of AFM allows accurate and high-resolution surface force measurements.

Electrical double-layer forces have been investigated with the AFM in various systems. Early studies (Butt, 1991; Weisenhorn et al., 1992; Atkins and Pashley, 1993; Li et al., 1993) dealt with the dependence of double-layer forces on the ionic strength. When two oppositely charged surfaces approach each other, they experience a repulsive force. As the concentration of background electrolyte increases, the double layers on the surfaces are compressed and the Debye lengths decrease. This phenomenon results in a smaller repulsive force, a lesser decay length, and the emergence of the van der Waals force. The force measurements were found in good agreement with theoretical calculations. A similar behavior was observed in asymmetric electrolytes (Butt, 1991; Meagher, 1992; Kékicheff et al., 1993).

The influence of the solution pH on the double-layer forces has also been investigated. Cappella and Dietler (1999) studied the double-layer forces on a stearic acid sample with a silicon nitride tip at different pH conditions. At pH less than the pK of the stearic acid, the surface has no charge and there is no double-layer force. However, a jump-to-contact due to the van der Waals force appears. The surface starts to charge at pH slightly higher than the pK and the jump-to-contact vanishes as the double-layer force counterbalances the van der Waals force. Then, the double-layer force emerges when pH is greater than pK. The transition from supremacy of double-layer force to supremacy of van der Waals force and vice versa was observed in several studies (Butt, 1991; Senden et al., 1994; Raiteri et al., 1996b; Karaman et al., 1997).

This phenomenon was also employed to determine the point of zero charge of surfaces. If two interacting surfaces have the same point of zero charge, they bear surface charge of the same sign at all pH conditions, and the force between them is always

repulsive. On the other hand, if the surfaces have different points of zero charge, the interaction force depends on the pH of the solution. A repulsive force is observed when the surfaces carry surface charge of the same sign, and attraction is noticed as they bear the opposite charges. The double-layer force was also used to monitor sorption of surfactants (Manne et al., 1994; Larson et al., 1997; Hu et al., 1997; Kane and Mulvaney, 1998).

The dependence of forces on applied potentials is currently one of the most interesting issues. Fréchette and Vanderlick (2001) measured the interaction forces between mica and polycrystalline gold as a function of the applied electrode potential. The measured forces were found to be strongly influenced by the applied potential. The results were compared to DLVO predictions. The long-range forces correspond well to DLVO predictions, including evidence of saturation in forces at high-applied potentials while there is a deviation in forces from theory at short ranges.

The interaction forces were investigated in systems of silica–silica and silica–gold in the presence of a series of alkalide–halide electrolyte solutions (Hillier et al., 1996). The interaction between the two similar surfaces was always repulsive and corresponded to DLVO predictions. On the other hand, the silica–gold interaction was a strong function of the potential applied to the gold. The force measurements showed that the effective potential of the gold surface decreased as the applied potential was varied from positive to negative. This behavior indicated that sorbed anions were removed from the gold surface. Different electrolyte species exhibited distinct behaviors at the same applied potential. The relationship between the potential of zero force (E_{pzf}) and the potential of zero charge (E_{pzc}) was also studied.

The effect of the solution pH was studied by Hu et al. (1997). A strong repulsive force was detected between a silica probe and a TiO_2 electrode at high pH. The magnitude of the interaction force decreased as the pH was reduced and the force became attractive at pH below 5.5. Various potentials were applied to the electrode at pH 5.5, where the silica bears negative charge. At negative electrode potentials, the negative charge was uniformly distributed over the charged layer; therefore, the interactions between the probe and the electrode were repulsive. As the potentials became more positive, the positive charges overcame the negative ones and finally an excess positive charge appeared in the charged layer and, therefore, the force converted to attraction. Once the background electrolyte solution was added with a polymeric anion, there was an indication that the polymeric anion competed with the OH^- to sorb on the electrode surface and this behavior led to a shift of the isoelectric point of TiO_2 to lower pH and an increase in the net negative surface charge.

Raiteri et al. (1996a) applied high electrical potential on both platinum and gold substrates and measured their interactions with a standard silicon nitride tip in aqueous solutions. All measurements were performed at alkaline conditions to ensure that the tip bears negative charge. They observed a very steep increase in forces over a small potential window and force saturation at potential beyond this range. A similar effect was detected by Döppenschmidt and Butt (1999). Arai and Fujihira (1996) controlled the potential of both interacting surfaces. Their theoretical fits indicated values of surface potential higher than expected. Later, Raiteri et al. (1998b) controlled the potential of both interacting surfaces with similar results.

The external potential was not only applied to the surface but also to the tip. Ishino et al. (1994) controlled the electrical potential of a gold-coated cantilever and measured force between the cantilever and glass substrates covered with different monolayers.

The interaction of a less noble metal electrode, such as copper with a silica sphere at low pH and concentrated $MgSO_4$ solutions, was investigated under a variety of electrode potentials (Dedeloudis et al., 2000). The results revealed that the double-layer interaction governed the total interactions as seen in diluted electrolytes. The formation of an sorbed oxygen layer on copper was found at neutral pH; however, after removal of that oxygen layer, the force became identical to the one measured in acidic conditions.

The influence of an applied electrochemical potential on the interfacial properties of the electrode surface was examined by means of electrostatic, adhesive, and friction forces (Campbell and Hillier, 1999). These properties were potential-dependent in rigid-surface systems. Nevertheless, the potential-dependent friction was absent at polymer film/electrolyte interfaces. This behavior is a result of the elimination of electrolyte-containing solvent from the tip/sample interface, hence, the electrostatic force does not operate during contact, and the friction coefficient is constant.

Potential-dependent interactions have not only been studied on solid surface materials, but also on soft matters such as polymer films. Wang et al. (2002) showed that the polymer used in their study, a poly(vinylferrocene), has a potential-dependent behavior that differs from that previously reported for an electronically conducting polymer film electrode (Wang and Brad, 2001).

In order to interpret force measurements in electrochemical systems, it is important to distinguish between the electrode potential and the surface potential (Bockris and Khan, 1985). The working electrode potential is measured with respect to a reference electrode while the surface potential is the potential used in the Poisson–Boltzmann equation assuming that the solution potential is zero. The DLVO theory gives the surface potential while the potentiostat controls the electrode potential. Although the electrode potential controls the surface potential, there is no direct relationship between the two (Fréchette and Vanderlick, 2001).

5.3. Theoretical Calculations

According to the DLVO theory, the total interaction energy between two charged surfaces in solution is the sum of the van der Waals interaction energy and the electrostatic interaction energy. In this work, the electrostatic potential in *z*:*z* symmetric electrolytes is calculated by using the well-known Poisson Equation:

$$\frac{d^2\psi}{dx^2} = -\frac{\rho}{\varepsilon} \tag{5.1}$$

where ψ is the electrostatic potential, ρ is the number density of ions of valence z at any point x between two surfaces, and ε is a relative permittivity, static dielectric constant.

The Boltzmann distribution of counterions at any point x is:

$$\rho = \bar{e}\left[zN_o \exp\left(-\frac{z\bar{e}\psi}{k_B T} \right) - zN_o \exp\left(\frac{z\bar{e}\psi}{k_B T} \right) \right] \tag{5.2}$$

$$\rho = -2\bar{e}zN_o \sinh\left(\frac{z\bar{e}\psi}{k_B T} \right) \tag{5.3}$$

where $\bar{e}$ is the electron charge (1.602×10^{-23} Coulomb), N_o is the Avogadro's constant (6.022×10^{-23} mol^{-1}), k_B is the Boltzmann constant (1.38×10^{-23} J K^{-1}), and T is the temperature (K).

The Poisson–Boltzmann equation is a combination of Eqs. (5.1) and (5.3).

$$\frac{d^2\psi}{dx^2} = \frac{2\bar{e}zN_o}{\varepsilon} \sinh\left(\frac{z\bar{e}\psi}{k_B T} \right) \tag{5.4}$$

This equation is solved for the system showed in Figure 5.1 in order to find the profile of potential in the gap. The following boundary conditions are applied:

$$\text{At } x = 0 \text{ , } \psi = \psi_{1,o} \tag{5.5}$$

$$\text{At } x = D \text{ , } \psi = \psi_{2,o} \tag{5.6}$$

$$\text{At } x = a \text{ , } \psi = \psi_a \tag{5.7}$$

and $$\left(\frac{d^2\psi}{dx^2}\right)_{x=a} = 0 \qquad (5.8)$$

where $\psi_{1,o}$ and $\psi_{2,o}$ are the potentials on the first and second surfaces, respectively, D is the separation distance, a is the point where the potential presents a minimum, and ψ_a is the potential at $x = a$.

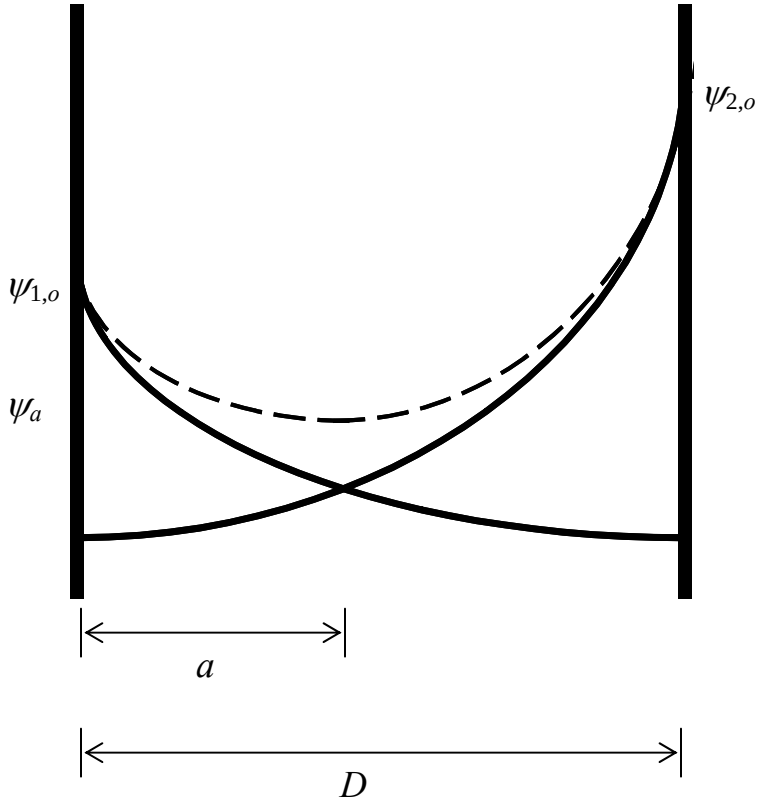

Figure 5.1. Schematic of potential profiles between two approaching surfaces.

Multiplying both sides of Eq. (5.4) by $2(d\psi/dx)$ and integrating we have:

$$2\left(\frac{d\psi}{dx}\right)\frac{d^2\psi}{dx^2} = 2\left(\frac{d\psi}{dx}\right)\frac{2\bar{e}zN_o}{\varepsilon}\sinh\left(\frac{z\bar{e}\psi}{k_BT}\right) \tag{5.9}$$

$$\frac{d}{dx}\left[\left(\frac{d\psi}{dx}\right)^2\right] = \frac{4\bar{e}zN_o}{\varepsilon}\sinh\left(\frac{z\bar{e}\psi}{k_BT}\right)\left(\frac{d\psi}{dx}\right) \tag{5.10}$$

$$d\left[\left(\frac{d\psi}{dx}\right)^2\right] = \frac{4\bar{e}zN_o}{\varepsilon}\sinh\left(\frac{z\bar{e}\psi}{k_BT}\right)d\psi \tag{5.11}$$

$$\left(\frac{d\psi}{dx}\right)^2 = \frac{4N_ok_BT}{\varepsilon}\cosh\left(\frac{z\bar{e}\psi}{k_BT}\right) + \text{constant} \tag{5.12}$$

At high boundary surface potentials (ψ_o >> 25 mV), Verwey and Overbeek (1948) calculated the electric potential at the midplane (ψ_m). Therefore, we then assume that $\psi_a \cong \psi_m$ and $a \cong D/2$.

Therefore, at $x = D/2$, $\psi = \psi_m$ and $\left(\frac{d\psi}{dx}\right)_{x=D/2} = 0$ (5.13)

Then, Eq. (5.12) becomes

$$0 = \frac{4N_o k_B T}{\varepsilon} \cosh\left(\frac{z\bar{e}\psi_m}{k_B T}\right) + \text{constant} \tag{5.14}$$

Eq. (5.14) can be rewritten as

$$\text{constant} = -\frac{4N_o k_B T}{\varepsilon} \cosh\left(\frac{z\bar{e}\psi_m}{k_B T}\right) \tag{5.15}$$

Substituting this constant value back to Eq. (5.12), we have

$$\left(\frac{d\psi}{dx}\right)^2 = \frac{4N_o k_B T}{\varepsilon}\left[\cosh\left(\frac{z\bar{e}\psi}{k_B T}\right) - \cosh\left(\frac{z\bar{e}\psi_m}{k_B T}\right)\right] \tag{5.16}$$

Since the inverse Debye length, κ, depends only on the characteristic of the solution, i.e., it does not depend on ψ_1 and ψ_2, we can assume that for the cases in which $D>>1/\kappa$, $\psi(x)$ can be expressed as a combination of the expressions of the potential of a single planar surface.

$$T[\psi(x)] = A(x)G[\psi_1(x)] + B(x)H[\psi_2(x)] \tag{5.17}$$

Eq. (5.17) can be written as

$$\frac{\exp\left(\frac{\bar{e}\psi}{2k_BT}\right)-1}{\exp\left(\frac{\bar{e}\psi}{2k_BT}\right)+1}=\left(\frac{x}{D}\right)\left[\frac{\exp\left(\frac{\bar{e}\psi_{1,o}}{2k_BT}\right)-1}{\exp\left(\frac{\bar{e}\psi_{1,o}}{2k_BT}\right)+1}\right]\exp(-\kappa x)+\left(\frac{D-x}{D}\right)\left[\frac{\exp\left(\frac{\bar{e}\psi_{2,o}}{2k_BT}\right)-1}{\exp\left(\frac{\bar{e}\psi_{2,o}}{2k_BT}\right)+1}\right]\exp(-\kappa(D-x)) \tag{5.18}$$

The value of ψ_m can be obtained by solving the following equation, which is derived from Eq. (5.18)

$$\frac{\exp\left(\frac{\bar{e}\psi_m}{2k_BT}\right)-1}{\exp\left(\frac{\bar{e}\psi_m}{2k_BT}\right)+1}=\frac{\exp\left(\frac{-\kappa D}{2}\right)}{2}\left[\left[\frac{\exp\left(\frac{\bar{e}\psi_{1,o}}{2k_BT}\right)-1}{\exp\left(\frac{\bar{e}\psi_{1,o}}{2k_BT}\right)+1}\right]+\left[\frac{\exp\left(\frac{\bar{e}\psi_{2,o}}{2k_BT}\right)-1}{\exp\left(\frac{\bar{e}\psi_{2,o}}{2k_BT}\right)+1}\right]\right] \tag{5.19}$$

The value of $\psi_{1,o}$ is obtained from zeta potential measurements of silicon nitride. The calculations aim to obtain the value of $\psi_{2,o}$, which is the surface potential of the gold plate, by minimization of the relative error between the calculated interaction force and the one obtained by AFM measurements. The following iterative procedure is performed: 1) a value for $\psi_{2,o}$ is proposed, 2) the value of ψ_m is calculated from Eq. (5.19), 3) the electrostatic force per unit area between the two surfaces, f, is calculated from Eq. (5.20), and 4) the sum of the absolute errors between measured and calculated forces is evaluated. An optimization procedure is applied for adjusting the value of $\psi_{2,o}$ to minimize the sum of errors.

$$f\,[\mathrm{N/m^2}] = k_B T n \left[\exp\left(\frac{\bar{e}\psi_m}{k_B T} \right) + \exp\left(\frac{-\bar{e}\psi_m}{k_B T} \right) - 2 \right] \tag{5.20}$$

In this calculation, the tip is modeled as a half sphere. It is assumed that the area of interaction is given by the projected area of the round tip on the surface, considering that the tip bears the charge at the center.

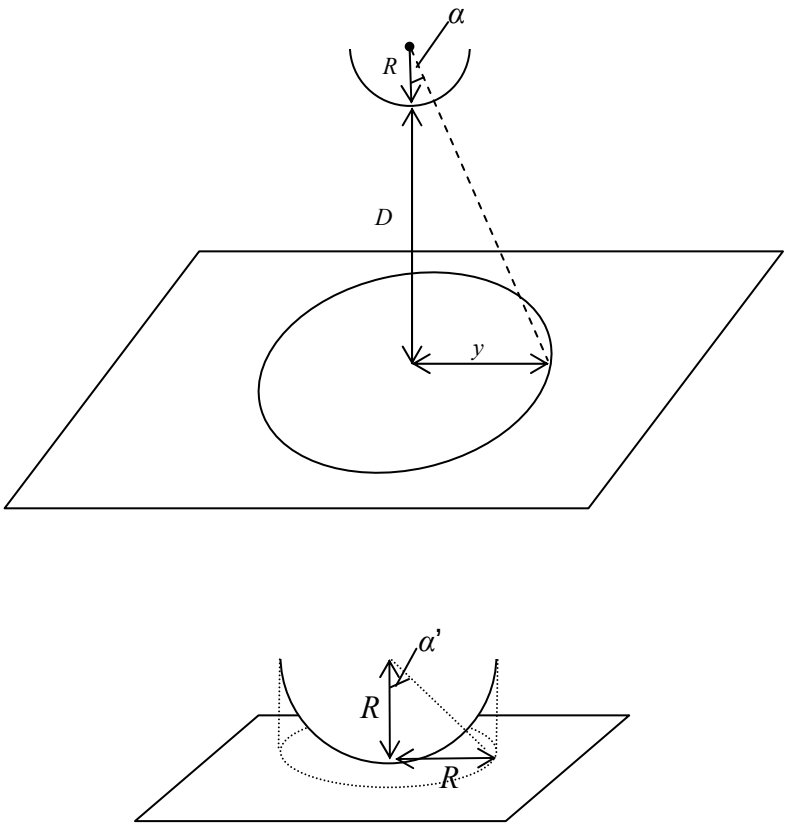

Figure 5.2. Schematic of an effective interaction area between a spherical particle and a planar surface.

Therefore, an effective area (A_{eff}) is

$$A_{eff} = \pi y^2 \tag{5.21}$$

where y is the radius of an effective area.

Expressing $y = y(D,R)$ (5.22)

Where R is the radius of the tip.

$$\alpha' = \alpha \tag{5.23}$$

where α and α' are the angles corresponding to two perpendicular/parallel sides.

So, $\tan\alpha' = \tan\alpha = 1$ (5.24)

From Figure 5.2 $\tan\alpha = \frac{y}{R+D} = 1$ (5.25)

Thus, $y = R + D$ (5.26)

Substitute y from Eq. (5.26) into Eq. (5.21),

$$A_{eff} = \pi(R + D)^2 \tag{5.27}$$

The electrostatic interaction force ($F_{electrostatic}$) between the two surfaces is obtained by

$$F_{electrostatic} = \pi(R+D)^2 * f\,[\mathrm{N/m^2}] \tag{5.28}$$

Eq. (5.28) depicts two opposite effects: a decrease of interaction area and an increase in interaction force per area as the separation distance between the two surfaces decreases. The relationship between interaction area and separation distance is quadratic. The potential at the midplane, ψ_m, is an implicit function of the separation distance. As the two surfaces approach each other, ψ_m becomes increasingly higher tending to an average value of the potential of the two surfaces. This change has a stronger effect on the value of the electrostatic force than the decrease of interaction area because it is exponential in nature.

Studies showed that the calculation approaches for the one-dimensional system of two planar surfaces, which is employed in this work, can be used to accurately estimate the interaction force in tip–surface system (Carnie et al., 1994; Stankovich and Carnie, 1996; Raiteri et al., 1996a).

The van der Waals force (F_{vdW}) can be approximated by

$$F_{vdW} = -\frac{AR}{6D^2} \tag{3.5}$$

The Hamaker constant for gold in water was reported to be 2.5×10^{-19} J (Ducker and Senden, 1992; Biggs and Mulvaney, 1994), while the Hamaker for Si_3N_4 in water is 5×10^{-20} J (Ackler et al., 1996). Therefore, the Hamaker constant for gold and Si_3N_4 in water is 1.12×10^{-19} J.

5.4. Materials and Methods

5.4.1. Chemicals

Solutions of NaCl were used as a background electrolyte and were prepared from reagent grade NaCl crystalline (Fisher Scientific, Fair Lawn, NJ) in deionized Millipore water with a conductivity of 18 MΩ/cm. The pH was adjusted by adding NaOH or HCl. Nitrogen was purged into the solution at least 30 min before starting an experiment.

Prior to use, the gold-coated substrate (Asylum Research, Santa Barbara, CA) with 20-nm continuous coating was cleaned with ethanol and then rinsed in copious amounts of purified water and blown dry under nitrogen gas.

5.4.2. AFM Measurements

All measurements were performed with a commercial AFM (model MMAFM-2, Digital Instruments, Santa Barbara, CA) using its standard electrochemical fluid cell. A three-electrode design was used for electrochemical measurements with the gold surface serving as the working electrode, a platinum counter electrode, and a commercial Ag/AgCl reference electrode. Electric potential was applied between the working electrode and the counter electrode. All electrode potentials are given with respect to the

Ag/AgCl reference. All electrodes were connected to a potentiostat (Petite Ampere, Model LC-3E, Bioanalytical Systems, West Lafayette, IN). Standard silicon nitride cantilevers of different spring constants were used (200 μm wide-legged with a spring constant of 0.12 N/m).

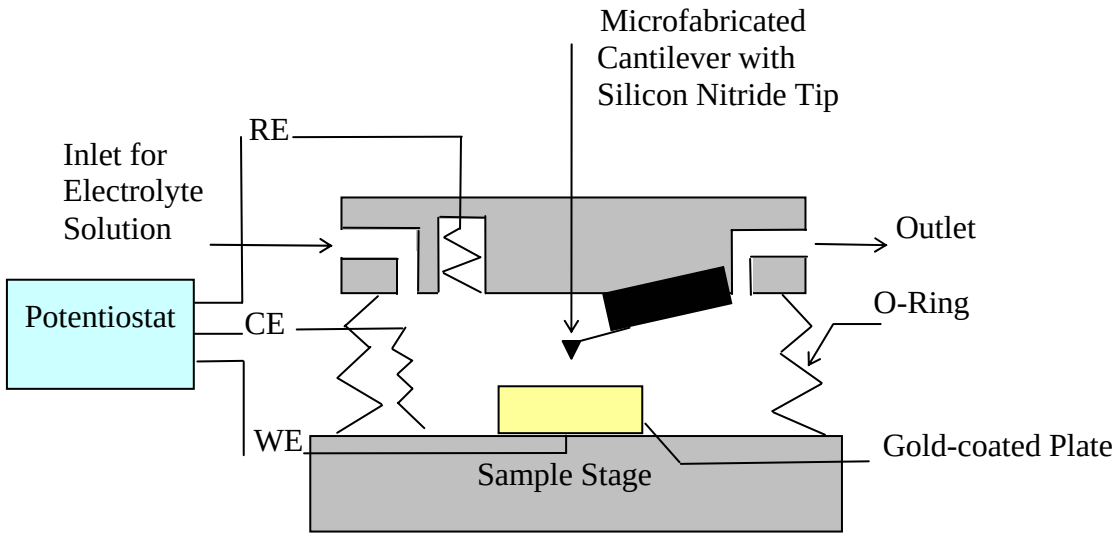

Figure 5.3. Electrochemical cell experimental setup. RE = Reference electrode, CE = Counter electrode, and WE = Working electrode.

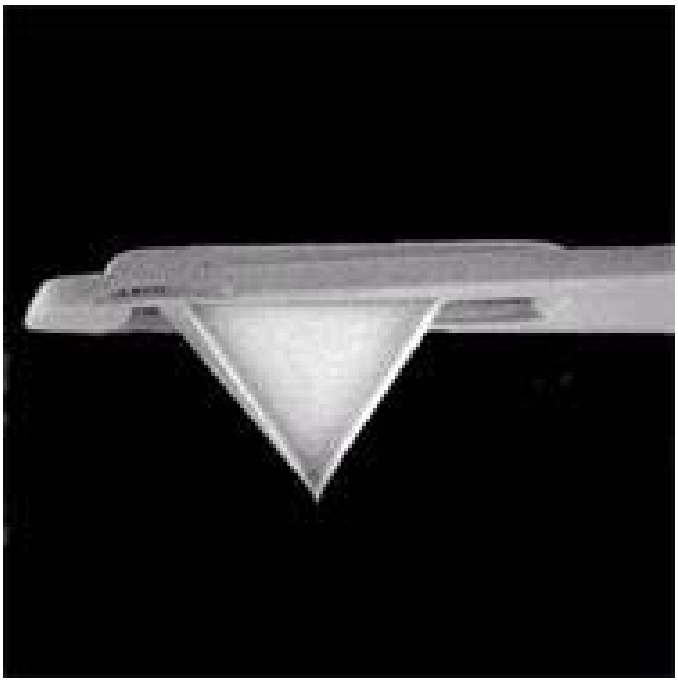

Figure 5.4. Image of a standard silicon nitride probe.

5.5. Results and Discussion

5.5.1. Effect of Solution pH at Low Ionic Strength

The solution pH was varied from around pH 5 to pH 9. The pH values below 5 were not selected since at that low pH the hydrogen ion would play a dominant role in the system. In Figures 5.5–5.13, symbols are used to represent force measurements at different externally applied potentials and the calculated results are represented by lines.

Figure 5.5 illustrates the interaction forces between a silicon nitride tip and the gold-coated plate in 0.0005 M NaCl solution at pH 5.18 at different applied potentials. Under open circuit conditions, the surface charge is determined solely by the coverage of OH^- and H^+ groups on the sorption sites on the surface. The force between a silicon nitride and the gold plate was attractive under open circuit potential (OCP). This behavior corresponds to the zeta potential measurements of both silicon nitride and gold. When the solution is at pH 5.18, the silicon nitride carries a positive charge since its isoelectric point is around pH 7 (as discussed in Chapter IV). The isoelectric point of gold was found at pH 4.5–5 (Arai et al., 1996; Giesbers et al., 2002, Barten et al., 2003a; Barten et al., 2003b); therefore, the gold plate bears a slightly negative charge. This behavior can also be explained by the fact that, besides OH^- ions, halide ions (i.e., Cl^-, Br^-, I^-) are found to bind strongly to gold and form a thin layer of negative charge on the surface (Jaschke et al., 1997). In this case, the concentration of OH^- ions is much lower than that of Cl^- ions, thus, chloride ions play an important role in the control of the surface charge of gold. The same behavior was observed by Giesbers et al. (2002). Once positive potential is applied, the positive charge counterbalances the negative charge on the surface and when the positive potential is increased, it overcompensates the negative charge.

Therefore, the interaction is repulsive at positive potentials. Applying negative potentials leads to more negative charge on the surface. As the potential moved from positive to negative values, the magnitude of the repulsive force decreased, and gradually attractive forces were observed as the tip was positively charged and the surface had a negative charge.

At pH 7.08, where the solution pH was unadjusted, attraction between the tip and the gold surface is observed at OCP (Figure 5.6). The silicon nitride has a slight positive charge at this solution pH due to its isoelectric point. Again, the Cl^- ions regulate the surface charge on gold at this pH value. Nevertheless, the behavior of the force curves as a function of applied potential is similar to that observed in the previous case. It can be concluded that the solution pH has no effect on the interaction forces between the silicon nitride tip and the gold-coated plate with different values of applied electric potential under the pH range of study.

At high pH, for example pH 9.21, gold is negatively charged as a result of sorption of both OH^- ions and Cl^- ions on the surface. The silicon nitride also bears a negative charge at this pH value; therefore, the interaction between the two surfaces is repulsive. As shown in Figure 5.7, the force converted from repulsive to attractive as the applied potential was varied from negative to positive. This behavior qualitatively agrees with the results of Raiteri et al. (1996a).

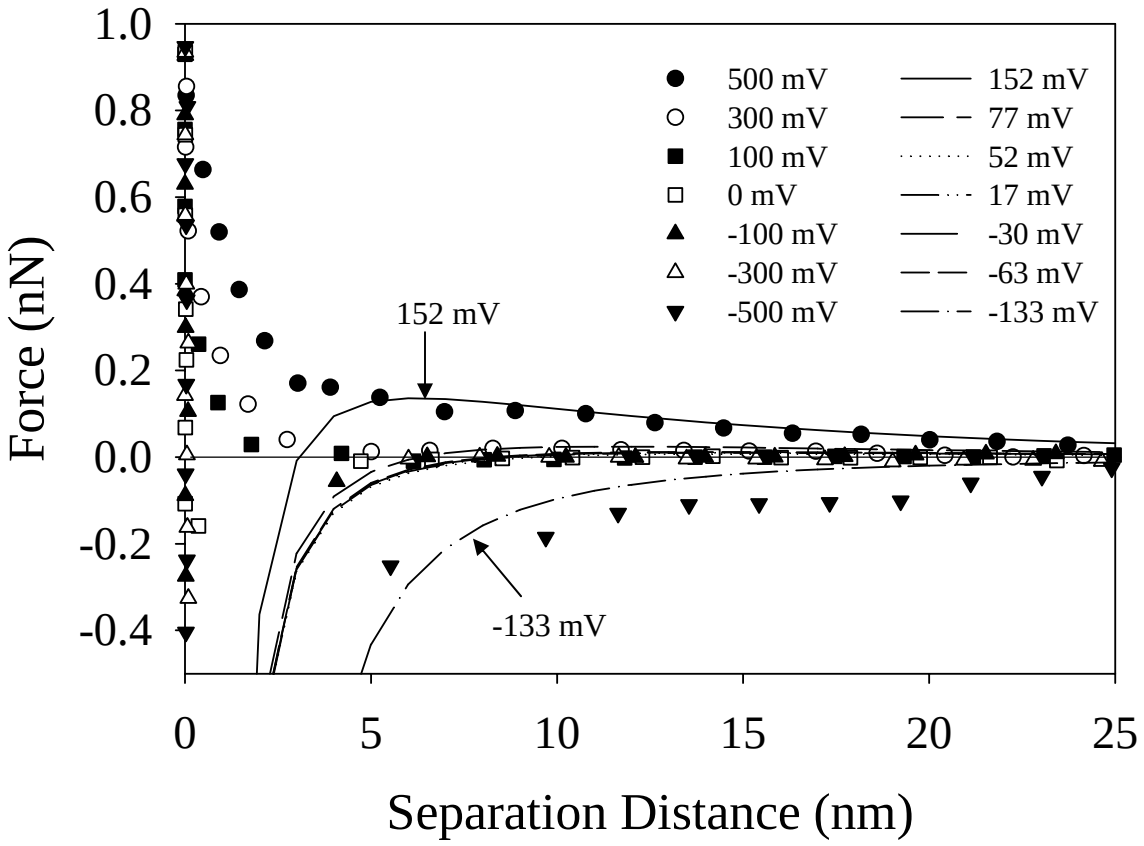

Figure 5.5. Measured and theoretical forces between a silicon nitride tip and the gold-coated plate in a 0.0005 M NaCl solution at pH 5.18 as a function of applied potential (vs. Ag/AgCl).

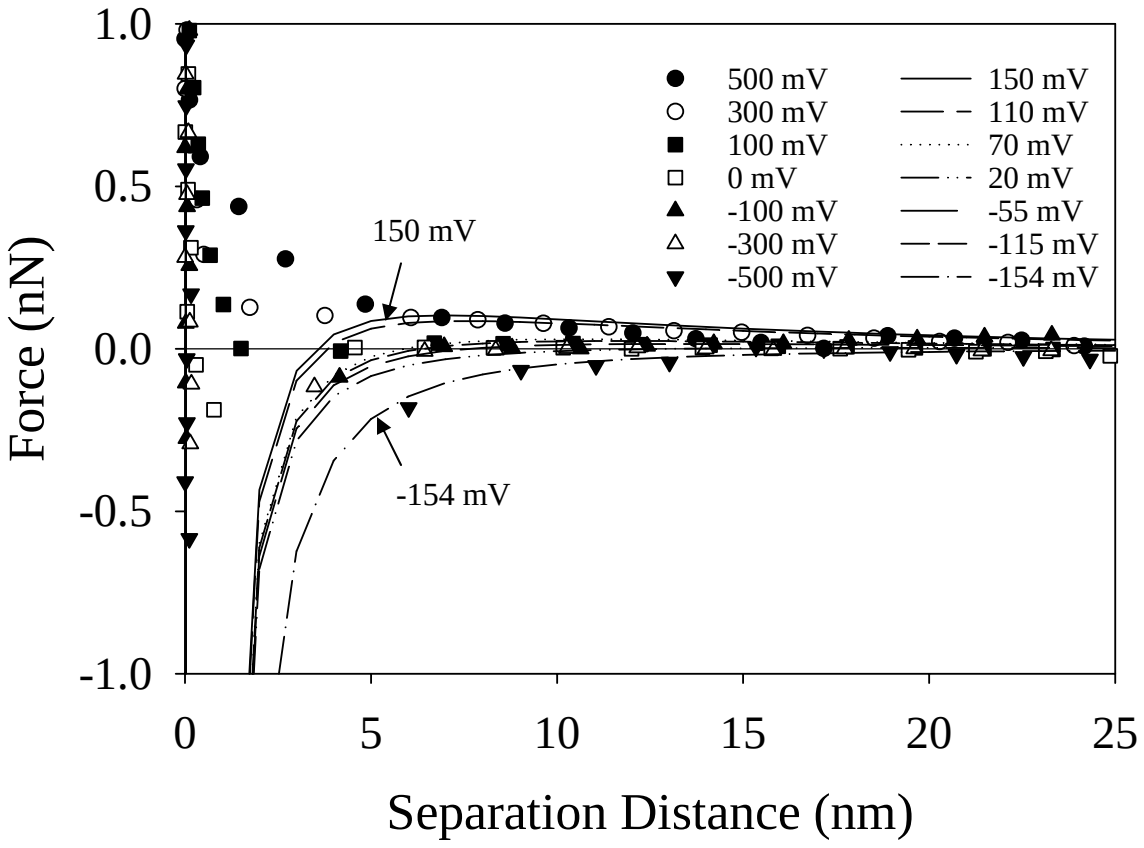

Figure 5.6. Measured and theoretical forces between a silicon nitride tip and the gold-coated plate in a 0.0005 M NaCl solution at pH 7.08 as a function of applied potential (vs. Ag/AgCl).

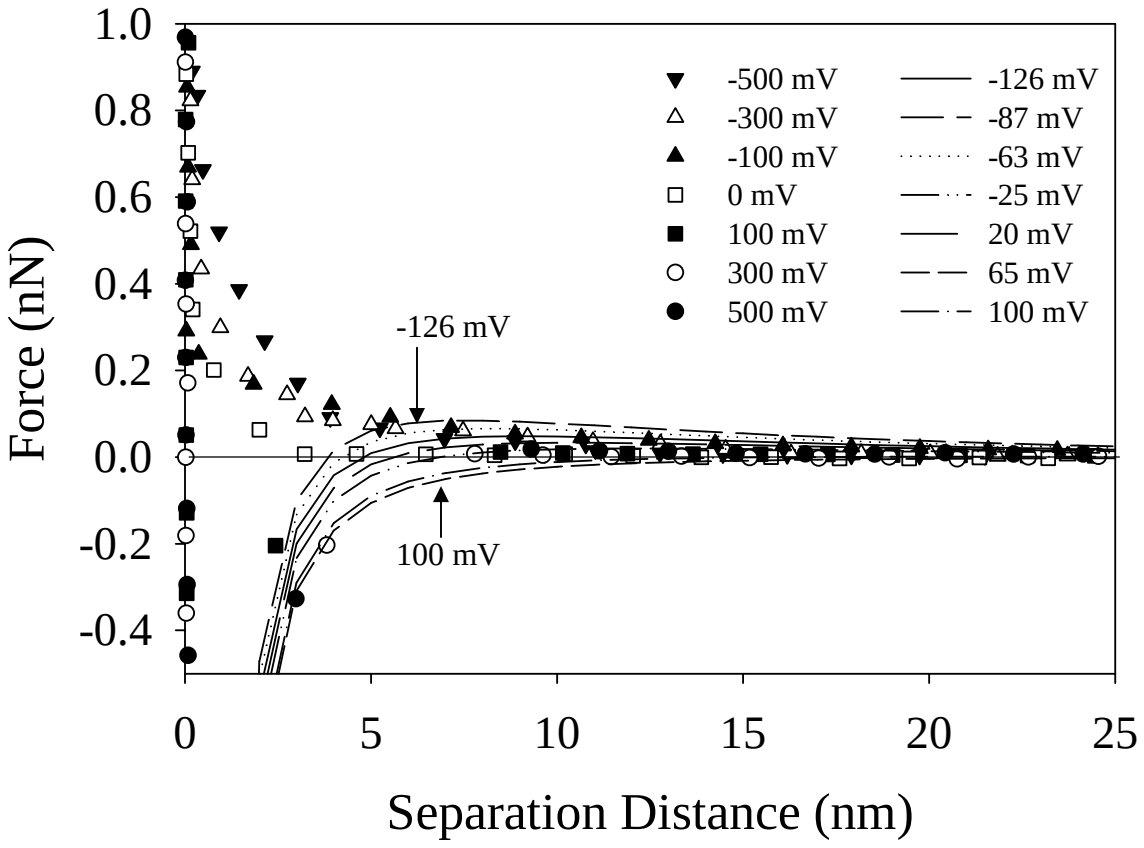

Figure 5.7. Measured and theoretical forces between a silicon nitride tip and the gold-coated plate in a 0.0005 M NaCl solution at pH 9.21 as a function of applied potential (vs. Ag/AgCl).

5.5.2. Effect of Ionic Strength

Force measurements were performed at intermediate ionic strength (0.005 M) with three different pH values under various values of applied potential. The behavior of all three force curves as a function of potential (Figures 5.8, 5.9, 5.10) is similar to the ones observed with the same values of solution pH at low ionic strength. However, since the ionic strength is greater, the Debye length is reduced, and hence, the magnitude of the forces is smaller at the same applied potential.

Most of the force measurements in electrochemical systems were performed in dilute electrolytes (e.g., Biggs et al., 1996; Raiteri et al., 1996a; Hu et al., 1997, Campbell and Hillier, 1999). In this work, the effect of high ionic strength on the interaction force with externally applied potential was studied. Solutions of 0.05 M NaCl were prepared with different pH values. At neutral pH (Figures 5.11 and 5.12), the forces between surfaces under these solution conditions are attractive at OCP due to their surface charge. A series of force measurements as a function of the applied potential to the gold surface indicated that the repulsive force decreased and finally changed to attractive force when moving towards more negative potentials in both cases. However, the change of the force-curve behavior from repulsion to attraction was less pronounced in this solution than in the lower ionic-strength solutions at this pH range. A similar result was seen by Dedeloudis et al. (2000), who measured the surface force between a silica sphere and a copper electrode in concentrated solutions.

Figure 5.13 shows a set of force curves between the tip and gold under potential control in 0.05 M NaCl at pH 9.63. The behavior of force curves is similar to that

obtained in different ionic strength solutions at the same pH. Then again, the transition of force from repulsive to attractive was less than in the lower ionic-strength solutions.

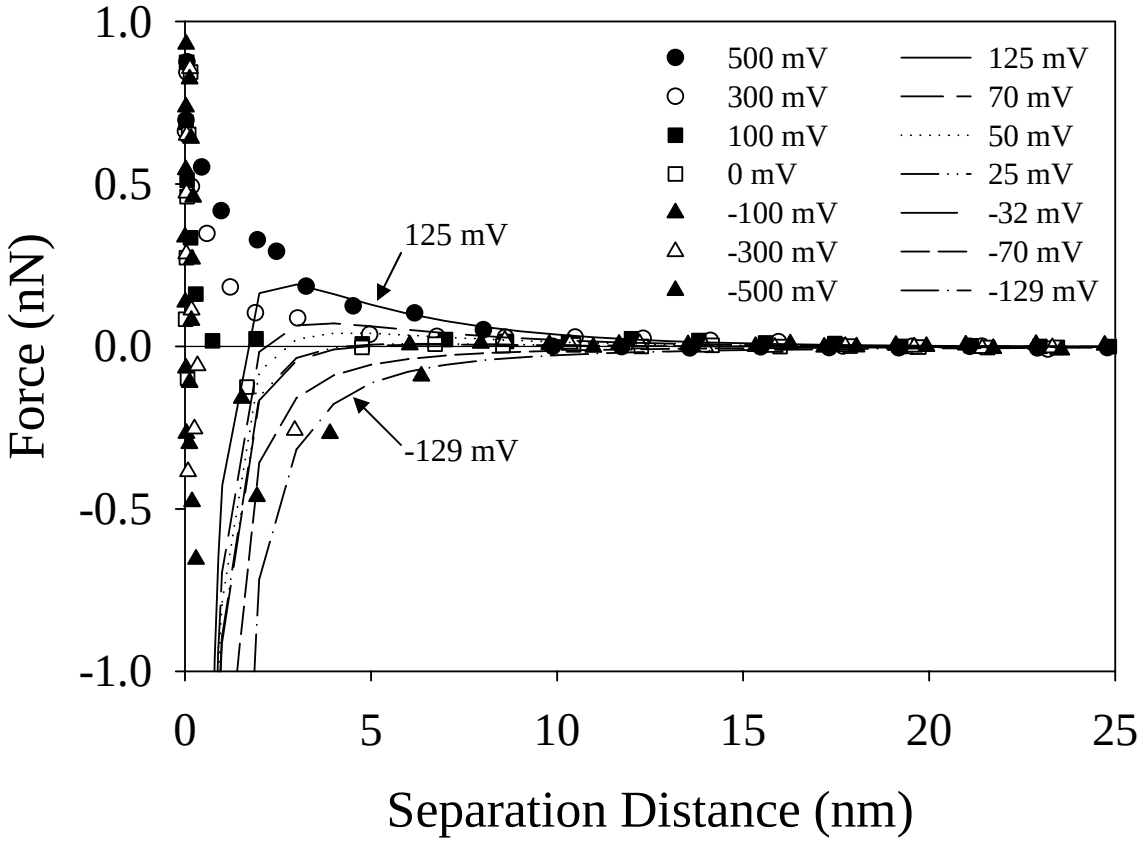

Figure 5.8. Measured and theoretical forces between a silicon nitride tip and the gold-coated plate in a 0.005 M NaCl solution at pH 5.07 as a function of applied potential (vs. Ag/AgCl).

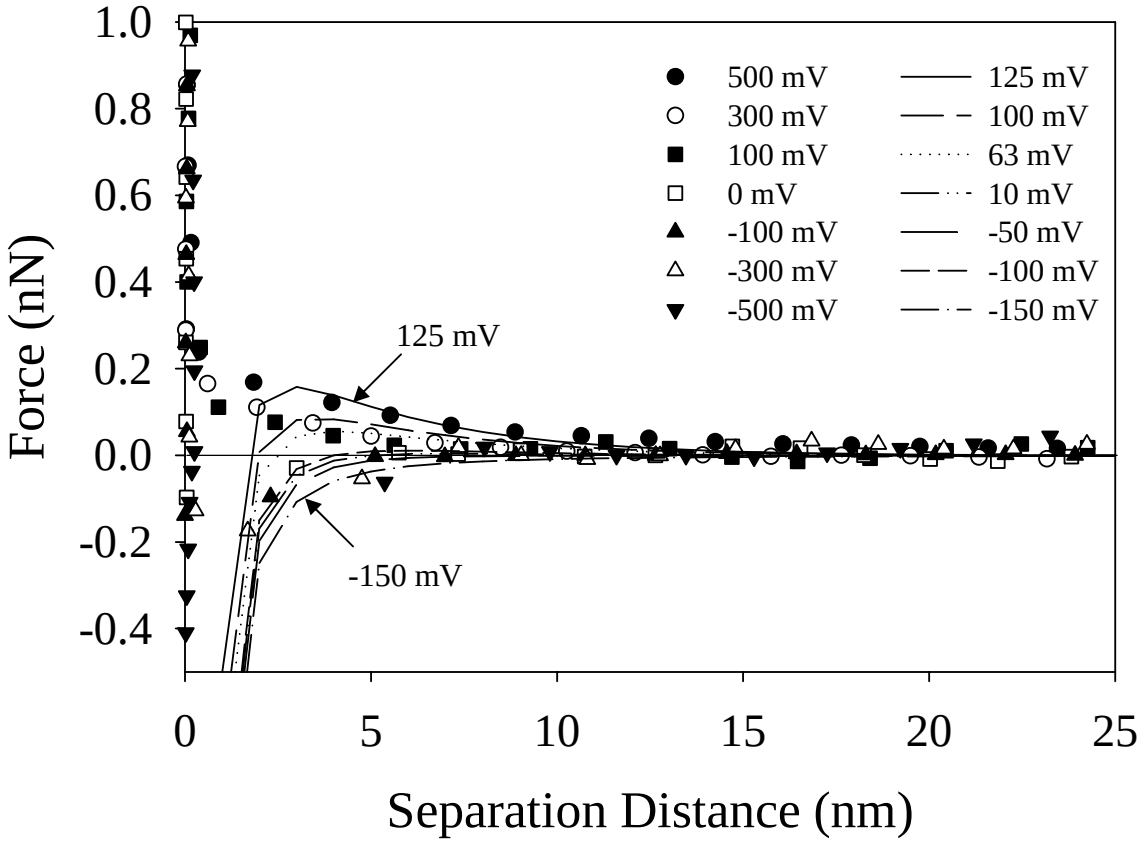

Figure 5.9. Measured and theoretical forces between a silicon nitride tip and the gold-coated plate in a 0.005 M NaCl solution at pH 6.42 as a function of applied potential (vs. Ag/AgCl).

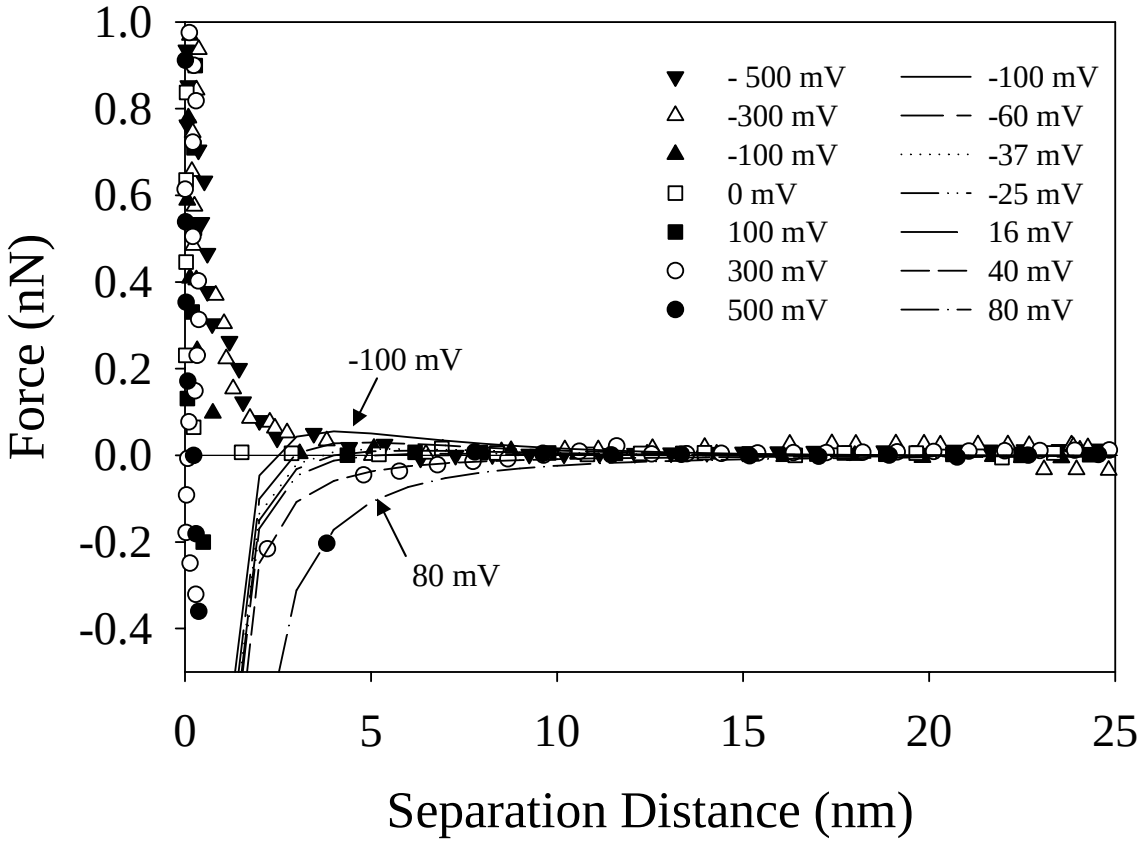

Figure 5.10. Measured and theoretical forces between a silicon nitride tip and the gold-coated plate in a 0.005 M NaCl solution at pH 9.08 as a function of applied potential (vs. Ag/AgCl).

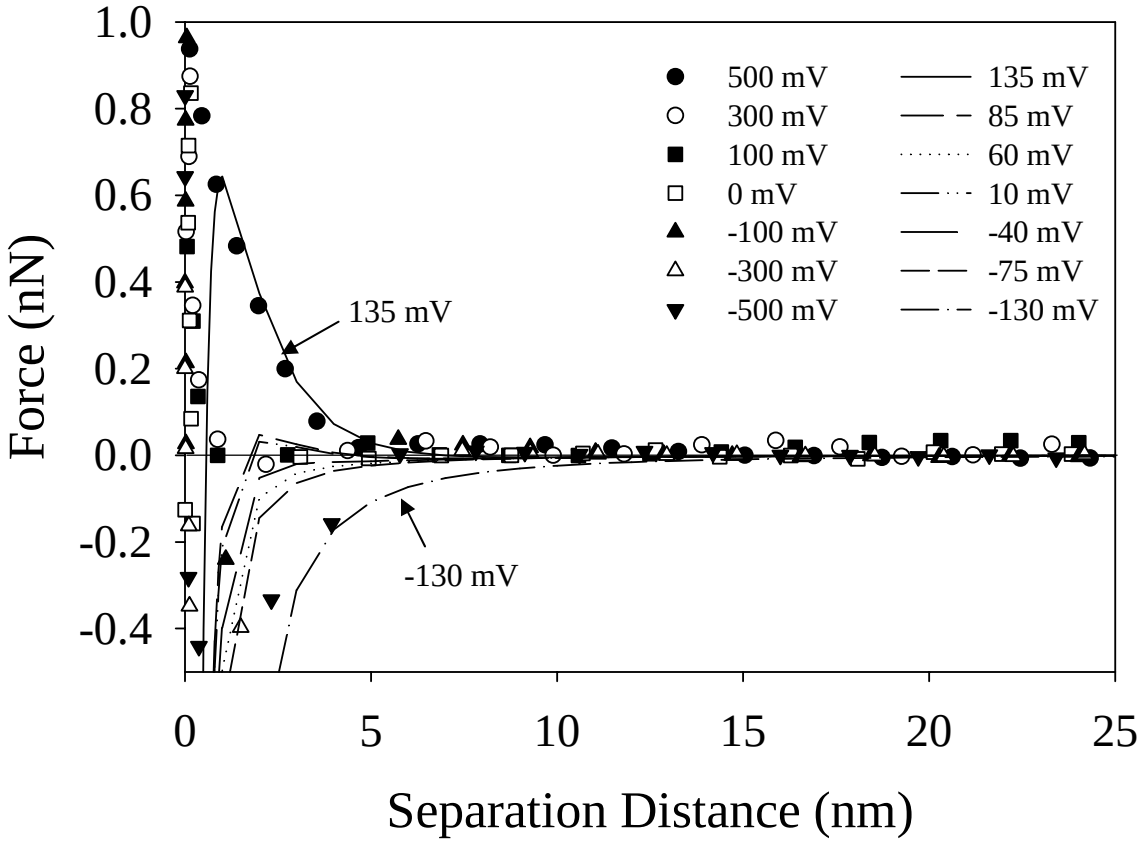

Figure 5.11. Measured and theoretical forces between a silicon nitride tip and the gold-coated plate in a 0.05 M NaCl solution at pH 5.34 as a function of applied potential (vs. Ag/AgCl).

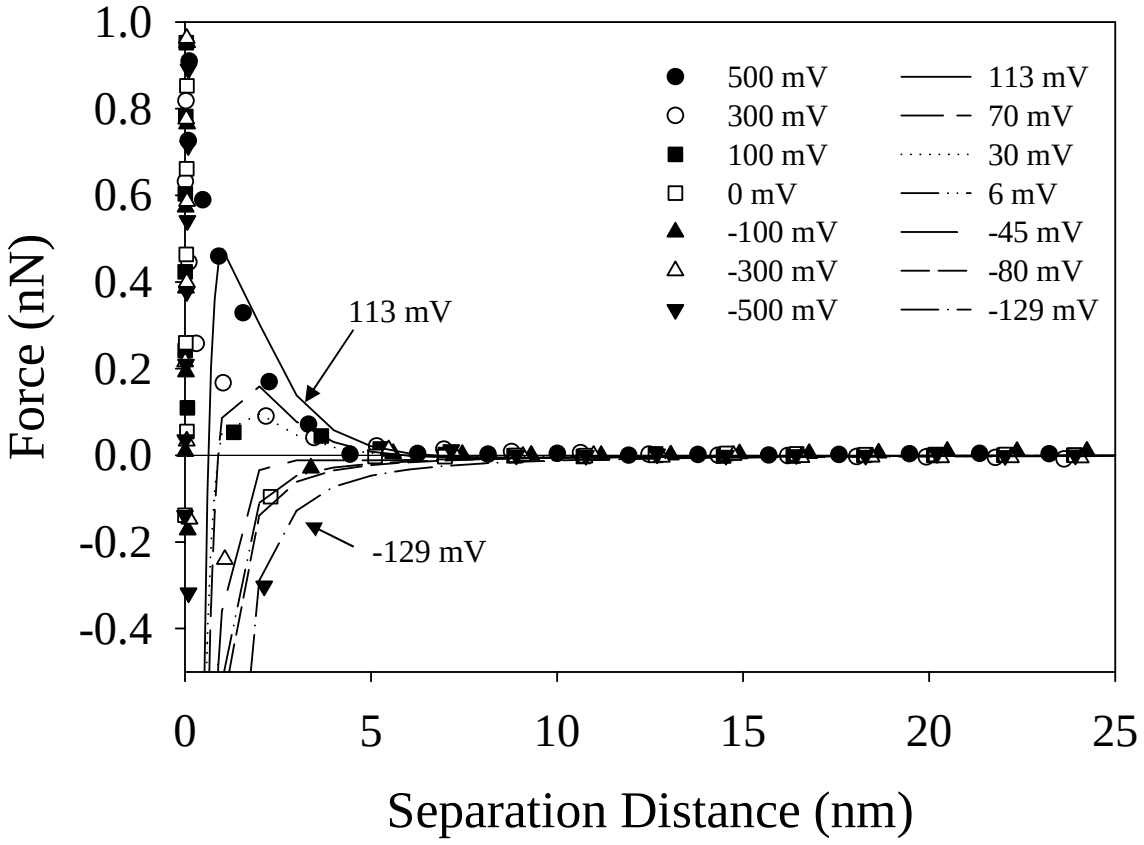

Figure 5.12. Measured and theoretical forces between a silicon nitride tip and the gold-coated plate in a 0.05 M NaCl solution at pH 6.00 as a function of applied potential (vs. Ag/AgCl).

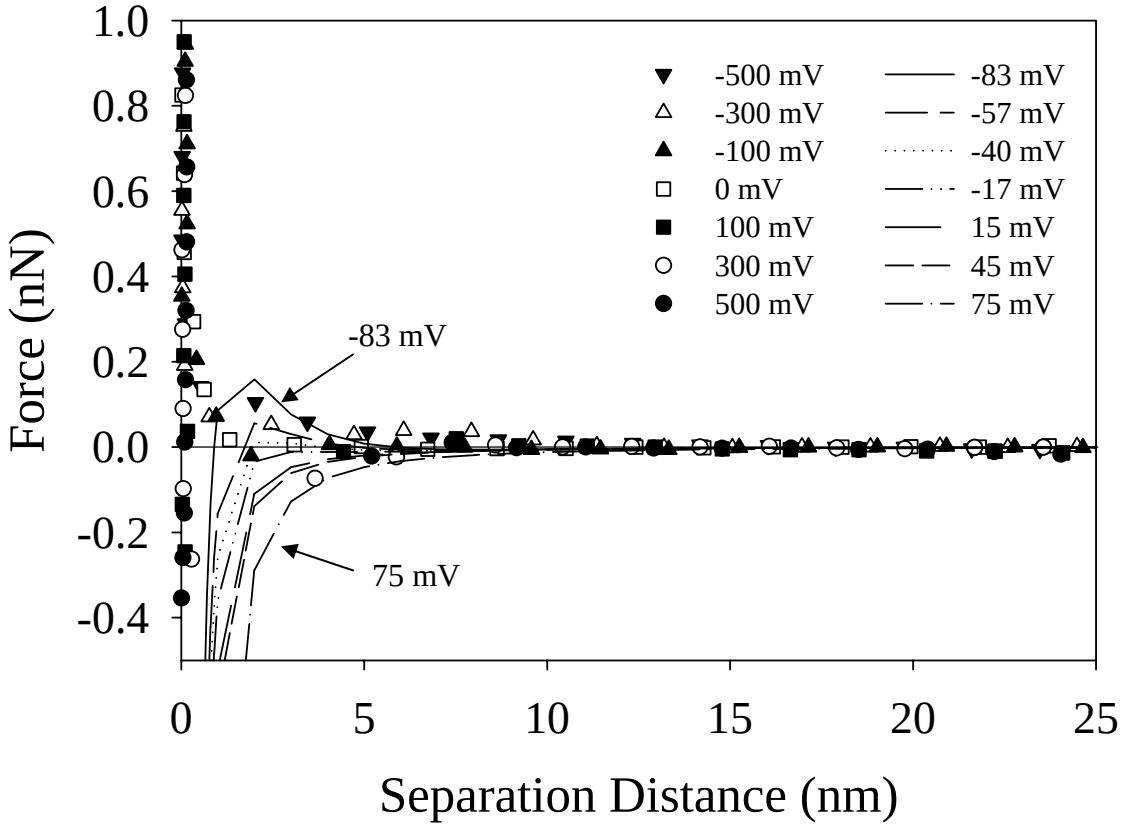

Figure 5.13. Measured and theoretical forces between a silicon nitride tip and the gold-coated plate in a 0.05 M NaCl solution at pH 9.63 as a function of applied potential (vs. Ag/AgCl).

5.5.3. Determination of Potential of Zero Charge

The potential of zero charge (E_{pzc}) is the applied potential where the surface charge is zero. There are many methods to determine the potential of zero charge, including: 1) cyclic voltammetry (Yang, 2003), 2) electrocapillarity method (Chen et al., 1996), 3) the crossed polarized metallic thread (Derjaguin et al., 1993), 4) the immersion method (Kim, 1973; Hamm et al., 1996), and 5) the differential capacity minimum method (Vorsina et al., 1939; Leikis et al., 1972). AFM can be used to provide alternative measurements of the potential of zero charge (Arai et al., 1996; Hillier et al., 1996).

In the force–distance curve, the effect of van der Waals and solvent interaction forces is negligible at larger separations. Therefore, the electrostatic force is dominant in this region. A change in applied potential that alters the repulsive force to an attractive one should reflect a surface potential at which the charge is zero, corresponding to the E_{pzc} (Hillier et al., 1996).

Figures 5.14–5.22 present the plots of the calculated surface potential using nonlinear Poisson–Boltzmann equation versus the externally applied potential onto gold surface. The results show that ionic strength has no significant effect on the E_{pzc}. On the other hand, the solution pH has a significant influence on E_{pzc}. At pH around 5 (Figures 5.14, 5.17, 5.20), the E_{pzc} occurred at an applied potential of approximately –50 mV. Once pH was increased, the E_{pzc} was shifted to the less negative potential as shown in Figs 5.15, 5.18, and 5.21. The change in E_{pzc} is as a result of the lower zeta potential of the gold surface. When the zeta potential is more positive, the applied potential has to be more negative to offset the positive charge. Thus, when the zeta potential is less positive, less negative applied potential is needed.

The summaries of the surface potentials determined by fitting the electrostatic force model at high solution pH are illustrated in Figures 5.16, 5.19, and 5.22. The relatively high potential of zero charge can be explained by the presence of a hydroxylated oxide layer at high pH (Thompson and Collins, 1992; Hu et al., 1997; Barten et al., 2003a). Therefore, the externally applied potential needs to be strongly positive to compensate for negative charges due to dissociated hydroxyl groups on the surface (Raiteri et al., 1996a).

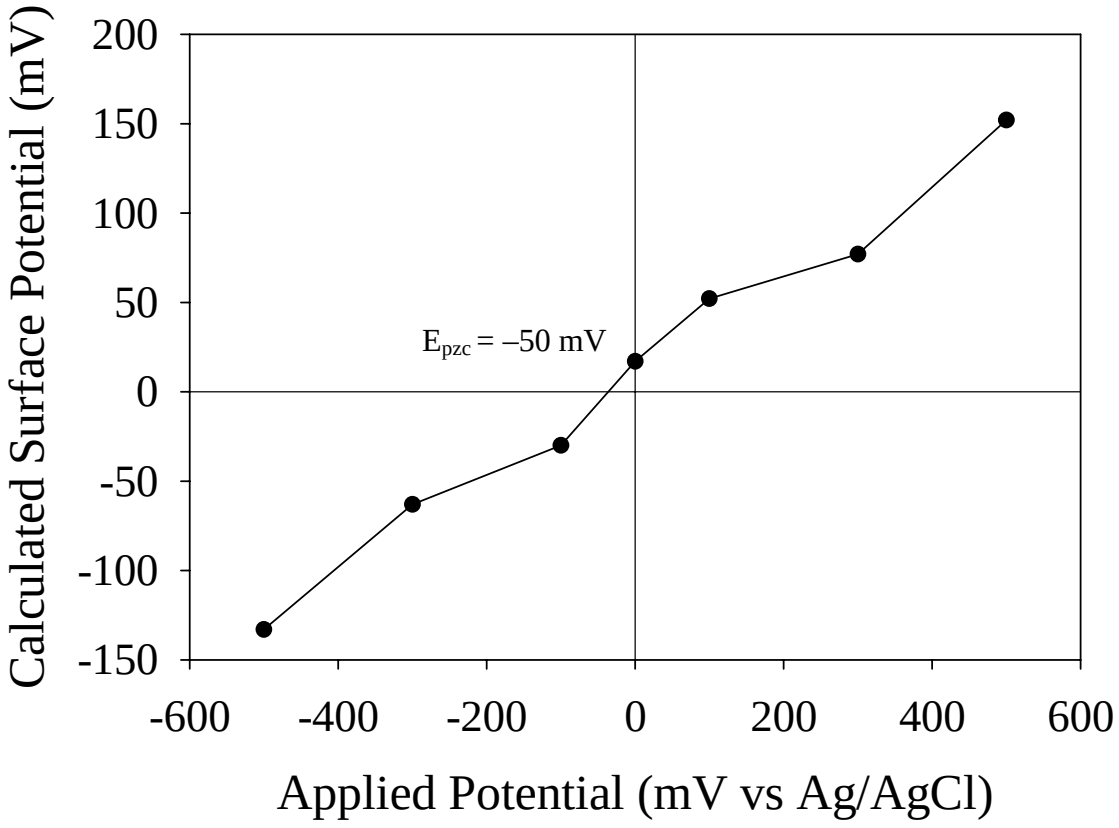

Figure 5.14. Surface potential of a gold substrate as a function of applied potential vs. Ag/AgCl as determined by a best fit of the theoretical model to experimental data in a 0.0005 M NaCl solution at pH 5.18.

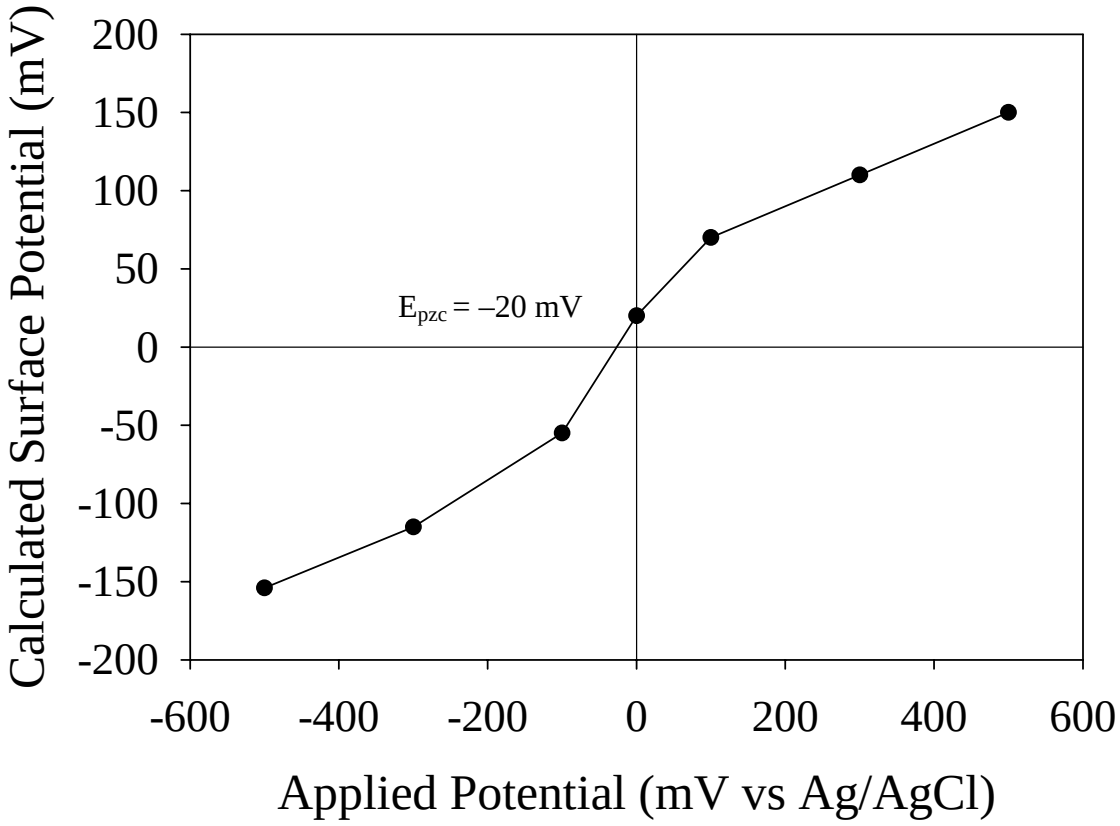

Figure 5.15. Surface potential of a gold substrate as a function of applied potential vs. Ag/AgCl as determined by a best fit of the theoretical model to experimental data in a 0.0005 M NaCl solution at pH 7.08.

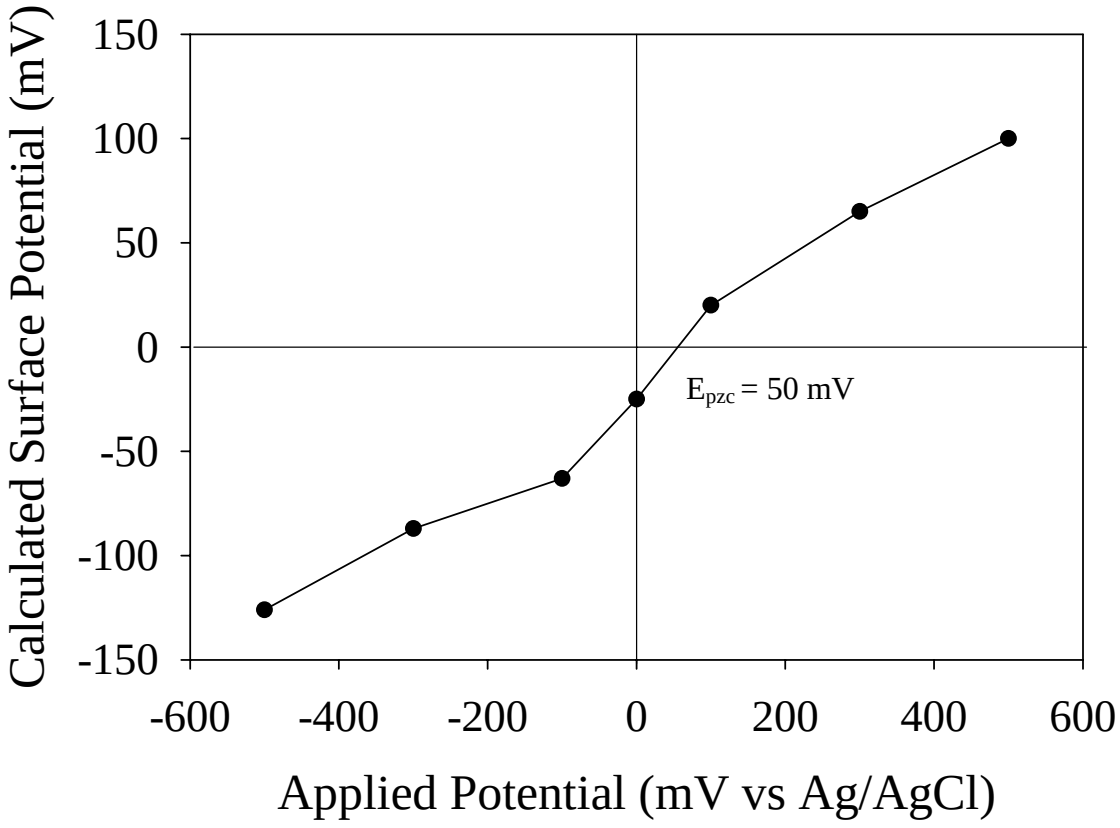

Figure 5.16. Surface potential of a gold substrate as a function of applied potential vs. Ag/AgCl as determined by a best fit of the theoretical model to experimental data in a 0.0005 M NaCl solution at pH 9.21.

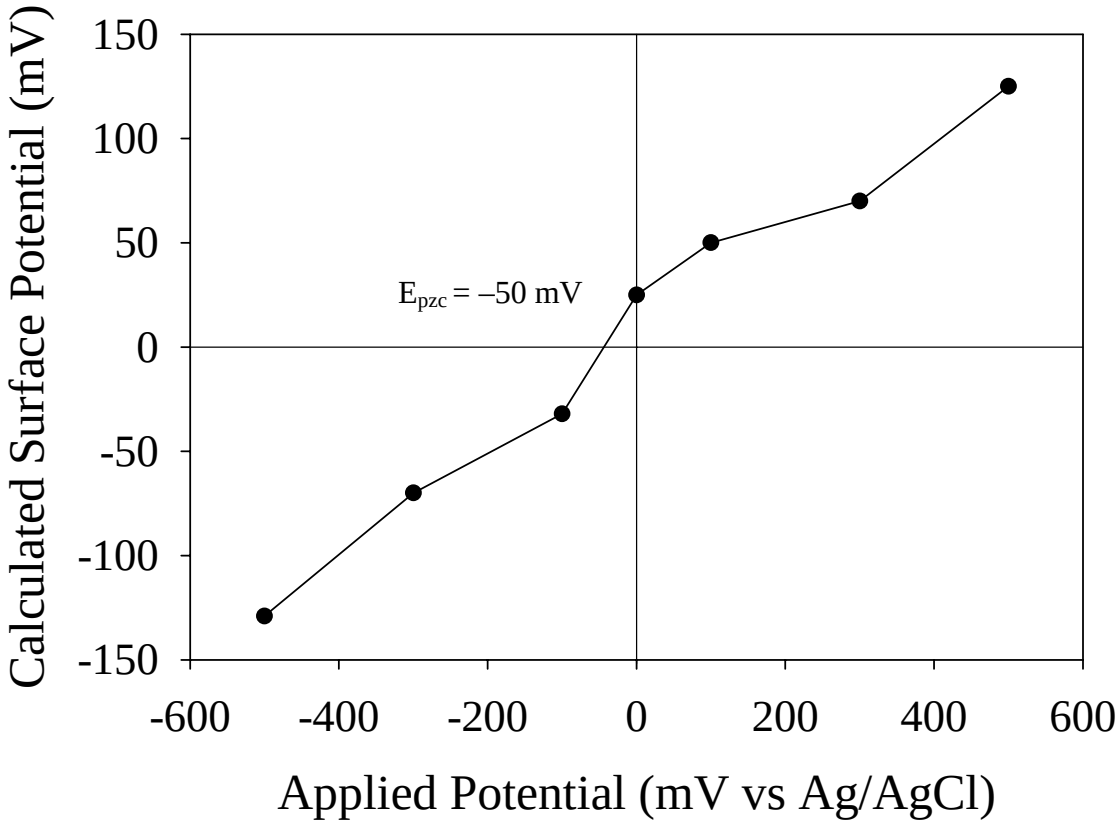

Figure 5.17. Surface potential of a gold substrate as a function of applied potential vs. Ag/AgCl as determined by a best fit of the theoretical model to experimental data in a 0.005 M NaCl solution at pH 5.07.

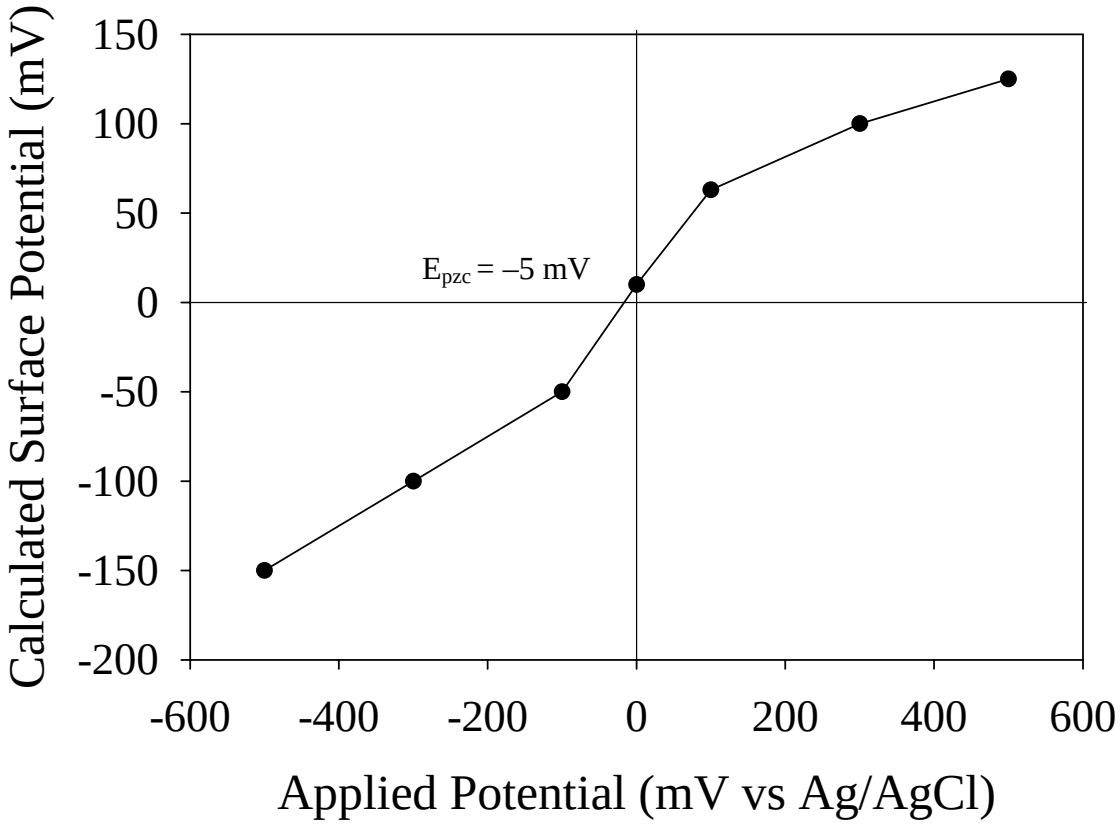

Figure 5.18. Surface potential of a gold substrate as a function of applied potential vs. Ag/AgCl as determined by a best fit of the theoretical model to experimental data in a 0.005 M NaCl solution at pH 6.42.

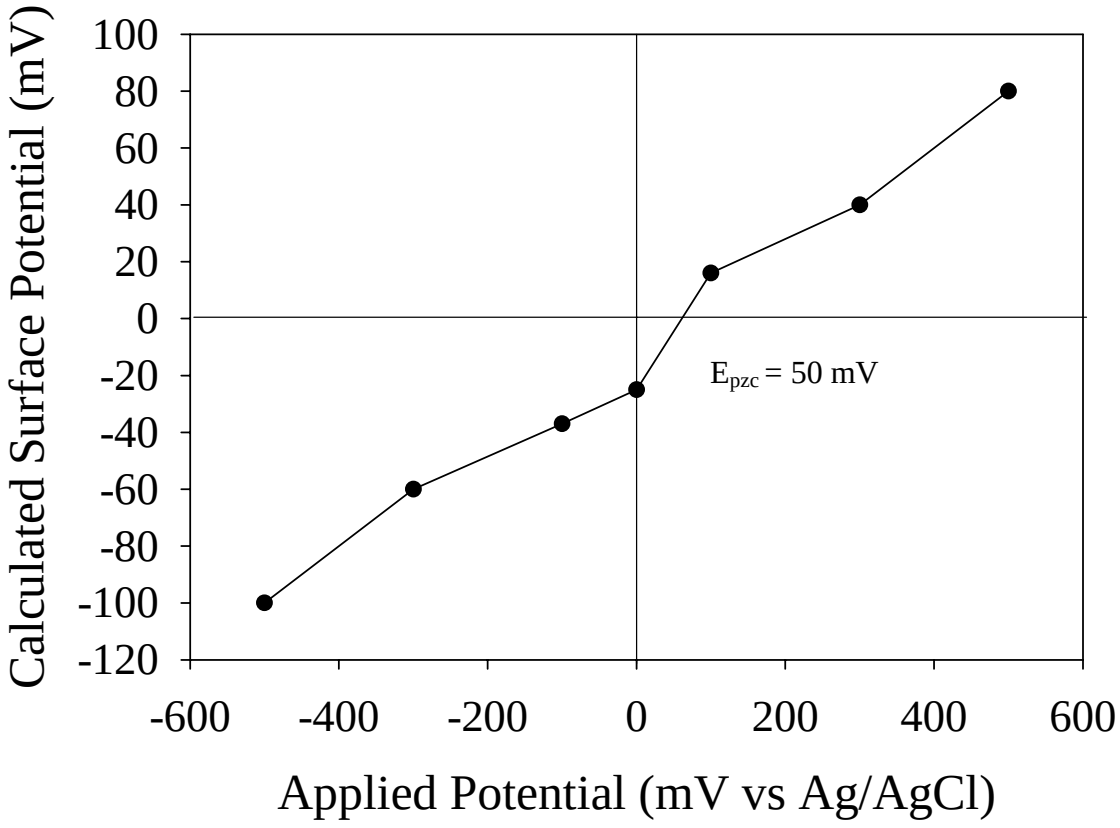

Figure 5.19. Surface potential of a gold substrate as a function of applied potential vs. Ag/AgCl as determined by a best fit of the theoretical model to experimental data in a 0.005 M NaCl solution at pH 9.08.

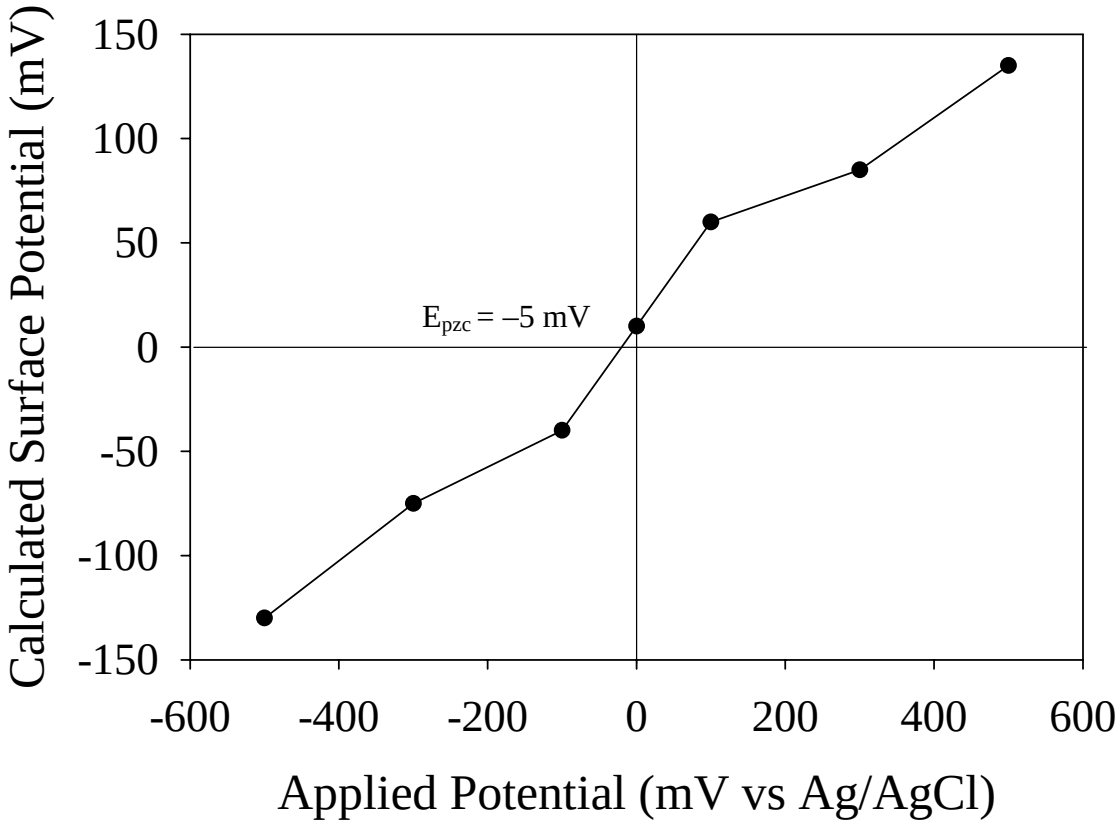

Figure 5.20. Surface potential of a gold substrate as a function of applied potential vs. Ag/AgCl as determined by a best fit of the theoretical model to experimental data in a 0.05 M NaCl solution at pH 5.34.

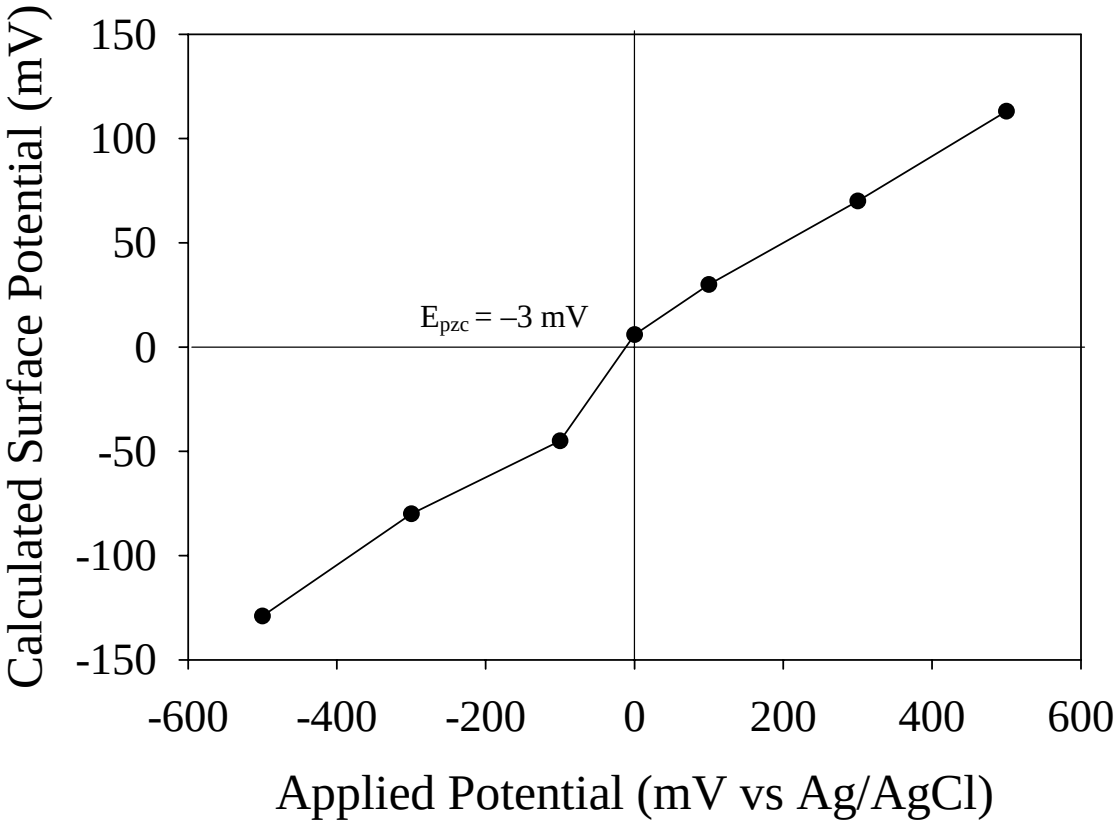

Figure 5.21. Surface potential of a gold substrate as a function of applied potential vs. Ag/AgCl as determined by a best fit of the theoretical model to experimental data in a 0.05 M NaCl solution at pH 6.00.

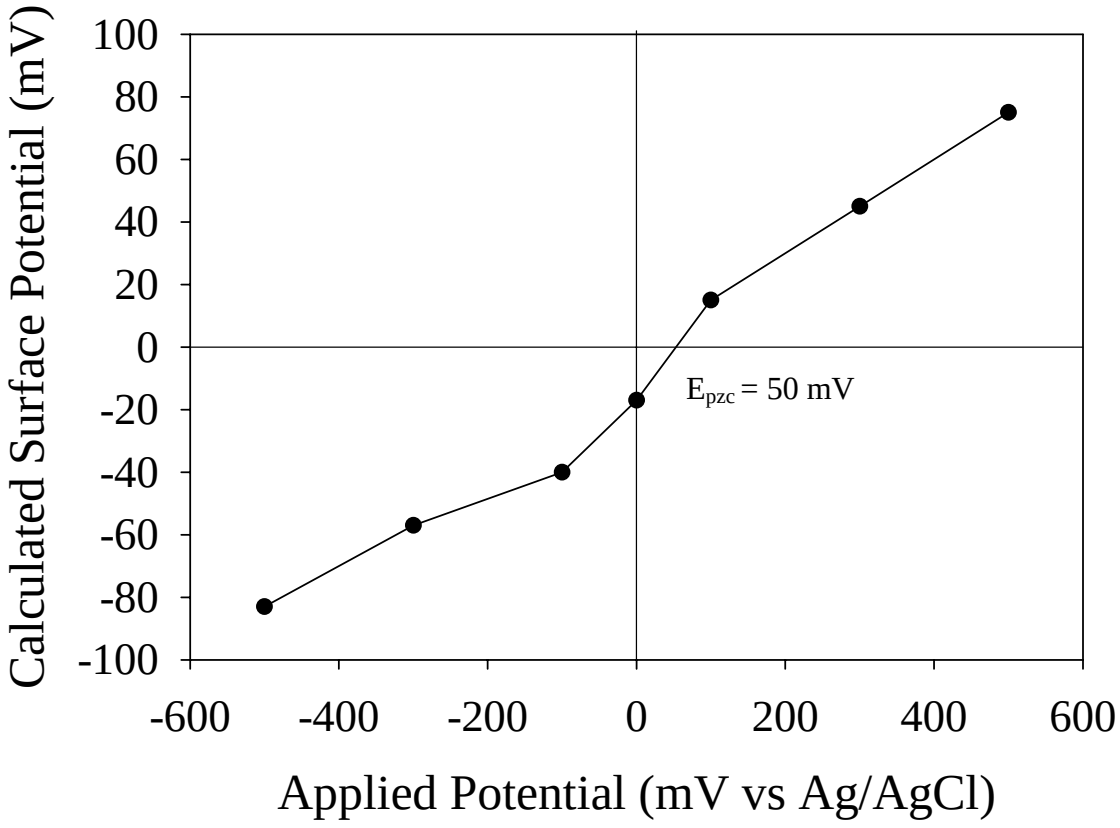

Figure 5.22. Surface potential of a gold substrate as a function of applied potential vs. Ag/AgCl as determined by a best fit of the theoretical model to experimental data in a 0.05 M NaCl solution at pH 9.63.

5.6. Summary

The electrostatic double layer strongly depends on the solution pH as well as on an externally applied potential. At open circuit potential, the interaction force between a silicon nitride tip and a gold-coated plate is due to their surface charges. At neutral pH values, where both surfaces have opposite charges, an attractive force is found. On the other hand, repulsion is observed at high solution pH since both surfaces have the same sign of surface charge.

An external potential is applied to gold surface and modifies its surface charge. Changes in measured force are obtained as the potential is varied. Results show that when the solutions are in the same pH range, the change of the force-curve behavior from repulsion to attraction is less pronounced in a high ionic-strength solution than in a low ionic-strength solution.

The potential of zero charge of a gold surface for all solution conditions is identified by means of force measurements. These findings allow a better understanding of the role of electrostatics in sorption processes and the possibilities for manipulating the sorption of charged macromolecules by applying an external potential to the interface.

CHAPTER 6

CHARACTERIZATION OF SORBED CETYLTRIMETHYLAMMONIUM BROMIDE ON A GOLD SURFACE BY FORCE MEASUREMENTS

6.1. Objectives

Recent studies have shown that the removal of organics from metal surfaces in a surfactant solution can be enhanced by applying potential to the surface (Rowe, 2000). An externally applied electric field leads to the modification of the surface charge (as discussed in Chapter V) and the rearrangement of surfactant molecules on the metal surface. To obtain a better understanding of this phenomenon, atomic force microscopy (AFM) is employed to investigate the effect of an applied electric field on the total interaction force between a standard silicon nitride AFM tip and a gold-coated plate in aqueous solutions of cetyltrimethylammonium bromide (CTAB), a cationic surfactant. The influence of surfactant concentration on the force curve is examined. Cyclic voltammetry is used to confirm the surfactant molecular reorganization that occurs on the gold surface as a function of the electrical potential.

6.2. Introduction

Sorption of surfactant molecules on surfaces in aqueous solutions has a critical importance in various industrial processes, such as detergency, water purification, colloidal stabilization, soil removal, oil recovery, and ore refinement by flotation.

Understanding the sorption mechanisms of surfactant molecules at the solid–liquid interface is an important step toward modeling these processes.

Surfactant molecules consist of two different parts: a hydrophilic headgroup and a hydrophobic tail group. A distinctive character of surfactant solutions is the formation of aggregates in the bulk at surfaces. In this work, we focus on surface aggregates. The main reason for the formation of aggregates is to minimize the interaction between the hydrophobic tail and the surrounding aqueous phase. The surfactant–surface interactions and head group interactions also play a role in aggregation. The presence of a charged headgroup governs an electrostatic driving force for sorption on oppositely charged surfaces. The surface charge on the substrate plays a significant role in determining the structure of the sorbed surfactant layer. The complexity of the surfactant interfacial behavior is enhanced by the interaction between co-ions and counterions with charged surfactant and surface groups (Tiberg et al., 2000). The differences in surface aggregates are due to the differences in surfactant–surface interactions (Jaschke et al., 1997). Hydrophilic surface interact mainly with surfactant headgroups and form the aggregate structures. These structures are dependent on the density of the electrostatically bound headgroups. In contrast, hydrophobic tail groups of surfactant preferentially sorb on hydrophobic substrates. For the sorption of nonionic surfactants, studies suggest that it occurs through the hydrogen bonding and/or dipole interactions (Rutland and Christenson, 1990; Rutland and Senden, 1993).

Sorption of surfactants molecules has been widely studied by means of neutron reflectometry, cyclic voltammetry, differential capacity, chronocoulometry, and AFM (Rusling and Couture, 1990; Adamczyk et al., 1999; Burgess et al., 1999; Schulz et al.,

1999; Atkin et al., 2000; Whitby et al., 2001; Burgess et al., 2001; Schulz et al., 2001; Avranas et al., 2002; Rojas et al., 2002; Zaman et al, 2002). The influence of the type and concentration of electrolyte as well as temperature, on the sorption of CTAB on a mercury surface, was studied by means of a cyclic voltammetry (Avranas et al., 2002). A condensed surfactant film at room temperature was formed on a mercury surface, as KBr was used as background electrolyte. In other electrolyte systems, the temperature must be quite low and the electrolyte concentration must be high for the formation of the condensed film. Rusling and Couture (1990) found that alcohols can induce sorption of CTAB and improve anion radical stability in reductions of organic compounds. Later, studies employed AFM to show the effect of alcohol on the surfactant structure and explain the interactions between alcohol molecules and surfactant micelles (Wall and Zukoski, 1999; Wanless et al., 1997).

The effect of solution pH on surfactant aggregates was also studied (Manne and Gaub, 1995). As the solution pH decreased, the space between CTAB micelles increased. The C_{14}TAB formed cylindrical aggregates on a hydrophilic surface of mica and showed meandering stripes. On the other hand, it formed hemicylindrical aggregates on hydrophobic substrates. Fleming et al. (2001) found that aggregation of CTAB on silica occurred at a significantly lower concentration at a high pH. This lower critical surface aggregation concentration results from the increased surface charge of the silica.

Liu and Ducker (1999) observed the temperature-dependent formation of the equilibrium CTAB structures on silica and mica substrates as well as a surfactant structural transition on a modified mica surface. They monitored the growth of

cylindrical domains with increasing temperature and the shrinkage of these domains with decreasing temperature.

Interaction forces between surfaces in surfactant solutions can be modified by adding a polyelectrolyte (Meagher et al., 2002). The polyelectrolyte alters the sign of the surface charge on both surfaces and leads to weak electrostatic interactions and the presence of attractive van der Waals forces. The higher the surfactant concentration, the more swelled the sorbed layer becomes. Liu et al. (1999) showed that the shape of surfactant aggregate was changed by the addition of salt. This phenomenon occurs because salt competes for binding sites on the substrate with coions coming from surfactant molecules. Increasing the surfactant counterion concentration also decreased the electrostatic repulsion between headgroups, resulting in the formation of aggregates above monomers and closer packing of headgroups. These results are similar to those obtained by Tiberg et al. (2000). The type of counterion also influences surfactant sorption, aggregate structure, and interaction forces (Velegol et al., 2000).

The different chain lengths of the surfactant tailgroup caused different polyelectrolyte-surfactant film morphologies (Liao and Higgins, 2002). The longer the chain length, the more protrusions were observed. Moreover, Sakamoto et al. (2002) discovered a stronger and longer-range attractive force when the chain length was increased.

Several studies have shown that force curves changed when the concentration of surfactant was varied from low to high. However, these experiments were performed on either hydrophobic surfaces or hydrophilic surfaces, while gold surfaces could not easily be categorized in either group (Jaschke et al., 1997). The hydrophobicity of a gold

surface depends on the counterion present in the solution. Halide anions have been known to have a specific sorption on the gold surface. When halide ions are present in the system, they sorb preferentially to the gold surface, resulting in a negative charge layer. In this case, gold would act as a hydrophilic surface and interact with charged headgroups of surfactant (Figure 6.1a). On the other hand, if halide ions are not present, hydrocarbon chains of surfactant sorb preferentially to the gold (Figure 6.1b).

Whitby et al. (2001) determined changes in the electrokinetic properties of surfaces due to the sorption of surfactant molecules. Similarly, the resulting coverage of surfactant onto electrode surface can be controlled by changing the electrode potential (Li and Kaifer, 1993; Suga et al., 1993; Marino and Brajter-Toth; 1993). The structure of surfactant aggregates at surfaces is of great importance in the removal of organics in industrial processes. Recent developments have shown that applied electric fields can aid in organic removal from metal surfaces (Rowe, 2002). The surfactant aggregates at the solution/surface interface change as the applied potential increases (Rowe, 2000; Burgess et al., 1999; Burgess et al., 2001). Therefore, AFM should be able to capture the effect of an externally applied potential on the surfactant sorption by means of force measurements. As electrosorption increases the local concentration of surface-active ions at the electrode interface, it may lead to the formation of various structures of surfactant such as spherical, semispherical, cylindrical, and semicylindrical micelles, as well as bilayers.

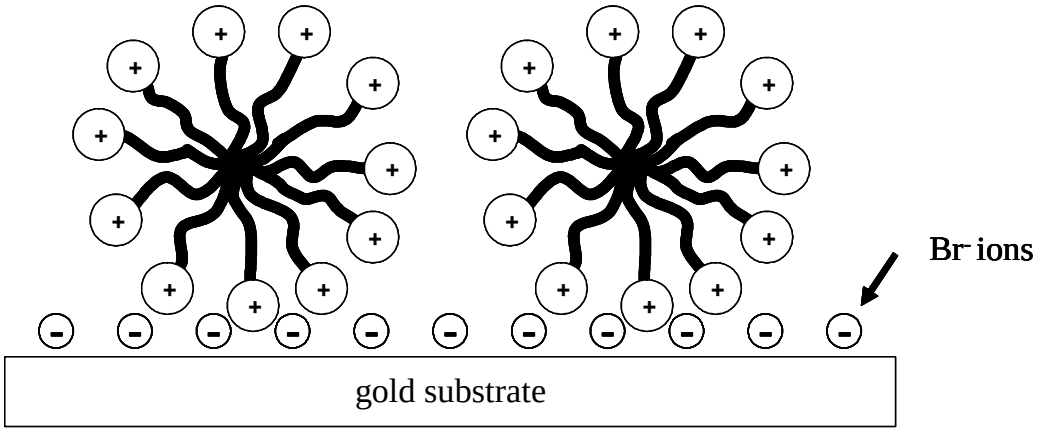

(a)

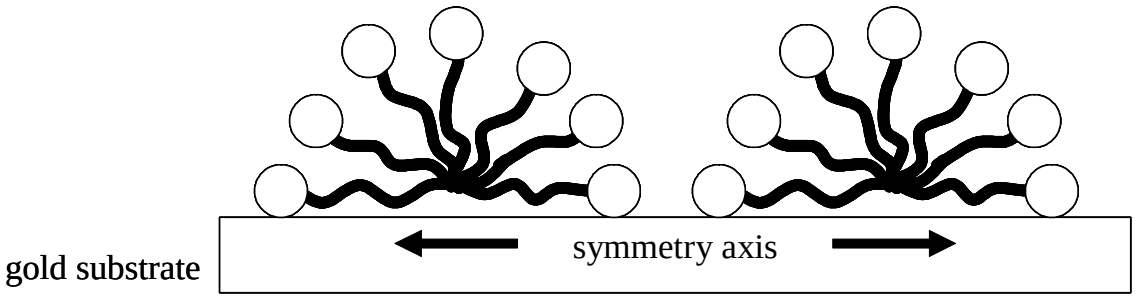

(b)

Figure 6.1. Cross-sectional models of two plausible C_{14}TAB aggregation morphologies proposed by Jaschke et al. (1997). (a) Halide ions are present in the system. (b) No halide ions are in the system.

6.3. Material and Methods

6.3.1. Chemicals

Cetyltrimethylammonium bromide (CTAB) from Aldrich (Milwaukee, WI) was used. All solutions were prepared using Millipore water with a resistivity of 18-MΩ/cm. Nitrogen was purged into the solution at least 30 min before starting an experiment to remove CO_2. HCl was purchased from Fisher Scientific (Fair Lawn, NJ) and methanol was purchased from Aldrich (Milwaukee, WI). It was found that the sorbed layer is in equilibrium with a bulk solution when the concentration is greater than the critical micelle concentration (CMC) (Schulz, 2000); therefore, the selected CTAB concentrations for the experiments were 1 mM (below CMC), 7mM (2.0 × CMC), and 10 mM CTAB solutions. The pH of CTAB solutions were between pH 6.7 and 7.

6.3.2. Cyclic Voltammetry

Cyclic voltammetry (CV) was performed by using a voltammetric analyzer (CV-50W) connected to a C2 stand (both from Bioanalytical Systems, West Lafayette, IN). The working electrode was a polished gold electrode. A platinum wire was used as an auxiliary electrode, and the reference electrode was Ag/AgCl electrode immersed in a 3-M NaCl electrolyte solution. A constant scan rate of 5 mV/s was used in all cyclic voltammetry experiments, and the resulting voltammograms were recorded using a computer. All solutions were prepared by using triply distilled 18-MΩ deionized water. Nitrogen was used to purge the solution and then flowed continuously over the top of the solution during the experiment. All measurements were conducted at room temperature.

6.3.3. AFM Measurements

Atomic force microscopy (model MMAFM-2, Digital Instruments, Santa Barbara, CA) was performed using a Nanoscope III instrument (Digital Instruments, Santa Barbara, CA) in contact mode with an E-scanner. Before use, the gold-coated substrate (Asylum Research, Santa Barbara, CA) with 20-nm continuous coating was freshly cleaned with ethanol (Aldrich, Milwaukee, WI) and a copious amount of DI water, then blown dry with nitrogen. Silicon nitride N-P cantilevers (Digital Instruments, Santa Barbara, CA) with nominal spring constants of 0.12 N/m were cleaned with DI water/HCl/DI water/Methanol/DI water prior to use.

All measurements were performed with a commercial AFM using its standard electrochemical fluid cell. A three-electrode design was used for electrochemical measurements, with the gold surface serving as the working electrode, a platinum counter electrode, and a commercial Ag/AgCl reference electrode. Electric potential was applied between the working electrode and the counter electrode. All electrode potentials are given with respect to this Ag/AgCl reference. All electrodes were connected to a potentiostat (Petite Ampere, Model LC-3E, Bioanalytical Systems, West Lafayette, IN). Samples were manually injected into a liquid cell, sealed with an O-ring, and allowed to sorb for 30 min before measuring the interaction force. The scan rate was varied in the range of 5–10 Hz. The integral and proportional gains were between 0.5–1. All experiments were performed at room temperature.

6.4. Results and Discussion

6.4.1. Electrochemical Studies

Sorption of CTAB onto the gold surface was initially examined by means of cyclic voltammetry experiments. All experiments were conducted using a 7 mM CTAB solution without any addition of a supporting electrolyte. Since this concentration was twice the CMC, the solution was a mixture of micelles and the monomer of CTAB (Burgess et al., 1999).

Figure 6.2 shows the current versus potential curve of a 7 mM CTAB solution. There was only one distinct peak observed at an applied potential of 500 mV (vs. Ag/AgCl). This peak corresponded to the phase transition between state A (<500 mV vs. Ag/AgCl) and state B (>500 mV vs. Ag/AgCl). Burgess et al. (1999) studied the sorption of sodium dodecyl sulfate (SDS) onto gold and found the transition between a hemimicellar aggregation state and a condensed assembly of the surfactant molecules to occur around 390 mV (vs. Standard Calomel Electrode).

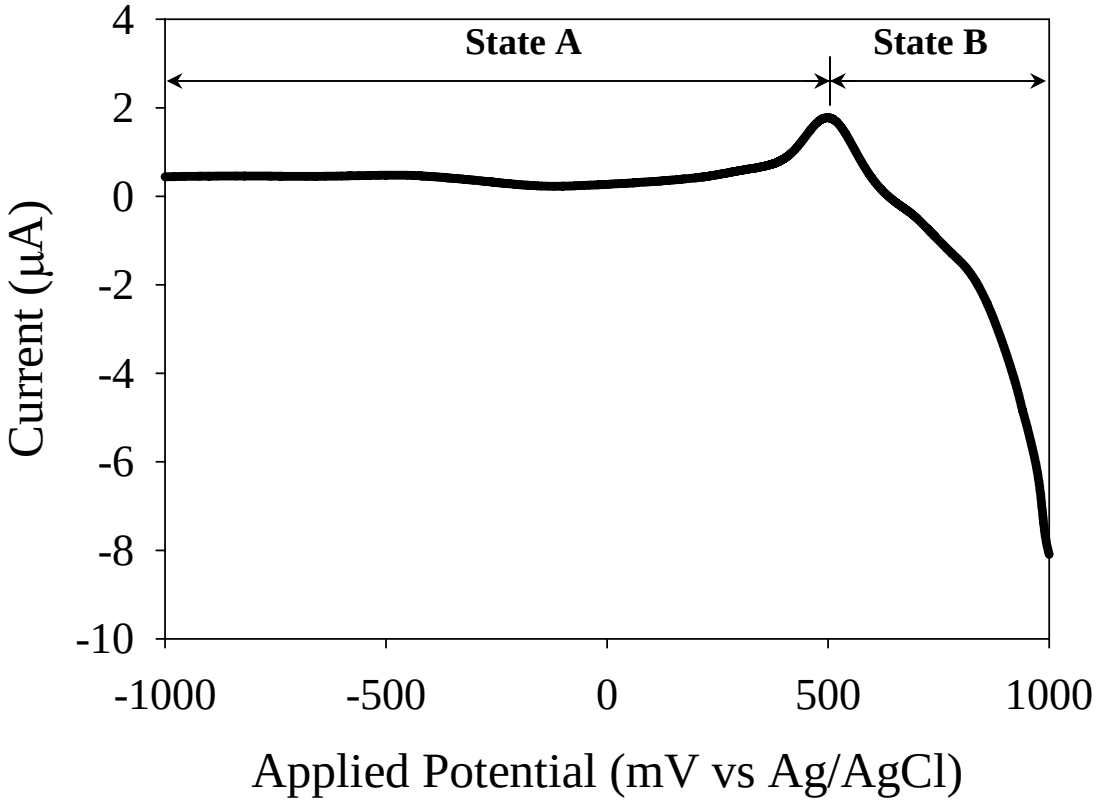

Figure 6.2. Cyclic voltammogram representing current vs. potential curve for a 7 mM C_{14}TAB solution at 5 mV/s.

6.4.2. AFM Measurements

Monitoring both the interaction force and surfactant image simultaneously can provide useful information on surfactant sorption. The interaction force should change as sorption changes the surface characteristics, such as the decay length of the repulsion, the force at which an instability occurs, and the magnitude of the instability (Fleming and Wanless, 2000).

Effect of Applied Potential

In order to compare the results from the electrochemical study, the applied potential was varied from –1000 to 1000 mV (vs. Ag/AgCl). As mentioned before, when halide ions are present in a system that consists of a gold surface, they sorb onto gold and form a negative layer on the surface. The sorption is driven primarily by the electrostatic interaction between the positively charged headgroups of CTAB and the surface, leading to full cylindrical aggregates (Jaschke et al., 1997) as shown in Figure 6.1a. The interaction forces between a silicon nitride tip and a gold surface in a 7 mM CTAB solution as a function of an applied potential is shown in Figure 6.3. At the open circuit potential (OCP), a force curve was qualitatively consistent with previous AFM studies of sorbed cationic surfactant layers (Liu and Ducker, 1999; Velegol et al., 2000; Teschke et al., 2001). When the tip approaches the surfactant structure, it experiences an electrostatic repulsion, until it reaches a so-called instability separation, where the tip pushes through the sorbed layer and contacts the substrate. This instability distance provides a measure of the sorbed layer thickness, which is ~5 nm in this case. This distance corresponds to the diameter of cylindrical micelle-like aggregates of CTAB (~5 nm) that were observed by

Sakai et al. (2001). At a sufficiently large applied force (~4.7 nN) the surfactant layer is removed from the space between the tip and the surface. Since the gold surface is negatively charged, it attracts the positively charged surfactant molecules. The tip is almost neutral charged at this pH. Therefore, the effect of surfactant molecules sorbed on the tip is negligible compared to the effect of molecules sorbed at the gold interface.

The force curves with the negatively applied potentials (–1000 to –250 mV (vs. Ag/AgCl)) were similar to that at OCP, but the instability distance decreased to around 3.8–4.4 nm, and the repulsive force was reduced to approximately 3.7–4.3 nN. This behavior can be explained by the hypothesis that, when the surface bears negative charge, halide ions are repelled from the surface. The surfactant molecules are allowed to contact with the surface. The surface attracts the positively charged headgroups of the surfactant, and surfactant molecules can form either full cylindrical aggregates or bilayers on it as shown in Figure 6.4a. As the applied potential becomes increasingly negative, halide ions are repelled from the surface at greater extent; therefore, the instability distance decreases with increasing negative potential. The slight reduction in the magnitude of the force with increasing negative potential on the surface can also be explained by the same hypothesis. Surfactant molecules are larger than halide ions, and there is a limit in the number of surfactant molecules that can be sorbed on the surface. This results in a limit in the capacity of the sorbed layer to neutralize the charge on the surface. As the surface charge becomes increasingly negative, the range of the electrostatic potential increases. Since the tip is positively charged at the experimental pH conditions, the effect is a net reduction in the magnitude of the repulsive interaction force.

It is observed that the characteristics of force curves--both magnitude of force and instability distance--for applied potentials of 250 and –250 mV (vs. Ag/AgCl) are almost identical. This could be because at 250 mV (vs. Ag/AgCl) the positive potential is insufficient to overcome the negative charge of the surface; therefore, the gold surface still carries a negative charge and as a result the surfactant aggregation is similar to that at –250 mV (vs. Ag/AgCl).

However, at higher potentials (500 to 1000 mV (vs. Ag/AgCl)), the positive charge overcompensates the charged layer of anions. The surface now bears a positive charge. Consequently, the layer of halide ions is still present and sorption of surfactant headgroups takes place. The shape of aggregate should be changed since both surface and headgroup have the same sign of charge. Some of the surfactant molecules are repelled from the surface, while the rest form the hemicylindrical aggregates on the surface (Figure 6.4b). This aggregation behavior is due to the exclusion of the hydrophobic tails of the surfactant molecules from an aqueous solution. The thickness of the sorbed layer is reduced, consistent with the results from force measurements. In addition, the repulsive force between the probe and the sample is weak, as an increasing positive potential is applied, suggesting that the surface is not fully covered with surfactant (Figure 6.4c).

Combining the results from the AFM experiment with those from the electrochemical experiment (cyclic voltammetry), the differences were observed in the magnitude of the repulsive force between the tip and the surface at potentials of states A (<500 mV vs. Ag/AgCl) and B (>500 mV vs. Ag/AgCl). The same was observed in the differences in the decay length. All force curves in state A are comparable. They have a larger instability distance and longer decay lengths than those of state B. We can also

make a comparison between CTAB experiments with SDS experiments that are reported in the literature (Burgess et al., 1999). In the experiments of Burgess et al., the change in force characteristics, as the potential moved from one phase to another, was determined. They found that SDS formed hemimicellar aggregates on a gold surface due to the absence of halide ions in the system. The instability force was 0.5 nN and the decay length was 3 nm, which was consistent with the length of SDS molecule. As the transition occurred, because SDS was in a condensed state, it required a higher force to remove the sorbed layer from the surface, and the decay length was longer than when it was in a hemimicellar state.

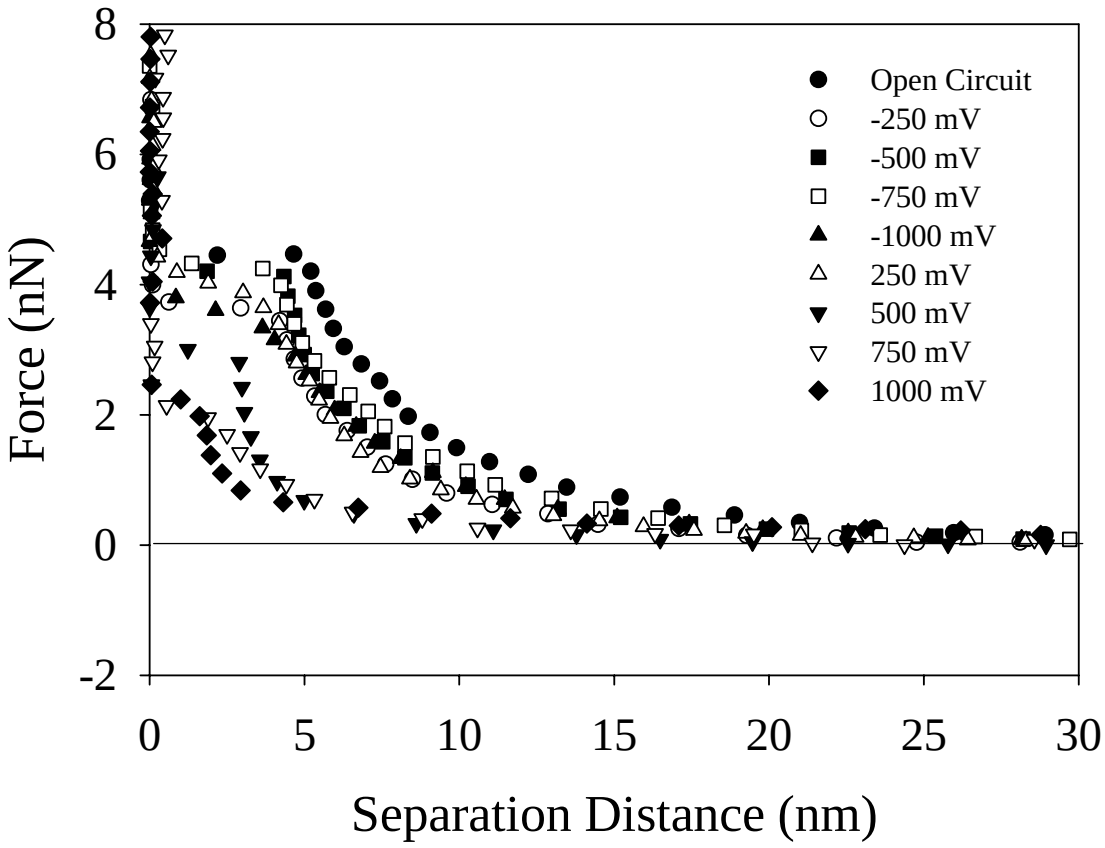

Figure 6.3. Force vs. separation distance curves between a silicon nitride tip and a gold surface in a 7 mM CTAB solution as a function of an applied potential.

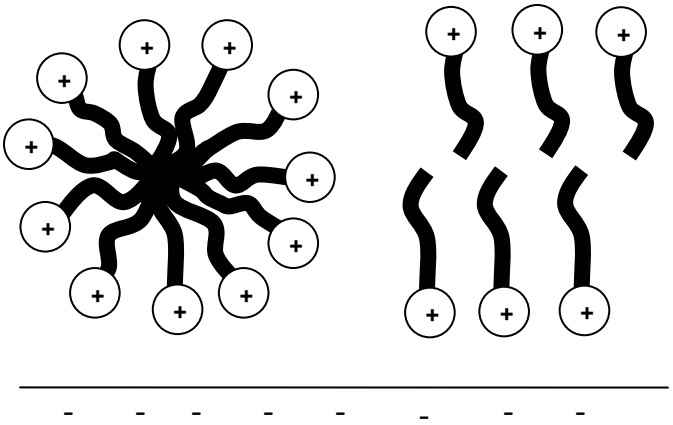

(a)

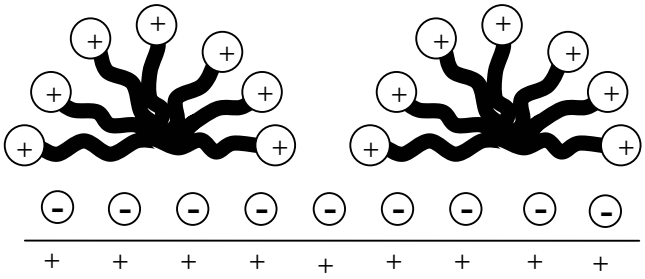

(b)

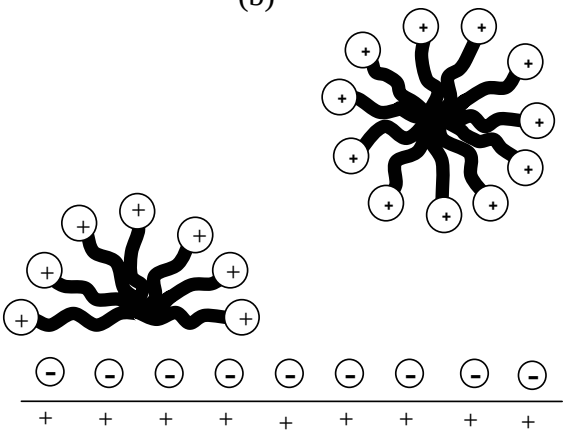

(c)

Figure 6.4. Plausible C_{14}TAB aggregate morphologies as a function of applied potential. (a) Full cylindrical aggregates and bilayers. (b) Hemicylindrical aggregates. (c) Hemicylindrical aggregates with partial coverage.

Effect of Surfactant Concentration

The force measured in DI water (pH 7.2) is shown in Figure 6.5. An attractive force is found due to the surface charge on both a silicon nitride tip and a gold surface. At this pH, the silicon nitride carries a positive to a nearly neutral charge, while the gold surface bears a negative charge. When the forces were measured in various surfactant concentrations, a repulsive force was observed, which became stronger as the surfactant concentration was increased.

Figure 6.6 illustrates the force versus separation distance between the tip and the gold substrate in a 1 mM CTAB solution under various potential values. This surfactant concentration was below CMC. At OCP, a weaker repulsive force with a jump-in distance of 3.9 nm was detected. The behavior of the interaction force under applied potential is similar to that observed previously in a 7mM CTAB solution.

Force measurements were also performed in a much higher concentration (10 mM) than the CMC of CTAB solution (Figure 6.7). A strong repulsion was observed, accompanied by a longer decay length. The instability is located at 5 nm. The applied potential exhibits the same effect on the force behavior as seen before. This result confirms that the aggregate morphology for pure ionic surfactant systems remains unchanged above the CMC (Tiberg et al., 2000).

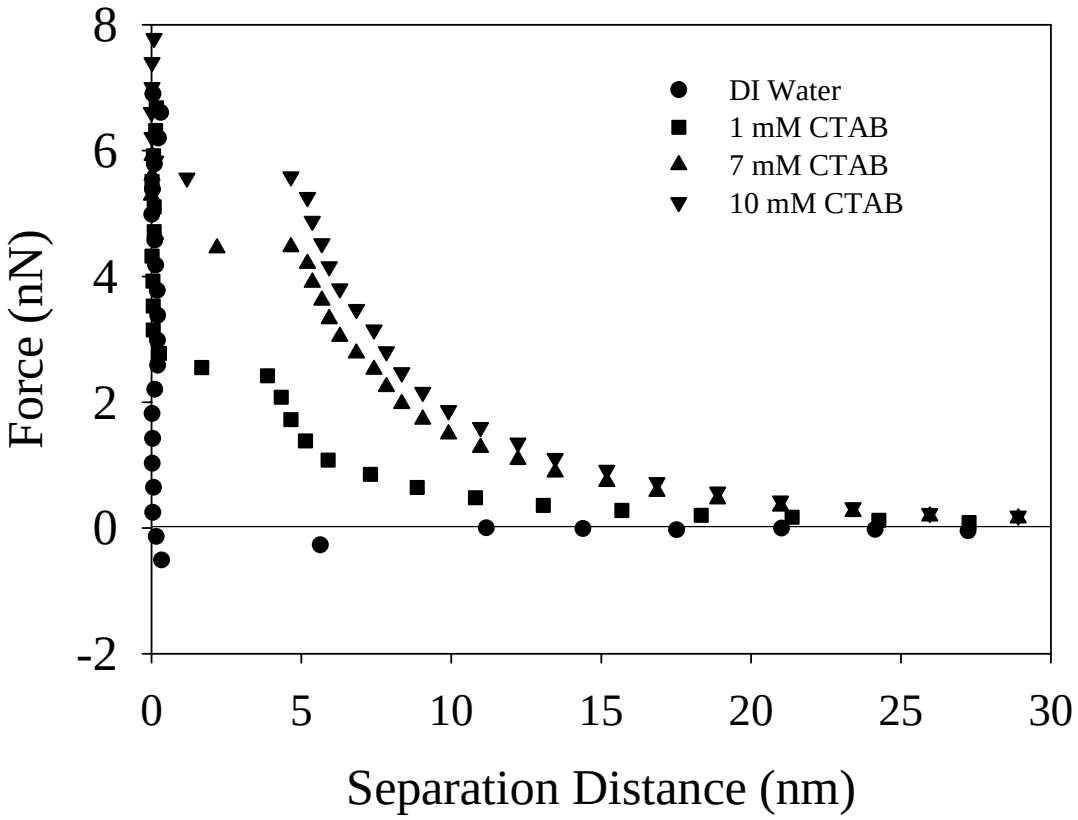

Figure 6.5. Effect of the surfactant concentration on force measurements.

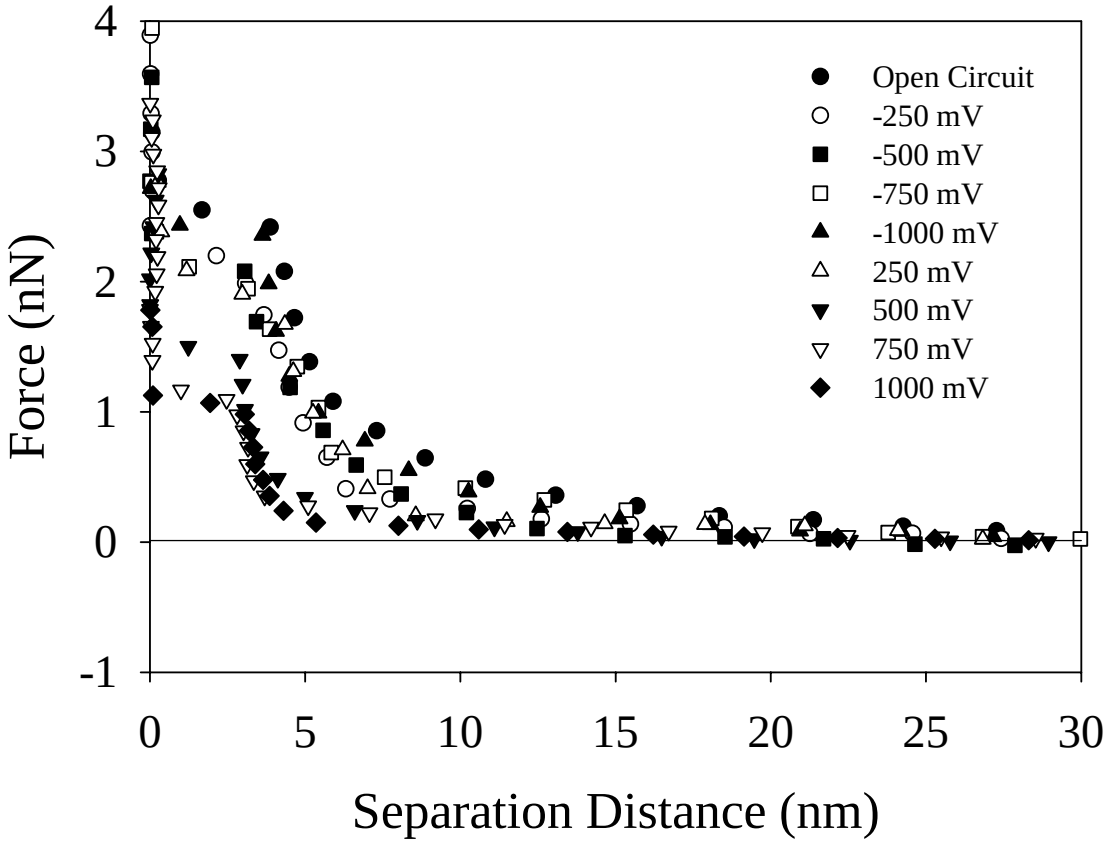

Figure 6.6. Force vs. separation distance curves between a silicon nitride tip and a gold surface in a 1 mM CTAB solution as a function of an applied potential.

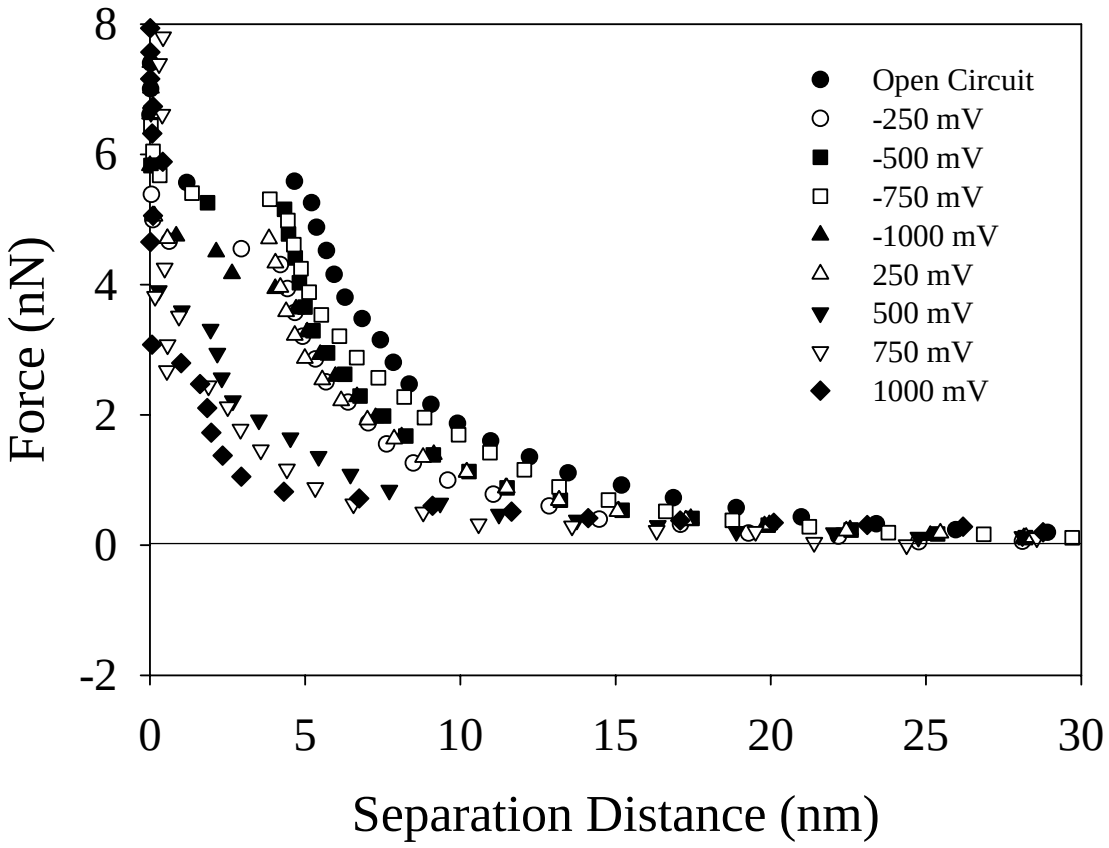

Figure 6.7. Force vs. separation distance curves between a silicon nitride tip and a gold surface in a 10 mM CTAB solution as a function of an applied potential.

6.5. Summary

AFM is used to study the total interaction force between a standard silicon nitride AFM tip and a gold-coated plate in a cationic surfactant solution of cetyltrimethylammonium bromide (CTAB), under various values of applied potential. The force measured in a system containing only DI water exhibits an attractive force. However, when surfactant is in the system, a repulsive force is observed. As the surfactant concentration increases, the repulsion becomes stronger and the decay length is longer. Under an applied potential from –1000 to 250 mV (vs. Ag/AgCl), the features of force curves are similar. At a higher positive potential, the repulsive force is weaker, the decay length is shorter, and the instability distance decreases indicating the formation of hemicylindrical aggregates. Results from an electrochemical study (cyclic voltammetry) indicate that the surfactant molecular reorganization that occurs is a function of the electrical potential. Further studies involving structural imaging by AFM are needed to investigate the formation of surfactant aggregates and confirm further these results.

CHAPTER 7

CONCLUSIONS AND RECOMMENDATIONS

7.1. Conclusions

In this work, AFM was used as a tool to study the sorption of different species, including copper ions and surfactant molecules, from aqueous solutions and effects of sorption on interparticle forces. An externally applied potential was also employed to modify surface charges and electrostatic forces. This process is called electrosorption.

The interaction force between a spherical silica particle and a smooth glass plate was directly measured using AFM. The influence of metal ion concentration and solution pH and ionic strength on metal ion sorption by a single silica particle on the force measured between the particle and a plate was also investigated. Results showed that the interaction force changed as a function of time during sorption, and a surface charge reversal was revealed. The maximum concentration that had no effect on the original force was determined. The zeta potential of the silica particle during sorption was determined by comparing the results from force measurements to theoretical values.

Use of force volume mode AFM allowed measurements of the interparticle force and surface topography simultaneously. The selected model system consisted of a silicon nitride tip and a silica substrate. The reason for using silica was that its surface charge can be modified by regulating the pH. The phase of silicon nitride used in commercial AFM cantilever tips was also determined in this work. Previous studies (Subramaniam et

al., 2001; Chin et al., 2002) demonstrated copper uptake by silica. Our hypothesis was that metal ion sorption not only changes the surface charge but also causes or enhances surface heterogeneities with respect to surface charge. The effect of metal ion concentration was studied with AFM at a low ionic strength. This study proved the hypothesis by showing changes in the interaction force, as well as in the surface topography, as a result of copper sorption. The solution ionic strength was also varied and the measurements were repeated in order to confirm the sorption effects. The hypothesis was that since the Debye length decreases as the ionic strength increases and vice versa, this effect should be reflected in the surface charge topography. This hypothesis was also proven.

An external potential was also applied to an electrically conductive surface in order to induce sorption by altering the surface charge and the electrical double layer of the surface (Yang et al., 2001). AFM was employed to probe the double layer force between a standard silicon nitride tip and a gold-coated substrate. The potential was applied only to the gold surface. At open circuit potential, the observed force was due to the zeta potential of both silicon nitride and gold. As the potential was varied, the interaction changed. The influences of solution pH and ionic strength were also studied. The measured force was compared to theoretical calculations using a nonlinear Poisson–Boltzmann equation. The potential of zero charge of gold surface for each set of solution conditions was also identified by means of force measurements.

The potential applied on the sorbed surface could also control the sorption of surfactant molecules (Li and Kaifer, 1993; Suga et al., 1993; Marino and Brajter-Toth; 1993). The total interaction force between a standard silicon nitride AFM tip and a gold-

coated plate in cationic surfactant solutions of cetyltrimethylammonium bromide (CTAB) was examined under various applied potential values. The force measured for a system containing only DI water exhibited a weak attractive force due to the surface potentials. The force was found to change significantly in the presence of surfactant. The effect of surfactant concentration was investigated. The features of the force–distance curve that were found to change are the thickness of sorbed layer, the decay length, and the magnitude of force at instability. Electrochemical experiments were also conducted to verify the findings from AFM.

Based on the findings of this study, the following conclusions can be drawn:

- AFM force measurements agree with the DLVO theory, except at very small separation distances, in all the solution conditions examined. The constant-surface-charge model can correctly describe the interaction force between two charged surfaces.
- A discrepancy between experimental data and expected results from the DLVO theory is consistently shown at short distances, where a maximum in the force is predicted. This is probably due to non-DLVO repulsion.
- The force–distance profiles between a silica sphere and a glass plate in a variety of NaCl solutions without copper ions indicate that the magnitude of the electrostatic repulsion decreases with increasing ionic strength.
- The rate of sorption decreases as the copper ion concentration is decreased.
- The ionic strength of background electrolyte has no significant or little effect on sorption dynamics of copper ions by silica.

- Metal concentration and solution ionic strength have no effect on sorption equilibrium indicating that, for the experimental conditions used in this study, the surface sites of the silica particle are fully monolayer covered by copper ions.
- The transient zeta potential of the silica particle during sorption of copper ions is determined *in situ* by representing the direct force measurements with the DLVO theory.
- The standard silicon nitride AFM tip employed in this study behaves as silicon nitride of alpha phase silicon nitride or electronic grade silicon nitride, which consists of 94% alpha phase and 6% beta phase.
- Force-volume AFM can be used to detect heterogeneously charged regions on surfaces.
- The appearance of islands along with results from force measurement suggest that copper ions sorb on the silica surface.
- Copper sorption increases as the concentration of metal ions is increased.
- The size of islands is decreased as the solution ionic strength is increased. This behavior is due to shortening in the Debye length.
- The islands represent the positively charged regions on the surface that result from the sorption of copper ions.
- The silicon nitride–gold interaction is accurately predicted by the DLVO theory, except at very small separations, where additional repulsion is observed.
- A divergence at small separations is attributed to an overestimate of the Hamaker constant, an ill-defined location for the plane of surface charge, and the presence of repulsive solvent forces.

- The electrostatic double layer shows a strong dependence on the solution pH as well as on an externally applied potential. When the solutions are of the same pH range, changes in the behavior of force from repulsion to attraction are less pronounced in a high ionic strength solution than in a low ionic strength one.
- When CTAB is present in the system, a repulsive force is observed. As the surfactant concentration is increased, the repulsion becomes stronger and the decay length is longer.
- The features of force–distance curves are similar for all experiments performed with the applied potential at and below 250 mV (vs. Ag/AgCl). At a higher potential, the repulsive force is weaker, the decay length is shorter, and the instability distance decreases suggesting the formation of the hemicylindrical aggregates.

7.2. Recommendations

Experimental results showed that AFM can be employed to successfully measure changes in the interaction force between a silica particle and a smooth glass substrate in the presence of copper ions as a function of time. This finding proves that copper ions sorb on a silica surface. Moreover, the measured force was found in a good agreement with theoretical predictions. However, the discrepancy at very small separation distances cannot be explained by the standard DLVO theory. Non-DLVO forces should be included in the calculations to correct the force at small separation distances.

The study of surface charge mapping was performed experimentally by force-volume AFM. Results showed the presence of islands suggesting the sorption of copper ions on the silica. Another technique, however, is needed to identify the species of the

sorbed copper by AFM. In addition, there are still questions on the nature of the heterogeneously charged regions. Therefore, surface spectroscopy, such as X-ray photoelectron spectroscopy (XPS) and X-ray diffraction (XRD), should be performed to confront surface charge data with surface chemical composition. A microscopic insight into the nature of the interactions and the structure of the overlapping electrical double layers (EDLs) can be obtained by developing a simulation protocol of a replica of the experimental set-up. The goal would be to probe the ions spatial distributions and calculate the interaction force between the colloidal particle and different regions of the charged surface.

The double-layer force between a silicon nitride tip and a gold-coated substrate was directly probed as a function of an externally applied potential. The nonlinear Poisson–Boltzmann equation was employed in the theoretical calculation due to the high surface potentials. Nonetheless, the DLVO theory is insufficient to describe the force at small separation distances. Non-DLVO forces should be included in the theoretical calculations to correct an additional repulsive force at small separations.

The interaction force between a silicon nitride tip and a gold substrate in the presence of a cationic surfactant under various external applied potentials was measured. Electrochemical experiments using cylcic voltammetry were performed to verify AFM results. However, direct information on surfactant aggregates using AFM imaging was not obtained in this study. Further studies involving a structural imaging and neutron reflectivity (NR) experiments are needed to further investigate the formation of surfactant aggregates and confirm the results presented in this thesis.

REFERENCES

Ackler, H. D., French, R. H., and Chiang, Y. M., "Comparisons of Hamaker constants for ceramic systems with intervening vacuum or water: From force laws and physical properties," *Journal of Colloid and Interface Science*, **179**, 460–469 (1996).

Adamczyk, Z., Para, G., and Warszynski, P., "Influence of ionic strength on surface tension of cetyltrimethylammonium bromide," *Langmuir*, **15**, 8383–8387 (1999).

Adler, J. J., Rabinovich, Y. I., and Moudgil, B. M., "Origins of the non-DLVO force between glass surfaces in aqueous solution," *Journal of Colloid and Interface Science*, **237**, 249–258 (2001).

Arai, T., Aoki, D., Okabe, Y., and Fujihira, M., "Ananlysis of surface forces on oxides in aqueous solutions using AFM," *Thin Solid Films*, **273**, 322–326 (1996).

Arai, T., and Fujihira, M., "Effects of electric potentials on surface forces in electrolyte solutions," *Journal of Vacuum Technology B*, **14**, 1378–1382 (1996).

Atkin, R., Craig, V. S. J., and Biggs, S., "Adsorption kinetics and structural arrangements of cationic surfactants on silica surfaces," *Langmuir*, **16**, 9374–93800 (2000).

Atkins, D. T., and Pashley, R. M., "Surface forces between zns and mica in aqueous electrolytes," *Langmuir*, **9**, 2232–2236 (1993).

Avranas, A., Retter, U., and Malasidou, E., "The adsorption and condensed film formation of cetyltrimethylammoniom bromide at the mercury/electrolyte interface," *Journal of Colloid and Interface Science*, **248**, 347–354 (2002).

Balooch M., and Hamza A. V., "Hydrogen and water vapor adsorption on and reaction with uranium," *Journal of Nuclear Materials*, **230**, 259–270 (1996).

Barten, D., Kleijn, J. M., Duval, J., Leeuwen, H. P. V., Lyklema, J., and Stuart, M. A. C., "Double layer of a gold electrode probed by AFM force measurements," *Langmuir*, **19**, 1133–1139 (2003a).

Barten, D., Kleijn, J. M., and Stuart, M. A. C., "Adsorption of a linear polyelectrolyte on a gold electrode," *Physical Chemistry Chemical Physics*, **5**, 4258–4264 (2003b).

Batchelor J. D., Olteanu, A., Tripathy, A., and Pielak, G. J., "Impact of protein denaturants and stabilizers on water structure," *Journal of the American Chemical Society*, **126**, 1958–1961 (2004).

Bhat S., and Agarwal P. K., "The effect of moisture condensation on the spontaneous combustibility of coal," *Fuel*, **75**, 1523–1532 (1996).

Biggs, S., and Mulvaney, P., "Measurement of the forces between gold surfaces in water by atomic force microscopy," *The Journal of Chemical Physics*, **100**, 8501–8505 (1994).

Biggs, S., Mulvaney, P., Zukoski, C. F., and Grieser, F., "Study of anion adsorption at the gold-aqueous solution interface by atomic force microscopy," *Journal of the American Chemical Society*, **116**, 9150–9157 (1996).

Binnig, G., Quate, C. F., and Gerber, C. H., "Atomic force microscopy," *Physical Review Letters*, **56**, 930–933 (1986).

Bockris, J. O., and Khan, S. U. M., "On the evolution of concepts concerning events at the semiconductor solution interface," *Journal of the Electrochemical Society*, **132**, 2648–2655 (1993).

Bouslah, N., and Amrani, F., "Miscible blends of styrene-cinnamic acid copolymers with poly(ethyl methacrylate)," *Polymer International*, **50**, 1384–1390 (2001).

Bousse, L., and Mostarshed, S., "The zeta potential of silicon nitride thin films," *Journal of Electroanalytical Chemistry*, **302**, 269–274 (1991).

Bremmell, K. E., Jameson, G. J., and Biggs, S., "Forces between surfaces in the presence of a cationic polyelectrolyte and an anionic surfactant," *Colloids and Surfaces A: Physicochemical and Engineering Aspects*, **155**, 1–10 (1999).

Burgess, I., Jeffrey, C. A., Cai, X., Szymanski, G., Galus, Z., and Lipkowski, J., "Direct visualization of the potential-controlled transformation of hemimicellar aggregates of dodecyl sulfate into a condensed monolayer at the Au(111) electrode surface," *Langmuir*, **15**, 2607–2616 (1999).

Burgess, I., Zamlynny, V., Szymanski, G., Lipkowski, J., Majewski, J., Smith, G., Satija, S., and Ivkov, R., "Electrochemical and neutron reflectivity characterization of dodecyl sulfate adsorption and aggregation at the gold-water interface," *Langmuir*, **17**, 3355–3367 (2001).

Butt, H.-J., "Electrostatic interaction in atomic force microscopy," *Biophysical Journal*, **60**, 777–785 (1991).

Butt, H.-J., "Measuring local surface charge densities in electrolyte solutions with a scanning force microscope," *Biophysical Journal*, **63**, 578–582 (1992).

Butt, H.-J., "A technique for measuring the force between a colloidal particle in water and bubble," *Journal of Colloid and Interface Science*, **166**, 109–117 (1994).

Camesano, T. A., and Logan, B. E., "Probing bacterial electrostatic interactions using atomic force microscopy," *Environmental Science Technology*, **34**, 3354–3362 (2000).

Campbell, S. D., and Hiller, A. C., "Nanometer–scale probing of potential–dependent electrostatic forces, adhesion, and interfacial friction at the electrode/electrolyte interface," *Langmuir*, **15**, 891–899 (1999).

Cappella, B., and Dietler, G., "Force–distance curves by atomic force microscopy," *Surface Science Reports*, **34**, 1–104 (1999).

Carnie, S. L., Chan, D. Y. C., and Gunning, J. S., "Electrical double-layer interaction between dissimilar sphericals and between a sphere and a plate–The linearized Poisson-Boltzmann theory," *Langmuir*, **10**, 2993–3009 (1994).

Cerovic, L.S., Milonjic, S.K., Bahloul-Hourlier, D., and Doucey, B., "Surface properties of silicon nitride powders," *Colloids and Surfaces A: Physicochemical and Engineering Aspects*, **197**, 147–156 (2002).

Chen, J. H., Nie, L. H., and Yao, S. Z., "A new method for rapid determination of the potential of zero charge for gold/solution interfaces," *Journal of Electroanalytical Chemistry*, **414**, 53–59 (1996).

Chin, C. J., Yiacoumi, S., and Tsouris, C., "Influence of metal ion sorption on colloidal surface forces measured by atomic force microscopy," *Environmental Science Technology*, **36**, 343–348 (2002).

Choi, C. J., Lee, B. W., Jung K. H., and Tschuikowreux, E., "Collisional energy-transfer in the 2-channel thermal unimolecular reactionof chloroethane-1,1,2-D(3)," *The Journal of Physical Chemistry*, **98**, 1139–1144 (1994).

Cleveland, J. P., and Manne, S., "A nondestructive method for determining the spring constant of cantilevers for scanning force microscopy," *Review of Scientific Instruments*, **64**, 403–405 (1993).

Colic, M., Fisher, M. L., and Fuerstenau, D. W., "Electrophoretic behaviour and viscosities of metal oxides in mixed surfactant systems," *Colloidal and Polymer Science*, **276**, 72–80 (1998).

Considine, R. F., Dixon, D. R., and Drummond, C. J., "Laterally-resolved force microscopy of biological microspheres-oocysts of *Cryptosporidium Parvum*," *Langmuir*, **16**, 1323–1330 (2000a).

Considine, R. F., and Drummond, C. J., "Long-range force of attraction between solvophobic surfaces in water and organic liquids containing dissolved air," *Langmuir*, **16**, 631–635 (2000b).

Crawford, R. J., Harding, I. H., and Mainwaring, D. E., "The zeta potential of iron and chromium hydrous oxides during adsorption and coprecipitation of aqueous heavy metals," *Journal of Colloid and Interface Science*, **181**, 561–570 (1996).

Crossley, A., Sofield, C. J., Goff, J. P., Lake, A. C. I., Hutchings, M. T., and Menelle, A., "A study comparing measurements of roughness of silicon and SiO_2 surfaces and interfaces using scanning probe microscopy and neutron reflectivity," *Journal of Non-Crystalline Solids*, **187**, 221–226 (1995).

Davis, J. A., James, R. O., and Leckie, J. O., "Surface ionization and complexation at the oxide/water interface," *Journal of Colloidal and Interface Science*, **63**, 480–499 (1978).

Dedeloudis, C., Fransaer, J., and Celis, J.-P., "Surface force measurements at a copper electrode/electrolyte interface," *The Journal Physical Chemistry B*, **104**, 2060–2066 (2000).

Derjaguin, B. V., Titijevskaia, A. S., Abrikossova, I. I., and Malkina, A. D., "Investigations of the forces of interaction of surfaces in different media and their application to the problem of colloid stability," *Discussions of the Faraday Society*, **18**, 24–41 (1954).

Derjaguin, B. V., and Abrikossova, I. I., "Direct measurements of molecular attraction between solids in vacuum," *Doklady Akademii Nauk SSSR*, **108**, 613–616 (1956).

Derjaguin B. V., and Landau L. D., "Theory of the stability of strongly charged lyophobic sols and of the adhesion of strongly charged particles in solution of electrolytes," *Acta physicochimica URSS*, **14**, 633–662 (1941).

Derjaguin, B. V., Voropayeva, T. N., Kabanov, B. N., and Titiyevskaya, A. S., "Surface forces and the stability of colloids and disperse systems," *Progress in Surface Science*, **43**, 83–105 (1993).

Döppenschmidt, A., and Butt, H.-J., "Measuring electrostatic double-layer forces on HOPG at high surface potentials," *Colloids and Surfaces A: Physicochemical and Engineering Aspects*, **149**, 145–150 (1999).

Ducker, W. A., and Senden, T. J., "Measurement of forces in liquids using a force microscope," *Langmuir*, **8**, 1831–1836 (1992).

Ducker, W. A., and Wanless, E., "Surface-aggregate shape transformation," *Langmuir*, **12**, 5915–5920 (1996).

Ducker, W. A., and Wanless, E., "Adsorption of hexadecyltrimethylammonium bromide to mica: nanometer-scale study of binding-site competition effects," *Langmuir*, **15**, 160–168 (1999).

Ducker, W. A., Xu, Z., and Israelachvili, J. N., "Measurement of hydrophobic and DLVO forces in bubble-surface interactions in aqueous solutions," *Langmuir*, **10**, 3279–3289 (1994).

Dzombak, D. A., and Morel, F. M. M., "Adsorption of inorganic pollutants in aquatic systems," *Journal of Hydraulic Engineer*, **113**, 430–475 (1987).

Dzombak, D. A., and Morel, F. M. M., "Surface Complexation Modeling: Hydrous Ferric Oxide," John Wiley and Sons, New York (1990).

Elimelech, M., Gregory, J., Jia, X., and Williams, R., "Particle Deposition & Aggregation: Measurement, Modelling and Simulation," Butterworth–Heinemann Ltd., Oxford (1995).

Estel, K., Kramer, G., and Schmitt, F.-J., "Charges in the interaction characteristics of polyelectrolyte complex covered silica surfaces," *Colloids and Surfaces A: Physicochemical and Engineering Aspects*, **161**, 193–202 (2000).

Fielden, M. L., Hayes, R. A., and Ralston, J., "Surface and capillary forces affecting air bubble-particle interactions in aqueous electrolyte," *Langmuir*, **12**, 3721–3727 (1996).

Fleming, B. D., and Wanless, E. J., "Soft-contact atomic force microscopy imaging of adsorbed surfactant and polymer layers," *Microscopy and Microanalysis*, **6**, 104–112 (2000).

Fleming, B. D., Biggs, S., and Wanless, E. J., "Slow organization of cationic surfactant adsorbed to silica from solutions far below the cmc," *The Journal of Physical Chemistry*, **105**, 9537–9540 (2001).

Fréchette, J., and Vanderlick, T. K., "Double layer forces over large potential ranges as measured in an electrochemical surface forces apparatus," *Langmuir*, **17**, 7620–7627 (2001).

Frisbie, C. D., Rozsnyai, L. F., Noy, A., Wrighton, M. S., and Lieber, C. M., "Functional group imaging by chemical force microscopy," *Science*, **265**, 2071–2074 (1994).

Gadegaard, N., Almdal, K., Larsen, N. B., and Mortensen, K., "The lamellar period in symmetric diblock copolymer thin films studied by neutron reflectivity and AFM," *Applied Surface Science*, **142**, 608–613 (1999).

Giesbers, M., Kleijn, J. M., and Stuart, A. C., "The electrical double layer on gold probed by electrokinetic and surface force measurements," *Journal of Colloid and Interface Science*, **248**, 88–95 (2002).

Hamm, U. W., Kramer, D., Zhai, R. S., and Kolb, D. M., "The pzc of Au(111) and Pt(111) in a perchloric acid solution: An ex situ approach to the immersion technique," *Journal of Electroanalytical Chemistry*, **414**, 85-89 (1996).

Harada, T., Matsuoka, H., Ikeda, T., and Yamaoka, H., "Comparison of USAXS information with RMSA prediction for the effect of added salt on colloidal crystal structure," *Journal of Polymer Science Part B-Polymer Physics*, **39**, 78–90 (2001).

Harame, D. L., Bousse, L. J., Schott, J. D., and Meindl, J. D., "Ion-sensing devices with silicon nitride and borosilicate glass insulators," *IEEE Transactions on Electron Devices*, **34**, 1700–1707 (1987).

Hartley, P. G., Grieser, F., Mulvaney, P., and Stevens, G. W., "Surface forces and deformation at the oil-water interface probed using AFM force measurement," *Langmuir*, **15**, 7282–7289 (1999).

Hartley, P., Matsumoto, M., and Mulvaney, P., "Determination of the surface potential of two-dimensional crystals of *Bacteriorhodopsin* by AFM," *Langmuir*, **14**, 5203–5209 (1998).

Hiemenz, P. C., and Rajagopalan, R., "Principles of Colloid and Surface Chemistry," 3rd Edition, Marcel Dekker, New York (1997).

Hiller, A. C., Kim, S., and Bard, A. J., "Measurement of double-layer forces at the electrode/electrolyte interface using the atomic force microscope: potential and anion dependent interactions," *The Journal of Physical Chemistry*, **100**, 18808–18817 (1996).

Hu, K., Fan, F.-R. F., Bard, A. J., and Hiller, A. C., "Direct measurement of diffuse double-layer forces at the semiconductor/electrolyte interface using an atomic force microscope," *The Journal of Physical Chemistry B*, **101**, 8298–8303 (1997).

Hüttl, G., Beyer, D., and Müller, E., "Investigation of electrical double layers on SiO_2 surfaces by means of force vs. distance measurements," *Surface and Interface Analysis*, **25**, 543–547 (1997).

Imae, T., Funayama, K., Aoi, K., Tsutsumiuchi, K., Okada, M., and Furusaka, M., "Small-angle neutron scattering and surface force investigations of poly(amido amine) dendrimer with hydroxyl end groups," *Langmuir*, **15**, 4076–4084 (1999).

Ishino, T., Hieda, H., Tanaka, K., and Gemma, N., "Measurements of electrostatic double-layer forces due to charged functional groups on Langmuir–Blodgett films with an atomic force microscope," *Japanese Journal of Applied Physics*, **33**, 4718–4722 (1994).

Ishino, T., Hieda, H., Tanaka, K., and Gemma, N., "Imaging charged functional groups with an force microscope operated in aqueous solutions," *Journal of Electroanalytical Chemistry*, **438**, 225–230 (1997).

Israelachvili, J. N., "Direct measurements of forces between surfaces in liquids at the molecular-level," *Proceeding of the National Academy of Sciences of the United States of America*, **84**, 4722–4724 (1987).

Israelachvili, J. N., "Intermolecular and Surface Forces," 2nd Edition, Academic Press, London (1992).

Israelachvili, J. N., and Adams, G. E., "Measurement of forces between 2 mica surfaces in aqueous-electrolyte solutions in range of 0–100 nm," *Journal of the Chemical Society–Faraday Transactions I.*, **74**, 975–979 (1978).

James, R. O., and Healy, T. W., "Adsorption of hydrolyzable metal ions at the oxide-water interface II. Charge reversal of SiO_2 and TiO_2 by adsorbed Co(II), La(II), and Th(IV) as model systems," *Journal of Colloid and Interface Science*, **40**, 42–52 (1972a).

James, R. O., and Healy, T. W., "Adsorption of hydrolyzable metal ions at the oxide-water interface I. Co(II) adsorption on SiO_2 and TiO_2 as model systems," *Journal of Colloid and Interface Science*, **70**, 42–52 (1972b).

Jaschke, M., Butt, H.-J., Gaub, H. E., and Manne, S., "Surfactant aggregates at a metal surface," *Langmuir*, **13**, 1381–1384 (1997).

Johnson, A. S., Nehl, C. L., Mason, M. G., and Hafner, J. H., "Fluid electric microscopy for charge density mapping in biological systems," *Langmiur*, **19**, 10007–10010 (2003).

Kado, H., Yokoyama, K., and Tohda, T., "Atomic force microscopy using ZnO whisker tip," *Review of Scientific Instruments*, **63**, 3330–3332 (1992).

Kanda, Y., Nakamura, T., and Higashitani, K., "AFM studies of interaction forces between surfaces in alcohol-water solutions," *Colloids and Surfaces A: Physicochemical and Engineering Aspects*, **139**, 55–62 (1998).

Kane, V., and Mulvaney, P., "Double-layer interactions between self-assembled monolayers of omega-mercaptoundecanoic acid on gold surfaces," *Langmuir*, **14**, 3303–3311 (1998).

Karaman M. E., Pashley, R. M., Waite, T. D., Hatch, S. J., and Bustamante, H., "A comparison of the interaction forces between model alumina surfaces and their colloidal properties," *Colloids and Surfaces A: Physicochemical and Engineering Aspects*, **130**, 239–255 (1997).

Karim, A., Douglas, J. F., Satija, S. K., Han, C. C., and Goyette, R. J., "Frustrated coalescence in a chemically reactive polymer blend film," *Macromolecules*, **32**, 1119–1127 (1999).

Kékicheff, P., Marcelja, S., Senden, T. J., and Shubin, V. E., "Charge reversal seen in electrical double-layer interaction of surfaces immersed in 2-1 calcium electrolyte," *The Journal of Chemical Physics*, **99**, 6098–6113 (1993).

Kim, S. H., "Method for potential of zero charge determination–Electrode pretreatment," *The Journal of Physical Chemistry*, **77**, 2787–2789 (1973).

Kramer, G. K., Estel, K., Schmitt, F.-J., and Jacobasch, H.-J., "Laterally resolved measurement of interaction forces between surfaces that are partly covered with electrolytes," *Journal of Colloid and Interface Science*, **208**, 302–309 (1998).

Larson, I., Chan, D. Y. C., Drummond, C. J., and Grieser, F., "Use of atomic force microscopy force measurements to monitor citrate displacement by amines on gold in aqueous solution," *Langmuir*, **13**, 2429–2431 (1997).

Larson, I., Drummond, C. J., Chan, D. Y. C., and Grieser, F., "Direct force measurements between TiO_2 surfaces," *Journal of the American Chemical Society*, **115**, 11885–11890 (1993).

Larson, I., Drummond, C. J., Chan, D. Y. C., and Grieser, F., "Direct force measurements between dissimilar metal oxides," *The Journal of Physical Chemistry*, **99**, 2114–2118 (1995).

Larson, I., and Pugh, R. J., "Qualitative adsorption measurements with an atomic force microscope," *Langmuir*, **14**, 5676–5679 (1998).

Leikis, D. I., Rybalka, K. V., and Panin, V. A., "Measurement of electrical double-layer capacity at a polycrystalline cadmium electrode," *Journal of Electroanalytical Chemistry*, **40**, 9–20 (1972).

Li, Y. Q., Tao, N. J., Pan, J., Gracia, A. A., and Lindsay, S. M., "Direct measurement of interaction forces between colloidal particles using the scanning force microscope," *Langmuir*, **9**, 637–641 (1993).

Li, J., and Kaifer, A. E., "Surfactant monolayer on electrode surfaces–Self-assembly of a viologen derivative having a cholesteryl hydrophobic residue," *Langmuir*, **9**, 591–596 (1993).

Liang, L., and Morgan, J. J., "Chemical aspects of iron oxide coagulation in water: laboratory studies and implications for natural systems," *Aquatic Science*, **52**, 33–55 (1990).

Liao, X., and Higgins, D. A., "Scanning probe microscopy studies of mesostructured nonstoichiometric polyelectrolyte-surfactant complexes," *Langmuir*, **18**, 6259–6265 (2002).

Liu, J.-F., and Ducker, W. A., "Surface-induced phase behavior of alkyltrimethylammonium bromide surfactants adsorbed to mica, silica, and graphite," *The Journal of Physical Chemistry B*, **103**, 8558–8567 (1999).

Liu, J.-F., Min, G., and Ducker, W. A., "AFM study of adsorption of cationic surfactants and cationic polyelectrolytes at the silica-water interface," *Langmuir*, **17**, 4895–4903 (2001).

London, F., "The general theory of molecular forces," *Transaction of Faraday Society*, **33**, 8–26 (1937).

Manne, S., Cleveland, J. P., Gaub, H. E., Stucky, G. D., and Hansma, P. K., "Direct visualization of surfactant hemimicelles by atomic force miscroscopy of the electrical double-layer," *Langmuir*, **10**, 4409–4413 (1994).

Manne, S., and Gaub, H. E., "Molecule organization of surfactants at solid-liquid interfaces," *Science*, **270**, 1480–1482 (1995).

Marino, A., and Brajter-Toth, A., "Ionic surfactants as molecular spacers at graphite-electrodes," *Analytical Chemistry*, **65**, 370–374 (1993).

McLachlan, A. D., "Retarded dispersion forces between molecules," *Proceedings of the Royal Society of London Series A–Mathematical and Physical Sciences*, **271**, 387–390 (1963).

McNamee, C. E., Matsumoto, M., Hartley, P. G., Mulvaney, P., Tsujii, Y., and Nakahara, M., "Interaction forces and zeta potentials of cationic polyelectrolyte coated silica surfaces in water and in ethanol: effects of chain length and concentration of perfluorinated anionic surfactants on their binding to the surface," *Langmuir*, **17**, 6220–6227 (2001).

Meagher, L., "Direct measurement of forces between silica surfaces in aqueous $CaCl_2$ solutions using an atomic force microscope," *Journal of Colloid and Interface Science*, **152**, 293–295 (1992).

Meagher, L., Maurdev, G., and Gee, M. L., "Interaction forces between a bare silica surface and α–alumina surface bearing adsorbed polyelectrolyte and surfactant," *Langmuir*, **18**, 2649–2657 (2002).

Meyer, E., Howald, L., Overney, R., Brodbeck, D., Luthi, R., Haefke, H., Frommer, J., and Guntherodt, H. J., "Structure and dynamics of solid-surfaces observed by atomic force microscopy," *Ultramicroscopy*, **42**, 274–280 (1992).

Miyatani, T., Horii, M., Rosa, A., Fujihira, M., and Marti, O., "Mapping of electrical double-layer force between tip and sample surfaces in water with pulsed-force-mode atomic force microscopy," *Applied Physics Letters*, **71**, 2632–2634 (1997).

Miyatani, T., Okamoto, S., Rosa, A., Marti, O., and Fujihira, M., "Surface charge mapping of solid surfaces in water by pulsed-force-mode atomic force microscopy," *Applied Physics A*, **66**, 349–352 (1998).

Nalaskowski, J., Veeramasuneni, S., Hupka, J., and Miller, J. D., "AFM measurements of hydrophobic forces between a polyethylene sphere and silanated silica plates–The significant of surface roughness," *Journal of Adhesion Science and Technology*, **13**, 1519–1533 (1999).

Nietzsche, R., and Friedrich, H., "Application of electrokinetic methods to characterize fine ceramic powders, demonstrated by the example of Si_3N_4," *Proceedings of the Symposium on the Electrokinetic Phenomena*, **11**, 123–137 (1989).

Philip, J., Gnanaprakash, G., Jayakumar, T., Kalyanasundaram, P., and Raj, B., "Three distinct scenarios under polymer, surfactant, and colloidal interaction," *Macromolecules*, **36**, 9230–9236 (2003).

Preuss, M., and Butt, H.-J., "Direct Measurement of Particle-Bubble Interactions in Aqueous Electrolyte: Dependence on surfactant," *Langmuir*, **14**, 3164–3174 (1998a).

Preuss, M., and Butt, H.-J., "Measuring the contact angle of individual colloidal particles," *Journal of Colloid and Interface Science*, **208**, 468–477 (1998b).

Rabinovich, Y. I., and Derjaguin, B. V., "Calculation of the surface-charge and potential and of the structural component of disjoining pressure in an interlayer in KCl solutions between glass samples," *Langmuir*, **3**, 625–628 (1987).

Rabinovich, Y. I., and Yoon, R.-H., "Use of atomic force microscope for the measurements of hydrophobic forces," *Colloids and Surfaces A: Physicochemical and Engineering Aspects,* **93**, 263–273 (1994).

Rae, A., and Mason, R., "Intermolecular potential and lattice energy of benzene," *Proceedings of the Royal Society of London Series A-Mathematical and Physical Science*, **304**, 487–490 (1968).

Raiteri, R., Grattarola, M., and Butt, H.-J., "Measuring electrostatic double-layer forces at high surface potential with the atomic force microscope," *The Journal of Physical Chemistry*, **100**, 16700–16705 (1996a).

Raiteri, R., Margesin, B., and Grattarola, M., "An atomic force microscope estimation of the point of zero charge of silicon insulators," *Sensors and Actuators B,* **46**, 126–132 (1998a).

Raiteri, R., Martinoia, S., and Grattarola, M., "pH-dependent charge density at the insulator-electrolyte interface probed by a scanning force microscope," *Biosensors and Bioelectronics,* **11**, 1009–1017 (1996b).

Raiteri, R., Press, M., Grattarola, M., and Butt, H.-J., "Preliminary results on the electrostatic double-layer force between two surfaces with high surface potentials," *Colloids and Surfaces A: Physicochemical and Engineering Aspects*, **136**, 191–197 (1998b).

Rojas, O. J., Ernstsson, M., Neuman, R. D., and Claesson, P. M., "Effect of polyelectrolyte charge density on the adsorption and desorption behavior on mica," *Langmuir*, **18**, 1604–1612 (2002).

Rowe, A.W., "The Effect of pH and Applied Electrical Potential on Oil Removal from a solid Surface in the Presence of Four Types of Surfactant Solutions," Master Thesis, University of Tennessee, Knoxville, TN (2000).

Rusling, J. R., and Couture, E. C., "Alcohol-induced surface wlectrochemistry in solutions of hexadecyltrimethylammonium bromide," *Langmuir*, **6**, 425–432 (1990).

Rutland, M. W., and Christenson, H. K., "Effect of nonionic surfactant on ion adsorption and hydration forces," *Langmuir*, **6**, 1083–1087 (1990).

Rutland, M. W., and Senden, T. J., "Adsorption of the poly(oxyethylene) nonionic surfactant $C_{12}E_5$ to silica–A study using atomic force microscopy," *Langmuir*, **9**, 412–418 (1993).

Sakai, H., Nakamura, H., Kozawa, K., and Abe, M., "Atomic force microscopy observation of the nanostruture of tetradecyltrimethylammonium bromide films adsorbed at the mica/solution interface," *Langmuir*, **17**, 1817–1820 (2001).

Sakamoto, M., Kenda, Y., Miyahara, M., and Higashitani, K., "Origin of long-range attractive force between surfaces hydrophobized by surfactant adsorption," *Langmuir*, **18**, 5713–5719 (2002).

Schindler, P. W., Fürst, B., Dick, R., and Wolf, P. U., "Ligand properties of silanol groups I. Surface complex formation with Fe(III), Cu(II), Cd(II), and Pb(II)," *Journal of Colloid and Interface Science*, **55**, 469–475 (1976).

Schulz, J.C., "Interfacial Structures in Thin Surfactant Films," Ph.D. Thesis, University of Sydney, Sydney (2000).

Schulz, J. C., Warr, G. G., Hamilton, W. A., and Butler, P. D., "A new model for neutron reflectometry of adsorbed surfactant aggregates," *The Journal of Physical Chemistry B*, **103**, 11057–11063 (1999).

Schulz, J. C., Warr, G. G., Butler, P. D., and Hamilton, W. A., "Adsorbed layer structure of cationic surfactants on quartz," *Physical Review E*, **63**, 041604-1–041604-5 (2001).

Senden, T. J., Drummond, C. J., and Kékicheff, P., "Atomic force microscopy: imaging with electrical double layer interactions," *Langmuir*, **10**, 358–362 (1994).

Senden T. J., and Drummond, C. J., "Surface-chemistry and tip sample interactions in atomic-force microscopy," *Colloids and Surfaces A: Physicochemical and Engineering Aspects*, **94**, 29–51 (1995).

Shuman, L. M., "Effect of removal of organic matter and iron- or manganese-oxides on zinc adsorption by soil," *Soil Science*, **146**, 248–254 (1988).

Snyder, B. A., Aston, D. E., and Berg, J. C., "Particle-drop interactions examined with an atomic force microscope," *Langmuir*, **13**, 590–593 (1997).

Stankovich, J., and Carnie, S. L., "Electrical double layer interaction between dissimilar spherical colloidal particles and between a sphere and a plate: Nonlinear Poisson-Boltzmann theory," *Langmuir*, **12**, 1453–1461 (1996).

Stumm, W., and Morgan, J. J., "Aquatic Chemistry: Chemical Equilibria and Rates in Natural Waters," 3rd Edition, Wiley, New York (1996).

Subramaniam, K., Vithayaveroj, V., Yiacoumi, S., and Tsouris, C., "Copper uptake by silica and iron oxide under high surface coverage conditions: Surface charge and

sorption equilibrium modeling," *Journal of Colloid and Interface Science*, **268**, 12–22 (2003).

Subramaniam, K., Yiacoumi, S., and Tsouris, C., "Copper uptake by inorganic particles–equilibrium, kinetics, and particle interactions: Experimental," *Colloids and Surfaces A: Physicochemical and Engineering Aspects*," **177**, 133–146 (2001).

Subramanian, V., and Ducker, W. A., "Counterion effects on adsorbed micellar shape: Experimental study of the role of polarizability and charge," *Langmuir*, **16**, 4447–4454 (2000).

Subramanian, V., and Ducker, W. A., "Proximal adsorption of cationic surfactant on silica at equilibrium," *The Journal of Physical Chemistry B*, **105**, 1389–1402 (2001).

Suga, K., Bradley, M., and Rusling, J. F., "Probing the interface of cast surfactant films and an underlying metal by surface-enhanced raman-scattering spectroscopy," *Langmuir*, **9**, 3063–3066 (1993).

Sung, Youlboong, "Copper (II) Uptake from Aqueous Solutions by Silica Particles: Adsorption and Precipitation Experimental Studies," Special Research Project Report, Georgia Institute of Technology, Atlanta, GA (1999).

Terán Arce, F., Avci, R., Beech, I. B., Cooksey, K. E., and Wigglesworth-Cooksey, B., "Microelastic properties of minimally adhesive surfaces: A comparative study of RTV11™ and intersleek elastomers™," *The Journal of Chemical Physics*, **119**, 1671–1682 (2003).

Teschke, O., Ceotto, G., and de Souza, E. F., "Rupture force of adsorbed self-assemble surfactants layers effect of the dielectric exchange force," *Chemical Physics Letters*, **344**, 429–433 (2001).

Thompson, D. W., and Collins, I. R., "Electrical-properties of the gold aquoues-solution interface," *Journal of Colloid and Interface Science*, **152**, 197–204 (1992).

Tiberg, F., Brinck, J., and Grant, L., "Adsorption and surface-induced self-assembly of surfactants at the solid-aqueous interface," *Current Opinion in Colloid and Interface Science*, **4**, 411–419 (2000).

Toikka, G., and Hayes, R. A., "Direct measurement of colloidal forces between mica and silica in aqueous electrolyte," *Journal of Colloid and Interface Science*, **191**, 102–109 (1997).

Van Megen, W., and Snook, I., "The grand canonical ensemble Monte Carlo method applied to the electrical double layer," *Journal of Chemical Physics*, **73**, 4656–4662 (1980).

Veeramasuneni, S., Yalamanchill, M. R., and Miller, J. D., "Measurement of interaction forces between silica and α-alumina by atomic force microscopy," *Journal of Colloid and Interface Science*, **184**, 594–600 (1996).

Veeramasuneni, S., Yalamanchili, M. R., and Miller, J. D., "Interactions between dissimilar surfaces in high ionic strength solutions as determined by atomic force microscopy," *Colloids and Surfaces A: Physicochemical and Engineering Aspects*, **131**, 77–87 (1998).

Velegol, S. B., Fleming, B. D., Biggs, S., Wanless, E. J., and Tilton, R. D., "Counterion effect on hexadecyltrimethylammonium surfactant adsorption and self-assembly on silica," *Langmuir*, **16**, 2548–2556 (2000).

Verwey E. J. W., and Overbeek J. Th. G., "Theory of the Stability of Lyophobic Colloids," Elsevier, Amsterdam (1948).

Victor, K., Jacob, J., and Cafiso D. S., "Interactions controlling the membrane binding of basic protein domains: Phenylalanine and the attachment of the myristoylated alanine-rich C-kinase substrate protein to interfaces," *Biochemistry*, **38**, 12527–12536 (1999).

Vithayaveroj V., Yiacoumi, S., and Tsouris, C., "Modification of surface forces by metalion adsorption," *Journal of Dispersion Science and Technology*, **24**, 517–525 (2003).

Wall, J. F., and Zukoski, C. F., "Alcohol-induced structural transformations of surfactant aggregates," *Langmuir*, **15**, 7432–7437 (1999).

Wang, J., Feldberg, S. W., and Bard, A. J., "Measurement of double-layer forces at the polymer film/electrolyte interfaces using atomic force microscopy: Concentration and potential-dependent interactions," *The Journal of Physical Chemistry B*, **105**, 1389–1402 (2002).

Wang, J., and Bard, A. J., "Direct atomic force microscopic determination of surface charge at the gold/electrolyte interface–The inadequacy of classical GCS theory in describing the double-layer charge distribution," *The Journal of Physical Chemistry B*, **105**, 5217–5222 (2001).

Wangsa-Wirawan, N. D., Ikai, A., O'Neill, B. K., and Middelberg, A. P. J., "Measuring the interaction forces between protein inclusion bodies and an air bubble using an atomic force microscope," *Biotechnology Progress*, **17**, 963–969 (2001).

Wanless, E. J., Davey, T. W., and Ducker, W. A., "Surface aggregate phase transition," *Langmuir*, **13**, 4223–4228 (1997).

Weaver, J. M. R., and Wickramasinghe, H. K., "Semiconductor characterization by scanning force microscope surface photovoltage microscopy," *Journal of Vacuum Science and Technology B*, **9**, 1562–1565 (1991).

Weisenhorn, A. L., Maivald, P., Butt, H.-J., and Hansma, P. K., "Measuring adhesion, attraction, and repulsion between surfaces in liquids with an atomic force microscope," *Physical Review B*, **45**, 11226–11232 (1992).

Whitby, C. P., Scales, P. J., Grieser, F., and Healy, T. W., "The adsorption of dedecyltrimethylammonium bromide on mica in aqueous solution studied by x-ray diffraction and atomic force microscopy," *Journal of Colloid and Interface Science*, **235**, 350–357 (2001).

Xu, Z., Ducker, W., and Israelachvili, J., "Forces between crystalline alumina (sapphire) surfaces in aqueous sodium dodecyl sulfate surfactant solutions," *Langmuir*, **12**, 2263–2270 (1996).

Yang, K.-L., Ying, T.-Y., Yiacoumi, S., Tsouris, C., and Vittoratos, E. S., "Electrosorption of ions from aqueous solutions by carbon aerogel: An electrical double-layer model," *Langmuir*, **17**, 1961–1969 (2001).

Yang, K.-L., "Electrical double-layer formation at the nanoscale : molecular modeling and applications," Ph.D. Thesis, Georgia Institute of Technology, Atlanta, GA (2003).

Yiacoumi, S., and Tien, C., "Kinetics of Metal Ion Sorption from Aqueous Solutions: Models, Algorithms, and Applications," Kluwer Academic Publishers, Boston (1995).

Zachara, J. M., Ainsworth, C. C., Cowan, C. E., and Resch, C. T., "Adsorption of chromate by subsurface soil horizons," *Soil Science Society American Journal*, **53**, 418–428 (1989).

Zaman, A. A., Singh, P., and Moudgil, B. M., "Impact of self-assembled surfactant structures on rheology of concentrated nanoparticle dispersions," *Journal of Colloid and Interface Science*, **251**, 381–387 (2002).

Zimmerman, R. J., Kanal, K. M., Sanders, J., Cameron, I. L., and Fullerton, G. D., "Osmotic-pressure method to measure salt-induced folding unfolding of bovine serum-albumin," *Journal of Biochemical and Biophysical Methods*, **30**, 113–131 (1995).

Zhang, S. H., Jin, X., Painter, P. C., and Runt, J., "Dynamical heterogeneity in the thermodynamically miscible polymer blend of poly(vinyl ethyl ether) and styrene-co-p-hydroxystyrene copolymer," *Macromolecules*, **36**, 5710–5718 (2003).

VITA

The author, Viriya Vithayaveroj, was born on October 26, 1977 in Bangkok, Thailand. She received a Bachelor of Engineering degree in Environmental Engineering from Chulalongkorn University, Bangkok, Thailand, in 1998. She also obtained a Master of Science degree in Environmental Engineering from New Jersey Institute of Technology in 1999. In Fall 2000, she initiated her graduate studies at the Georgia Institute of Technology, Atlanta, GA. The author joined the research group of Dr. Sotira Yiacoumi in Spring 2001 and started her research focusing on surface interactions and the application of AFM to study sorption processes. The author completed her Ph.D. degree in September 2004.